CYCLIC IN–PLANE TESTING OF POST AND BEAM WALLS WITH STRAW-BALE IN-FILL AND STUCCO/PLASTER

by

Juan Carlos Ramírez

A thesis submitted in partial fulfillment of the
requirements for the degree of

Master of Science in Civil Engineering

University of Washington

1999

Approved by _____
Chairperson of Supervisory Committee

_____

_____

_____

Program Authorized
to Offer Degree _____

Date _____

Master's Thesis

In presenting this thesis in partial fulfillment of the requirements for a Master's degree at the University of Washington, I agree that the Library shall make its copies freely available for inspection. I further agree that extensive copying of this thesis is allowable only for scholarly purposes, consistent with "fair use" as prescribed in the U.S. Copyright Law. Any other reproduction for any purposes or by any means shall not be allowed without my written permission.

<div style="text-align: right;">

Signature_____

Date _____

</div>

University of Washington

Abstract

CYCLIC IN–PLANE TESTING OF POST AND BEAM WALLS
WITH STRAW-BALE IN-FILL AND STUCCO/PLASTER

by Juan Carlos Ramírez

Chairperson of the Supervisory Committee:
Gregory MacRae, Assistant Professor
Department of Civil and Environmental Engineering

Two large-scale single story wall units made with straw bale construction were subjected to repeated in-plane cyclic lateral loads at the roof level in order to determine their seismic performance. Both walls were constructed with a wooden post and beam frame. Straw-bales were used as frame in-fill and cement-stucco/mesh facing was placed on one side of the wall and gypsum-based plaster/mesh facing was used on the other side. The second wall had straw bales that were less wide than the first wall so that the facings were within the confines of the wooden post and beam frame.

It was found that both test units reached peak strengths of greater than $V = 0.0735d(b_p\sqrt{f'_{cp}} + b_s\sqrt{f'_{cs}})$, where f'_{cp} is the compressive strength of the plaster (MPa), f'_{cp} is the compressive strength of the stucco (MPa), b_p is the average thickness of plaster facing, b_s is the average thickness of stucco facing and d is the wall length. The second test unit was 27% stronger than the first test due to confinement of the facings within the frame. The flexibility of the straw-bale was high, and the lateral resistance was negligible. However, the straw limited the tendency of the facings to buckle.

Drifts of greater than 3% were reached for each frame before the strength dropped to less than 80% of the peak strength. Components of deformation at 3% drift were panel deformation, facing-frame connection deformation and uplift.

A simple model was developed to describe the relative component of facing panels, facing-frame connections and uplift drifts to the total drift, and to allow strength in each component to be obtained.

Finally, a typical straw-bale structure was analyzed by means of the UBC 1997, FEMA 302 (1998) and ATC-40 (1996) codes. It was found that while the structure did not meet the seismic criteria for these codes in zones of high seismicity, it was satisfactory for zones of lower seismicity. Also, a simple design relationship to determine the length of wall required per unit roof area was developed as a function of the seismic coefficient for walls similar to those tested in this study.

TABLE OF CONTENTS

LIST OF FIGURES

vii

LIST OF TABLES

GLOSSARY

Course. A horizontal layer of straw-bales (Steen et al. 1994)

Facing. Ornamentation of brick, concrete, stone, tile, or similar materials attached to a backing (FEMA 302, 1998). In the case of straw-bale walls, facings are used for the purposes of confinement and/or load bearing, and may be earthen based (adobe) or cement based (stucco) or lime based (plaster), among other materials.

Flakes. Slabs of straw removed from an untied bale, and used primarily to fill in gaps at end of stacked bales (State of California Guidelines for Strawbale Structures, 1995).

Hay. Green moist grass stems with leaves and seeds, full of grains and nutrients, used primarily for feeding animals (King, 1996).

Laid Flat. Stacking up of bales so that the sides with the largest cross-sectional area are horizontally oriented and the longest dimension of this area is parallel to the ground (State of California Guidelines for Strawbale Structures, 1995).

Laid On-Edge. Stacking up of bales so that the sides with the largest cross-sectional area are vertically oriented and the longest dimension of this area is parallel to the ground (State of California Guidelines for Strawbale Structures, 1995).

Seismic Performance. A measure of the degree of protection for the public and building occupants against the potential hazards resulting from the effects of earthquake motions on buildings.

Straw. Dry, dead plant stems of agricultural cereal grains left after the seed heads have been harvested (State of California Guidelines for Strawbale Structures, 1995).

Straw-Bale. Densely compacted rectangular hexahedron composed of cut straw and bound with polypropylene string or other ties (State of California Guidelines for Strawbale Structures, 1995).

LIST OF ABBREVIATIONS

ADRS. Acceleration-Displacement Response Spectra

ATC. Applied Technology Council

CAPGSBC. California Proposed Guidelines for Straw Bale Construction

CSA. Canada Standards Agency

CHMC. Canada House and Mortgage Corporation

CTPCAZBC. City of Tucson and Pima County Arizona Building Code

DE. Design Earthquake

EOM. Equation of Motion

FEMA. Federal Emergency Management Agency

ICBO. International Conference of Building Officials

OSB. Oriented Strand Board

MCE. Maximum Considered Earthquake

NEHRP. National Earthquake Hazard Reduction Program

NMBC. New Mexico Building Code

SDOF. Single Degree of Freedom

UBC. Uniform Building Code

ACKNOWLEDGMENTS

DEDICATION

Esta tésis está dedicada a mis padres,

Hilda y Hesiquio Ramírez,

quiénes siempre me han brindado todo su apoyo, cariño y compresión.

Sin ellos, jamás habría llegado tan lejos,

Gracias a ellos,

soy quién soy.

CHAPTER 1: INTRODUCTION

STATEMENT OF PROBLEM

Construction of simple one- and two-story structures has generally been carried out using a significant amount of timber. However, rising costs of timber mean that other previously little used construction materials, may become more viable. Agricultural straw, cut, compacted and bound as straw-bales, has been used as a construction material in simple one and two-story structures in different parts of the world. Straw bales have excellent insulation and sound absorption properties. While laboratory testing has been carried out to obtain the properties of straw-bales as well as the performance straw-bale and straw-bale/facing walls to lateral loading, theefficacy of straw-bale/facing construction to sustain earthquake type loading has not been documented.

If straw-bale/facing wall systems are to be used as primary lateral force resisting elements for structures in seismic zones it is necessary to understand the seismic characteristics.

A research program was initiated at the University of Washington in order to:

• understand the likely seismic performance of structures with walls containing straw-bales and facings designed according to standard guidelines for non-seismic regions,

• assess their performance according to current seismic codes, and

• to develop simple design recommendations for the design of the types of structure tested.

A review of literature regarding straw-bale construction is presented in Chapter 2 of this thesis. Chapter 3 shows the properties of each of the materials used. Chapter 4 documents the construction of the test unit and the test setup. Chapter 5 describes the

instrumentation used and the loading regime applied. Chapter 6 describes the behavior of the test units. Chapter 7 describes how the experimental results were interpreted. Chapter 8 presents design recommendations based on the test results. Chapter 9 compares the behavior or a structure designed for non-seismic regions with the seismic codes design requirements. Chapter 10 presents conclusions obtained from this study.

CHAPTER 2: LITERATURE REVIEW

2.1 BACKGROUND

The earliest use of straw as a building material has been attributed to the Egyptians, who used it to reinforce earthen building blocks. Subsequently, it has been used either as reinforcement into earthen mixtures or as a structural material by itself has been around the world, particularly in Africa, Latin America and Europe (Burkhardt 1996, King 1996). In the United States, the recorded longevity of structures using straw to provide the structural support is of over eighty years (Burkhardt 1996, Eisenberg 1995, King 1996, Welsch 1970). Some straw-bale houses found in Nebraska, dating from before 1900AD are still structurally sound. Straw-bales and plaster houses were generally used simply because there were no other building materials available in the region.

The structural use of straw-bales in the United States for simple one- and two-story structures was revitalized in the early 1970's after Welsch's (Welsch 1970) articles inspired people to look at straw-bales as an alternative building material (Eisenberg 1995, King 1996). Since then, simple one- and two-story straw-bale structures have proliferated in dry, low seismicity regions (Such as Arizona, New Mexico and Texas), particularly in the last few years. The recent gain in the popularity of straw-bale has been due in part to its appeal as a "sustainable" and renewable material. As a by-product of grain production, straw-bales are compressed, rectangular blocks that "recycle" the cellulose material remaining after harvesting. Production of straw-bales is particularly attractive in states where the pollution caused by agricultural burning has become a major environmental concern. Some designers have begun to look at straw-bale construction as an alternative to ordinary construction materials for economic reasons, acknowledging the rising costs of lumber, and masonry construction (Burkhardt 1996, King 1996).

2.2 MATERIALS USED IN STRAW-BALE BASED CONSTRUCTION

2.2.1 STRAW

Agricultural straw is the material remaining after harvesting of grains from crops such as wheat, rice, oats and barley. Agricultural straw contains cellulose, hemicellulose, lignings and silica, which differentiates it from hay, which is rich in nutrients, and primarily used as animal food. The specific chemicals found in straw depend on the grain from which it was obtained. Straw generally has a lower moisture content than hay. If not burned or returned to the soil as a fertilizing agent, the straw can be cut and implemented as a construction material for simple structural systems. The straw may be used as a construction material either by itself, or in combination with cementitious and earthen mixtures, such as plaster and adobe, or synthetic adhesives, such as those used to make low, medium and high density straw-based construction panels. Straw is readily available throughout the world, particularly after a harvest season, and is renewable on a regular basis.

2.2.2 STRAW-BALES

Straw-bales are produced when straw is cut, compressed and tied tightly with polypropylene string to form some volumetric shape. The use of mechanical balers has made the process of creating rectangular blocks more efficient. By automating bale production, fewer variations in the finished bales occur when compared to manual baling processes. Figure 1 shows a typical two and three string straw-bale produced by a mechanical baler. Mechanical balers produce bales with four similar and two dissimilar planes. The similar planes are those in contact with the polypropylene strings and are a combination of folded, cut and randomly oriented straw. The two dissimilar planes are along the length of the bale and not in contact with the string ties. The plane known as the "cut side" is made of sharp, cut ends of the straw, the other smoother plane, known as the "uncut side" is made of straw ends folded to form the flat plane. The resulting rectangular straw hexahedron is an anisotropic, heterogeneous block.

Figure 1: Typical Two and Three String Straw-Bale (Steen et al. 1994)

At present, straw-bales are produced by mechanical balers in two sizes: a smaller, less dense and moderately compressed two string bale, and a larger, denser and more heavily compressed three string bale. The compression applied by the mechanical balers usually yield straw hexahedrons with a dry density in the order of ρ_{ave}=112 to 160kg/m^3 (ρ_{ave}=7 to 10pcf) (King 1996). High-power mechanical balers are capable of producing denser, heavier blocks, but their use and acceptance has been very limited (King 1996). Certain balers can make custom bales, with variable densities and dimensions. The range of standard dimensions and weight of the two standard sizes of straw-bales produced are the following. For three string bales, 356 to 432mm (14 to 17in) high by 1067 to 1219mm (42 to 48in) long by 584mm (23in) wide, the dry weight ranges between 267 and 400N (60 and 90lbs). For the two string bales, 356 to 406mm (14 to 16in) high by 889 to 1016mm (35 to 40in) long by 457mm (18in) wide, the dry weight ranges between 156 and 289N (35 and 65lbs). The dimensions depend on the baler used and the weight on type of grain and characteristics at the time of cutting.

As with any other structural material, proper moisture control is crucial to the longevity and structural integrity of straw-bales. The moisture content of the straw depends on climatic conditions at the time of baling. Straw-bales need to be monitored for low

moisture content at the time of installation, with existing codes, proposed guidelines and experienced builders recommending a moisture content less than 20%. The connection to the foundation must be lined with an impermeable material to prevent water seepage into the straw-bales. When properly confined, straw-bales appear to be as reliable as any other construction material.

Tests to determine the material properties of straw-bales have been performed by some individuals over the last few years:

Bou-Ali (1993) carried out a number of laboratory tests using three polypropylene string wheat bales, with an average density ρ_{ave}=136kg/m^3 (ρ_{ave}=8.5pcf) and approximate dimensions of 406mm x 584mm x 1143mm (16in x 23in x 45in). Bou-Ali carried out unconfined compression tests on four bales with a laid flat orientation and on two with a laid on-edge orientation. He determined a range for the maximum compressive stress between 483 to 579kPa (70 to 84psi) for bales laid flat and 117 to 145kPa (17 to 21psi) for those laid on-edge. Loading of these units stopped when the applied force stopped increasing, at a compressive strain, ε, of approximately 50%. Bou-Ali also reported a range for the modulus of elasticity, E, between 414 to 1793kPa (60 to 260psi) and (78 to 211psi), for bales laid flat and on-edge, respectively. Poisson's ratio, μ, was estimated by Bou-Ali as 0.3. He observed that elastic rebound to the original height after compression occurred on all units laid flat, with no signs of plastic deformation or failure, including one subjected to a compressive stress, σ, of approximately 15.4kPa (2240psi). The compressive stress on the two bale units laid on-edge broke the middle polypropylene string. Bou-Ali stated that density of the bales was proportional to the maximum compressive stress.

Thompson et al. (1993) carried out some compression tests on a number of two polypropylene string wheat, barley and oat bales laid flat, with dimensions 457.2mm x 355.6mm x 914mm (18in x 14in x 36in). The average modulus of elasticity, E, was 124kPa (18psi) for barley, 135kPa (20psi) for wheat and 179kPa (26psi) for oats. The

Poisson's ratio, μ, for the different grains was documented as 0.1 for barley and wheat, and 0.13 for oats. Thompson et al. reported a maximum compressive stress range between 41 to 69kPa (6 to 10psi). They found that the density of the bales was proportional to the maximum compressive stress and that the type of grain had a negligible effect on this result.

2.2.3 STUCCO/PLASTER FACINGS

Facings should be applied to the sides of straw-bale walls both for confinement of the straw-bales and for structural reasons. The choice of plasters for the facings and application methods are variable. Lime- and gypsum-based as well as earthen plasters, such as adobe, are generally applied by hand; Cement stucco can be either applied by hand or pressured sprayed-on to the straw surface. Examples of spray-on systems are Quick Spray (Straw Bale Construction Management, Santa Fe) and pneumatically placed plaster, or gunite (1997 UBC Section 2510). Exterior facings are usually made of cement stucco, primarily because of its longevity, weather resistance, and known properties. However, dry climatic conditions and/or proper plaster stabilization may permit the efficient use of alternate plasters (Steen et al. 1994).

The use of wire reinforcement is an option for providing control of shrinkage cracks, increasing the ductility of the facings and permitting attachment to the framing elements in non-load bearing structures. The reinforcement utilized are usually 16 gauge 1inch-- 25.4mm galvanized woven wire stucco netting and expanded metal lath (ANSI A42.4-1995). The expanded metal lath is used for fastening the woven wire to a perimeter frame in non-load bearing structures. By having the reinforcement attached directly on to the bales, the in-fill straw-bale wall prevents catastrophic collapse when the capacity of the facing is exceeded, both in bearing and non-load bearing structures. Buckling of the facings is also successfully controlled by attachment of the reinforcement onto the bales, greatly reducing the unbraced length of the flat, thin facing "columns". Overall stability

of the wall system is also achieved due the facing's higher stiffness relative to that of the straw-bales.

2.2.4 PRECOMPRESSION METHODS

Creep occurs in straw-bale walls due to the weight of the roof and wall itself. This is a significant problem in load bearing assemblies, particularly if care is not taken to allow the wall to compress down under the roof and its own weight prior to the application of plaster for facings. Some precompression methods have been implemented both to expedite the creep induced on straw-bales by compression from dead loads and to increase the overall stability of inner straw wall (Steen et al. 1994, King 1996).

The first level of precompression is recommended as each course of bales is placed in a running bond. Once a course is laid, an individual should strike down his/her own foot on the bales to aid in the settling of the straw, and lacking the proper engineering terminology, straw-bale construction has adopted the term "stomping" for describing this process (Stafford and Tichy 1996). There will exist a large scatter in the magnitude of the compressive forces applied by this technique, even if done by the same person; Nevertheless, it greatly aids to reduce undesirable settling in the straw-bales (King 1996, Steen et al. 1994).

Extending threaded rods from the foundation through the top, or roof, plate and tightening down bolts once the straw-bales are in place is the most commonly used wall precompression technique in straw-bale construction. Bou-Ali (1993) and Thompson et al. (1993) both used 12.7mm (½in.) diameter mild-steel threaded rods with coupling nuts and washers as required for precompressing the walls they constructed.

Polyester strapping (Carlson Systems, Tacoma, WA) used for commercial packaging is another method of applying precompressive forces to a straw-bale wall. The strapping is run from the foundation of the wall, over the top plate, stretched to some established tension and cinched down securely. Polyester straps have elastic properties and show

brittle failure. Heavy fencing wire, 14 gauge and higher (ASTM A 185) can also be used to apply precompression and is utilized in a similar manner to polyester strapping. Once the desired tension level in the wire is reached, it is maintained by Gripple wire splicers (Gripple Ltd. Sheffield, England). Fencing wire generally behaves elastically, with plastic behavior dependent on the type of steel it is made of. Both of these methods have been used in several projects, but no laboratory testing studies have been carried to determine how efficiently tension is maintained (King, 1996).

Chapman and Platts (1996) have developed a precompression technique in which the 17-gauge stucco wire reinforcement is tightened down to apply a compressive force on the straw-bales. Their technique consists on first loading the wall excessively, beyond any expected long term creep, and then tensioning the wire mesh with hydraulic jacks at the top plate, where it is fastened. Firehouse Ltd. with Scanda Consultants Ltd (1996) tested Chapman and Platts' precompression method on wall panels 2.414m (8ft) high with lime-cement stucco facings. The wire mesh used was 22 gauge 1inch—25.4mm wire mesh (ANSI A42.4-1995) tensioned with approximately 8.8N/m (600lbs/ft). The results of this study are discussed in sections 2.3.2.1 and 2.3.2.2 of the following section.

2.3 STRAW-BALE/PLASTER FACING WALL SYSTEMS

2.3.1 BACKGROUND

Straw-bale construction is separated into separate categories for non-load bearing structures and load bearing type structures.

In a load bearing structure, the straw-bales are used to provide adequate initial support for the weight of the roof. The term "Nebraska style" has been used by straw-bale construction enthusiasts to describe load bearing straw-bale structures because most of the structures dating from the early 20th century were built in Nebraska and were of the load bearing type. The straw-bales tend to compress under the roof load due to their elastic characteristics, and it is common practice to wait some time for compression to

occur before adding confining facings to the sides of the walls. A common practice to ensure uniform settlement throughout the length of load bearing walls is to pre-compress the wall to a considerable degree in order to prevent the weight of the roof and the wall itself from compressing it further. Application of cement, lime or earthen plaster facings to a straw-bale wall provides not only the required confinement for proper straw reliability and longevity, but also makes the wall a "hybrid" structural system. This hybrid wall system needs to provide resistance to both vertical and horizontal forces. The contribution of each of the materials in this wall system to provide adequate shear capacity is dependent on numerous factors (King 1996). Some of these are: Density of bales, bond between straw and facing, thickness of facings, strength of the facings, application method for the facings, use or lack of straw and/or facing reinforcement, attachment of facing reinforcement to straw, wall pre-compression level or lack thereof, etc.

In a non-load bearing structure, the straw-bales primarily serve as an in-fill, insulating material. Straw-bales provide insulation with an average insulation value, R, of about 50, and ranging from R45 to R55, thickness dependent (Bainbridge, 1993). The vertical loads are supported by the framing structure (Such as wood, concrete or steel post and beam systems). Horizontal loads on a non-load bearing straw-bale structure are resisted by the framing structure in combination with the facings and, to a lesser extent, by the straw-bales. The facing is connected to the perimeter of the frame via reinforcing wire. Beyond the factors that affect the shear capacity of a load bearing wall, the rigidity of the connections between posts and beams in the frame, the facing/frame perimeter attachment as well as the material of the framing system need be added to the shear capacity for non-load bearing walls.

2.3.2 LABORATORY RESEARCH

2.3.2.1 VERTICAL COMPRESSION STUDIES

Canada Mortgage and Housing Corporation, or CMHC, (1984) carried out the first laboratory testing program on load bearing straw-bale walls to determine their structural capabilities (CMHC 1984, Hames 1997). The wall unit used was 3.67m (12ft) long by 2.44m (8ft) high by 0.5m (1.6ft) wide. It was a three-string bale load bearing wall without imbedded reinforcement and with 19.05mm (¾in.) thick cement-line-sand mortar facings. The straw-bales were laid flat and stacked on each other, forming columns with spacing in between. This spacing was later filled with joint mortar, which results in a variation of non-load bearing walls, commonly known as "honey comb matrix"wall (Thompson et al. 1993). No mention is made of reinforcement placed between courses of bales. The test wall contained window and door openings, with respective wooden frames. The first structural test carried out was a vertical compression test. The wall unit was subjected to a combined 79kN (17,760lbs) and 3.2kN (719.4lbs) maximum vertical compressive and out-of-plane transverse monotonic force, respectively, without measurable deflection. From the results of their studies, design loads were established for vertical and transverse loading of non-load bearing straw-bale walls, in accordance with the residential construction requirements (CSA A23.3-1978).

Bou-Ali (1993) tested three load bearing straw-bale walls for compressive strength. The walls had no precompression applied nor plaster facings. Reinforcement between courses of bales was provided by #4 A615 steel reinforcing bars with a minimum yield strength, F_y, of approximately 421kPa (60,000psi). The wall units were 3.67m (12ft) long by 2.44m (8ft) high, built with polypropylene-three-string wheat straw-bales, average density of ρ_{ave}=136kg/m^3 (ρ_{ave} =8.5pcf). At a stress level, σ= 33.6kN/m2 (4.88psi), the vertical deflection of each of the wall units was: 175.3mm (6.9in), 193mm (7.6in) and 198.1mm (7.8in). One of the units was reported to deform out of plane noticeably due to the lack of precompression. Bou-Ali calculated that this loading represented (82psf) of

roof load, or a roof area of about $1.49m^2$ per linear meter ($16ft^2$-per linear foot) of wall. He concluded the load capacity of the walls was higher than dead, live and wind loads combined.

Stafford and Tichy (1996) also carried out compressive tests on two load bearing walls made of wheat straw-bales bound with two polypropylene strings. The two wall assemblies had no plaster facings, and precompression was applied with three polyester straps, which had a tensile capacity of (800lbs). The wheat straw-bales were laid flat. The dimensions of the first wall were 3.67m (12ft) long by 2.84m (9.3ft), and 3.67m (12ft) long by 2.51m (8.2ft) for the second one. The vertical reinforcement between course of bales was provided by #4 A615 steel reinforcing bars. The average density of the two-string bales was ρ_{ave}=132.14 kg/m^3 (ρ_{ave}=8.25pcf). The following are the results they reported for this part of their study: The first unit was subjected to a compressive force of 15.9kN/m^2 (333psf), and deflected vertically approximately 101.6mm (4in). At this point the load was released, and the wall rebound to show only 63.5mm (2.5in) of deflection. The polyester straps were tightened, and the load application resumed, up to 18.1kN/m^2 (378psf), and a total vertical wall deflection of 111.7mm (4.4in). As reported, wall unit 1 failed by lateral buckling at this load. The second unit failed in the same manner at a load of 4.3kN/m^2 (89psf) and a total vertical deflection of 12.7mm (0.5in). Stafford and Tichy stated that "stomping" the bales during construction may have ameliorated to some extent the instability of the wall. They also determined that bales have different densities across their width, and that the uncut side is denser and stronger than the cut side.

Chapman and Platts (1996) had structural studies carried out on load bearing straw-bale wall panels to assess the effects of their precompression method. Firehouse Ltd. with Scanda Consultants Ltd (1996) tested wall panels precompressed with Chapman and Platts' method versus wall panels with the standard hand-tightened wire mesh. The wall panels had dimensions 2.41m (8ft) high by 0.92m (3ft) long, and were plastered with

18mm ($^3/_4$in) lime-cement stucco facings. The straw-bales were made of wheat, with an average density of ρ_{ave}=111kg/m^3 (ρ_{ave} 6.9=pcf) and bound by two polypropylene strings each. No reinforcement was used between courses of bales. The wire mesh used for the precompressed panels was 22 gauge 1inch—25.4mm wire mesh (ANSI A42.4-1995), tensioned with approximately 8.8N/m (600lbs/ft). The wire mesh used for the standard panels was 22 gauge 3inch—76.2mm wire mesh (ANSI A42.4-1995). The studies carried out yielded the following results: A vertical compressive load of 65.7kN/m (4500lbs/ft) yielded a deflection of 3mm ($^1/_8$in) in the wall assemblies with no precompression. This load represented the capacity of the testing setup, and thus no further load increments were possible. Chapman and Platts did not test the precompressed panels for compressive strength, assuming their capacity would be much higher than that of the testing setup.

2.3.2.2 LATERAL OUT-OF-PLANE LOAD STUDIES

CMHC (1984) carried out an out-of-plane monotonic transverse load test on the same load bearing wall unit used for their compressive strength study (see section 2.3.2.1). The wall unit was subjected to a combined 3.2kN (719.4lbs) and 79kN (17,760lbs) maximum out-of-plane transverse monotonic and vertical compressive force. The wall did not measurably deflect in neither vertical nor horizontal direction, as reported. From their results, some conservative design loads were established for vertical and transverse loading of non-load bearing straw-bale walls.

Bou-Ali (1993) carried out out-of-plane transverse load tests on three load bearing wall units duplicate to those used for his compressive strength study (See section 2.3.2.1). The wall units were transversely loaded to simulate a wind load of 44.7m/s (100mph), approximately 1.1kPa (23psf), and exhibited no structural failure, with an average maximum displacement of 25.4mm (1in) at the top of the wall. Bou-Ali mentions that longer reinforcing bars would probably improve the transverse capacity of straw-bale walls.

Simons (1993) also conducted tests on four load bearing straw-bale walls to determine the out-of-plane capacity of several wheat straw-bale wall panels. The vertical steel reinforcement consisted of #4 A615 steel reinforcing bars. The load was applied monotonically. Three wall units were 3.67m (12ft) long by 2.44m (8ft) high, with no plaster facings. These panels were loaded up to 1kPa (20psf), resulting in lateral deflections of (1.38in), (0.56in) and (0.37in) at the top of each of the wall panels. A fourth unit with duplicate dimensions had stucco facings applied to both sides and was loaded transversely up to 2.4kPa (50psf) with a deflection of 3.2mm ($^1/_8$in) at the top. Bryce reported that all four units rebounded back with no permanent deformations upon removal of the load. King (1996) concludes from Simmons' studies that the shear transfer between the facings through the straw is considerable, making the wall act structurally as sandwich panel.

Chapman and Platts (1996) had a lateral out-of-plane load test performed on load bearing straw-bale wall panel precompressed with their method. The panels for this test where the same used in the test to determine the vertical compressive strength (See section 2.3.2.1). The wall panel was built with two string wheat bales, with no lateral reinforcement between courses of bales. Lime-cement plaster facings were applied to the precompressed 22 gauge 1 inch—25.4mm wire mesh. Firehouse Ltd. with Scanda Consultants Ltd (1996) applied a monotonic lateral load on the wall unit with no roof load. The stucco facing on the wall showed surface cracks at 6.5kN/m^2 (135psf) but horizontal deformation was only noticeable at a 7.3kN/m^2 (153psf) load.

2.3.2.3 LATERAL IN-PLANE LOAD STUDIES

In-plane loading tests on straw-bale walls without facings have been carried out on both two and three string bale walls. The importance of in-plane tests is crucial for determination of the applicability of straw-bale walls as shear resisting elements for straw-bale structures.

Bou-Ali (1993) carried out in-plane monotonic load tests on three wheat straw-bale load bearing wall units. The properties of the materials, and the dimensions of these wall panels are the same as those used for the compressive and out-of-plane load studies (3.67m (12ft) long by 2.44m (8ft) high by 0.61m (2ft) wide straw-bale wall units with no facings, and with a straw-bale average density of ρ_{ave}=136kg/m^3 (ρ_{ave}=8.5pcf)). However, these wall units were precompressed using three 12.7mm (½in.) diameter mild-steel threaded rods, which were run from the foundation, through the straw-bales and up to the top beam, where the precompression was applied by tightening nuts over the top beam. Each of the walls had a different precompression level applied to it. The first one had the lowest precompression level, the nuts on the three rods being tightened by hand only. The second had the nuts tightened several turns with a wrench. The third had the highest precompression rate, having each of the nuts tightened with a wrench until it was difficult to turn them further. This highest level of precompression is most representative of common practice in straw-bale construction (Steen et al. 1994). Lateral in-plane monotonic forces were applied to the walls by means of a built up wood member as shown in Figure 2. It should be noted that the units used by Bou-Ali were not confined by framing elements; Instead, two 50.8mm x 152.4mm (2in x 6in) lumber sections, used together as a typical precompression top beam, were the only rigid elements incorporated into the wall units.

Figure 2 shows a schematic of how an in-plane point loading generates gradual displacements in a straw-bale wall, while a graphical representation of the measured deformations induced in the plane opposite load application is presented in Figure 3. As seen in the graphical interpretation, the wall's vertical planes have a tendency to deform into a curved shape, confirming the elastic properties of straw-bales. The drift at mid-height (1.22m (4ft)) and roof level (2.44m (8ft)) of the wall units are as shown. The maximum in-plane load applied to the wall units was 2.6kN per horizontal linear meter (178plf). This is equivalent to a shear stress, τ, of 6.6kPa (1psi). The wall with the highest level of precompression, wall # 3, had a top wall displacement of 58.4mm (2.3in).

The period of these wall units was 0.92s. The force was applied by means of a 108mm by 108mm (4in by 4in) wood member pulled against the vertical plane of the wall by means of a wire tensioned with a load by means of a pulley system. All the wall units slipped relative to the floor, since the walls were only confined one the side where the wood member applied the in-plane force, as shown in the wall schematic of Figure 3. The lines shown in Figure 3 have been corrected for the slippage at the floor level. It can be seen from Figure 3 that the deformation effects of the lateral load decay along the length of the wall, since the vertical plane where drift measurements were taken is not planar, particularly noticeable on wall # 3.
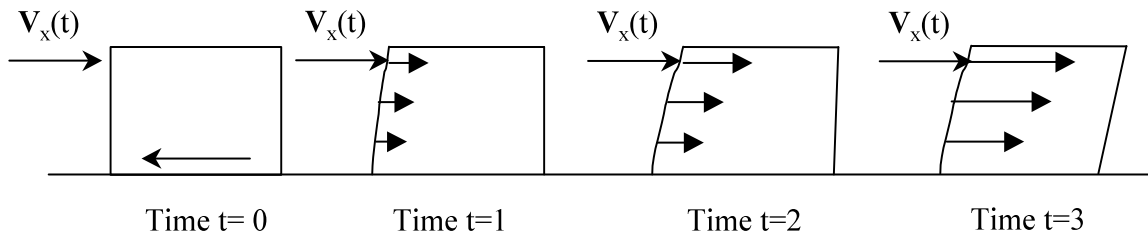
Figure 2: Schematic of Gradual Displacements in a Straw-Bale Wall due to In-plane Loads
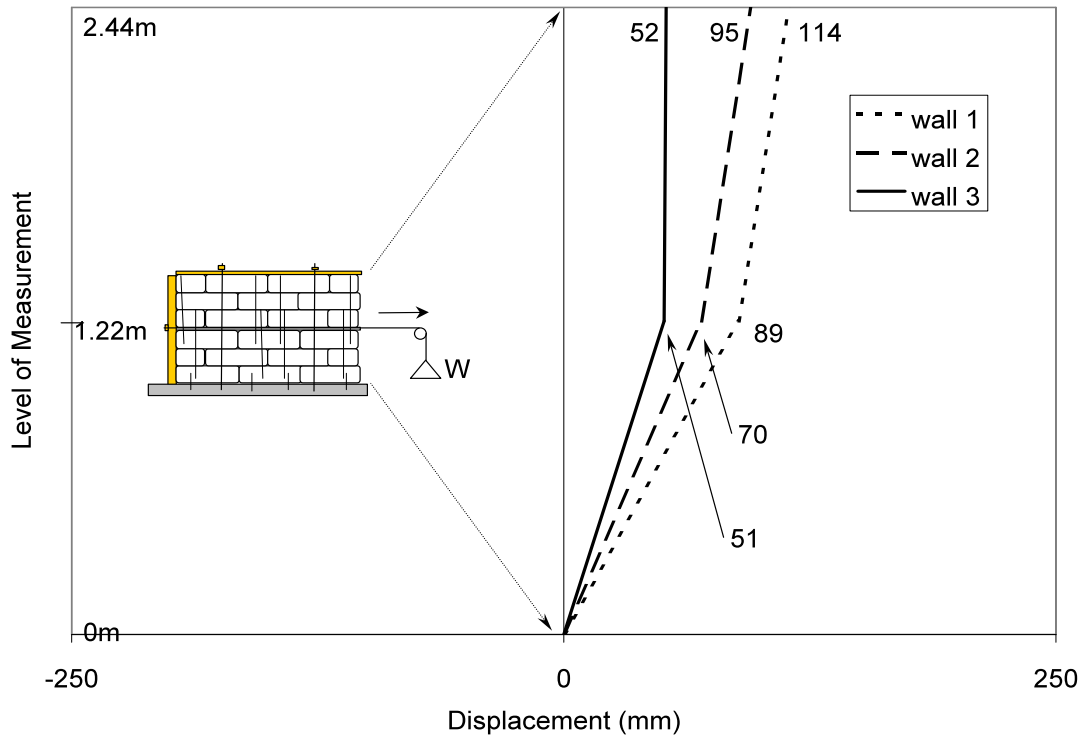
Figure 3: Graphical Representation of Deformation Induced by In-plane Loading on Load Bearing Straw-bale Walls w/out Facings

Figure 4 shows a plot of the lateral in-plane monotonic load/area of wall, τ, versus drift, γ. The idealized elastic response with initial shear modulus, G_i, is also presented in this figure to assess the degradation of the secant shear moduli of the walls, G_s. The secant shear modulus is directly dependent with wall precompression level. The shear stress, τ, at which the secant shear modulus is defined is equal to 4.2kPa (0.6kips), and the corresponding drift, γ, of each of the wall units, is presented in Figure 4.
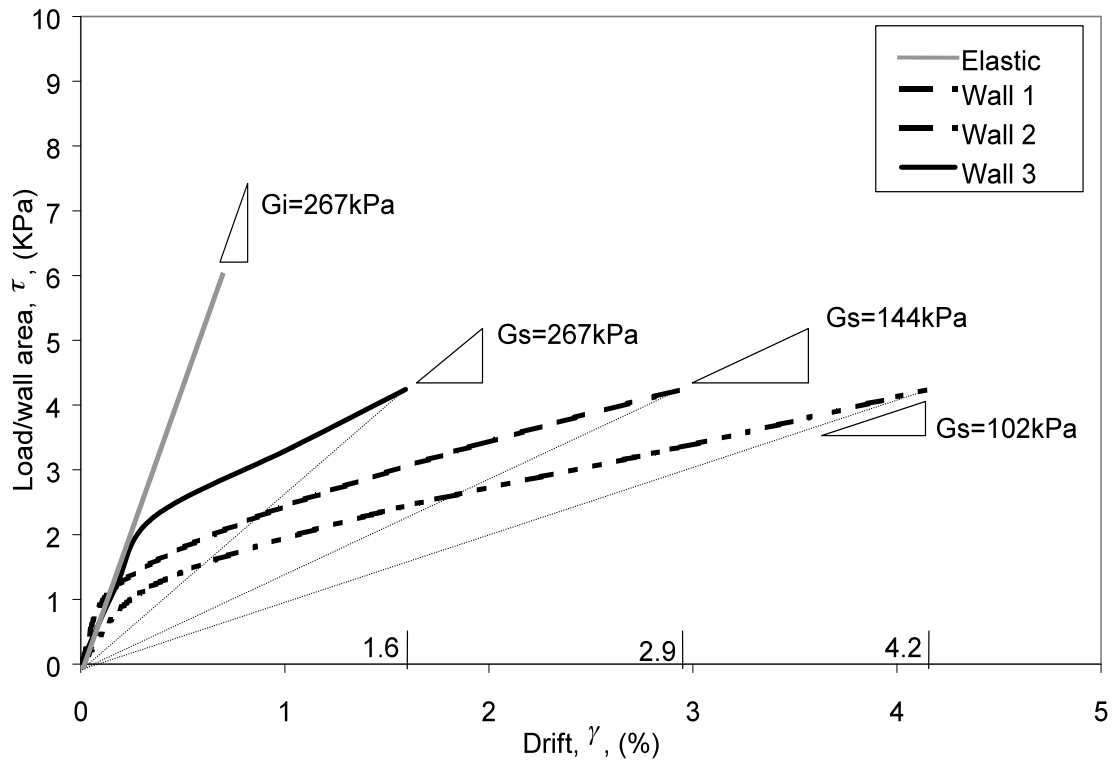
Figure 4: Lateral In-plane Monotonic Load per Area versus Drift

Stafford and Tichy (1996) performed in-plane loading of a 3.67m (12ft) long by 2.84m (9.3ft) high by 0.46m (1½ft) wide load bearing wall. The bales used were two-string wheat straw-bales, average density ρ_{ave}=132.14 kg/m^3 (ρ_{ave}=8.25pcf). Lateral reinforcement was provided by #4 A615 steel reinforcing bars pinning through the courses of bales. The walls had no facings. Precompression was applied by means of three polyester strapping, cinched tightly. The in-plane monotonic load applied was of 3.4kPa (83psf) at a top wall, which yielded a deflection of 146.1mm (5.75in). The period of this wall unit was 0.79s. Stafford and Tichy concluded that the lateral load resistance of their wall unit was limited, and not sufficient to meet building code criteria for one-story buildings in seismic zone 3.

White and Iwanicha (1997) also carried out an in-plane monotonic load test on a lumber post and beam, straw-bale in-fill wall with stucco facings. The wall unit tested was made of three string wheat bales, and had dimensions 2.414m (8ft) long by 1.62m (5.3ft) high by 0.61m (2ft) wide. Lateral reinforcement was provided by #4 A615 steel reinforcing bars pinning through the courses of bales. The strength of the plaster facings was f'_c=1.74kPa (f'_c=253psi). The average density of the bales used for this test was ρ_{ave}=112.12 kg/m^3 (ρ_{ave}=7.0pcf), lower than any of the other reported straw-bale test unit densities. The lumber perimeter frame was built out of TJI (Truss Joist MacMillan, Seattle, WA) wooden components and semi-rigid metal connections for the framing elements. Failure of the wall unit was first detected as the facing wire mesh reinforcement pulled away from the frame elements it was nailed onto. The maximum monotonic in-plane load this unit was subjected to was 54kN (12,300lbs) with a displacement of 29.1mm (1.15in). Subsequent loading cracked the TJI columns and the metal connections failed due to bending and axial stresses. The test was halted after the wall had reached a displacement of 198.12mm (7.8in), at an approximate load of 26.69kN (6000lbs). No recording was made of the loading rate at which the monotonic load was applied. The goal of White and Iwanicha's test was to observe the behavior of the wall and determine the shear capacity and deflection characteristics under monotonic loading.

2.3.2.4 COMPARISON OF RESULTS OBTAINED FOR IN-PLANE LOAD STUDIES

A graphical comparison of the lateral force, τ, plotted against drift, γ, is made for the tests by Bou-Ali (1993), Stafford and Tichy (1996) and White and Iwanicha (1997) in Figure 5. The initial wall system shear modulus, G, secant to the unloading portion of the force-displacement curves, is calculated from the following relationship of the applied lateral in-plane force and the resulting drift:

$$G = \frac{Force}{A_{wall} \cdot \gamma} \quad\dots\dots\dots\dots\dots\dots\dots\dots\dots\dots\dots\dots\dots\dots\dots(2.1)$$
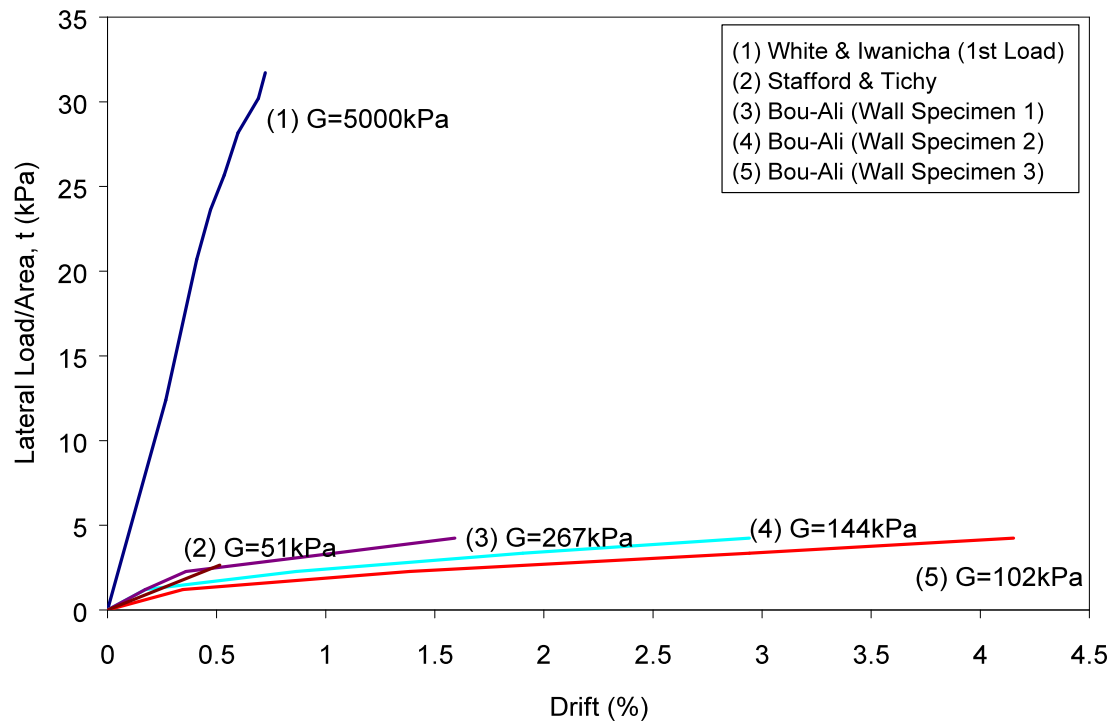
Figure 5: Comparison Lateral In-plane Force Vs. Drift for Previous
Studies

2.3.3 FIELD RESEARCH

2.3.3.1 BACKGROUND

Field experiments of straw-bale construction are limited. Most structures are built according to standard practice, following guidelines and suggestions from previous projects, but seldom are they monitored or instrumented. Numerous houses stand as testimony of the durability and adequate structural performance of straw-bale construction. Of particular interest are one-and two-story houses found in Nebraska, still structurally sound and inhabited, dating close to or before the 1900's (Eisenberg 1995, Hames 1997, King 1996).

2.3.3.2 VERTICAL COMPRESSION STUDIES

Smith, Theis and Swearingen (1994) applied and monitored a compressive vertical load on a load bearing straw-bale wall at the Shenoa Retreat and Learning Center cottage at Philo, CA. The straw-bales used were made of rice straw from California and bound by three strings. The dimensions of the wall were 3.67m (12ft) long by 2.44m (8ft) high by 0.6m (2ft) wide. The wall was precompressed 99mm (3.9in) by tightening three 12.7mm (½in.) diameter mild-steel threaded rods with a wrench. Then, the precompression was released to construct the test setup on the wall. Prior to the application of the stucco facings, the wall was subjected to a series of successively increasing loads, up to a maximum compressive load of 771N per linear meter (636lbs per linear foot), equivalent to a shear stress, 22.9kPa (3.3psi). The wall deflected 88.9mm (3.5in) at this maximum load, corresponding to a strain, ε, of 3.7%. The intent of this loading regime was to simulate loading and unloading of live loads. Wire mesh and 22.2mm ($^7/_8$in) thick stucco plaster facings on either side were applied, and the same load was reapplied to the wall for 96hours. No measurable deflections occurred, and no adverse effects were observed on the stucco facings (King 1996, Steen et al. 1994).

2.3.3.3 LATERAL OUT-OF-PLANE LOAD STUDIES

Luecke (1994) built a 5.5m (18ft) by 11m (36ft) studio in Boulder, CO. It is a load bearing structure, with a shed roof. The walls were precompressed with polyester strapping, rated at 4.7kN (1050lbs), and tensioned by hand tools. The placement of the strapping was at every 0.9m (3ft). The walls have plaster facings on either side. The studio has successfully stood wind loads in excess of 161kph (100mph) since built (King 1996, Steen et al. 1994).

Other examples of qualitative out-of-plane load field studies: The Real Goods Solar Living Center (Hopland, CA) and Twila Ard's house (Pensacola, FL) resisting windstorms and a hurricane, respectively.

2.3.3.4 LATERAL IN-PLANE LOAD STUDIES

The author of this thesis is not aware of any documented quantified in-plane load field studies for neither load bearing nor non-load bearing straw-bale structures. Qualitative evaluations of the resistance to in-plane loading can be made from numerous houses in seismically active zones, particularly those which have survived earthquakes in California. Bruner's (Douglas, WY) house resisted a 5.5 Richter-magnitude earthquake, at an epicentral distance of 33 miles (Steen et al. 1994).

2.4 OVERVIEW AND RANGES OF STRAW-BALE WALL STRUCTURES

There was no one standard before 1994, but structures were approved in an ad-hoc basis.

The largest interior area for a built straw-bale non-load bearing structure is $4645.5m^2$ ($5000ft^2$) (Fundación de Apoyo Infantil, Ciudad Obregon, MEXICO); for a non-load bearing structure, the largest area is $278.7m^2$ ($3000ft^2$) (Dorothy Nolan Senior Center, Florence, AZ).

The highest non-load bearing wall rises 9.4m (31ft) (Schwaesdall Winery Tasting Room, Ramona, CA). The tallest code-approved load bearing walls this author found, 3.1m (10ft) high, are those found in Michael and Spring Thomas' home in Port Townsend, WA. Probably the tallest load bearing walls overall are found in a two-story 1928 church (Pilgrim Holiness Church, Arthur, NB). The author of this thesis estimates the height of these walls as 6.4m (21ft) from a picture of the structure.

2.5 CODE REQUIREMENTS

2.5.1 LOCAL BUILDING CODES

2.5.1.1 BACKGROUND AND GENERAL REQUIREMENTS

The first building code to incorporate straw-bale construction was the City of Tucson Pima County Arizona Building Code (CTPCAZBC) in 1994. The inclusion of straw-bale

requirements was added as Appendix Chapter 72. Subsequently, other state legislatures, such as New Mexico an Texas, have used the CTPCAZBC as a model for their own proposed building codes.

The design parameters for load bearing and non-load bearing structures are different and some legislatures approve only the use of straw-bales for non-load bearing designs (NMBC, for example). The California 1995 Proposed Guidelines for Straw Bale Construction (CAPGSBC) have suggested building requirements that vary in some respects to those specified in the CTPCAZBC appendix. The CTPCAZBC and CAPGSBC are the guidelines most straw-bale structural designs are based on.

All existing and proposed codes require straw-bales to have a minimum density of $\rho_{min}=112$kg/m^3 ($\rho_{min}=7.0$pcf), a moisture content not to exceed 20% at the time of installation and a minimum dimension of 330.2mm (13in).

2.5.1.2 STRUCTURAL REQUIREMENTS FOR LOAD BEARING STRAW-BALE STRUCTURES

Straw-bales are to be laid flat and stacked in running bond for load bearing designs, which are limited to one story. The CTPCAZBC and the CAPGSBC specify 356mm (14in) as the nominal minimum bale wall width. The Arizona codes limit the unsupported length to width ratio for a load bearing wall to 13:1, while the code contemplated for California allows a 15.7:1 ratio. The wall height is limited by a height to width ratio of 5.5:1 under the CTPCAZBC while CAPGSBC suggests a 5.6:1 ratio.

The Arizona County's codes limit the allowable roof load to 17.24kPa (360psf) based on the vertical load requirements from Chapter 19 of the 1997 UBC, while the proposed California code allows 19.15kPa (400psf) as the maximum vertical roof load. Two #4 A615 grade 60 steel reinforcing bars (ASTM A615), with a minimum tensile strength of 421kPa (60,000psi), per bale are specified for pinning, and must be long enough to extend through four courses. There is an agreement by the mentioned codes that the horizontal shear resistance of a straw-bale wall should be determined according to

equation 14-1 in Chapter 19 of the 1994 UBC. This equation is presented here for reference.

$$Fp = (Z \cdot I \cdot C_p / R_w) \times W_{DL} \ldots\ldots\ldots\ldots\ldots\ldots\ldots\ldots(2.2)$$

The value obtained need not exceed the shear value of 2628 N/m (180lbs/ft) specified in Table 25-I (1994 UBC, Chapter 25) for the use of vertical diaphragms of lath and plaster. Hence the codes require the shear resistance be developed by the plaster facings alone. Plaster facings with proper wire reinforcement are required for all load bearing straw-bale walls. The codes permit the use of earthen, lime-based or cement-based plasters for exterior and interior facings.

2.5.1.3 STRUCTURAL REQUIREMENTS FOR NON-LOAD BEARING STRAW-BALE STRUCTURES

Few differences exist in the guidelines concerning the use of straw-bales for non-load bearing designs in the mentioned codes. The main difference is that bales are expected to "hold themselves up," serving only as insulation and in-fill material.

The CTPCAZBC and the CAPGSBC allow bales to be either laid flat or on-edge. The NMBC requires bales be laid flat, in a running bond and reinforced with at least two #4 A615 reinforcing steel bars per bale. It specifically restricts wall dimensions to 3.67m (12ft) in height and 6.11m (20ft) for unsupported lengths (Section 1). It also requires a minimum wall width of 457.2mm (18in), and makes reinforcement for the facings optional (Section 2). The post and beam frame around the in-fill straw-bale walls must be designed to carry all vertical and horizontal loads, as specified in Chapter 23 of the 1997 UBC, in addition to the provisions pertinent to the material selected for the frame. The structural requirements of the local building codes mentioned are tabulated below.

Table 1: Local Building Code Requirements for Straw-Bale/Facing Construction

Code	Structural System[*] Permitted	Minimum density/ Moisture Content	Maximum Roof Load Allowed	Minimum Wall Width	Maximum Wall Height	Maximum Unsupported Wall Length

CAPGSBC (1995)	LB & NLB	ρ_{min}=112kg/m^3 moisture ≤ 20%	LB-19.15kPa NLB-Not specified	356mm	LB- (H:W Ratio) 5.6:1 NLB- Not specified	LB-(L:W Ratio) 15.7:1
CTPCAZBC (1994)	LB & NLB	ρ_{min}=112kg/m^3 moisture ≤ 20%	LB-17.24kPa NLB-Not Specified	356mm	LB-(H:W Ratio) 5.5:1 NLB- Not specified	LB-(L:W Ratio) 13:1 NLB- Not specified
NMBC (1994)	NLB (only)	ρ_{min}=112kg/m^3 moisture ≤ 20%	NLB-Refers to the latest edition of UBC	457mm	NLB- 3.67m	NLB-6.11m

*LB (Load Bearing)
*NLB (Non-Load Bearing)

2.5.2 UNIFORM BUILDING CODE (UBC)

The UBC (ICBO 1997) lacks a specific section defining the use of straw-bales as a building material. Sections 104.2.8, 105 and 107 permit the use of straw-bales as an alternative material to those specifically prescribed in the code (Concrete, steel and wood, for example) based on approval by a building official. The UBC uses a linear design based on the inelastic response of typical structures, reducing the elastic earthquake forces by a numerical reduction coefficient factor, R.

Chapter 16, Division III requires all structures to have a minimum resistance to seismic ground motions on a site-specific basis. One- and two-family dwellings in seismic zone 1 are the only structures exempt from the UBC requirements of this Chapter. Under these provisions, the minimum design seismic forces may be calculated by the static lateral-force procedure. The straw-bale structure must be capable of resisting the base shear (V), period (T), vertical (V_x) and horizontal (F_t, F_x) distribution of forces, torsional and overturning moments, determined following the outlined design procedure in Chapter 16. The elastic story drift limitation is 0.025 of the wall height for most straw-bale structures, as they generally have a period T< 0.7s (per section 1630.10.2).

The maximum design shear value stucco facing, idealized as a very thin and slender wall of stucco, can be subjected to, is 2628 N/m (180lbs/foot). This shear value assumes an overall facing thickness of 22.23mm ($^7/_8$in) and properly attached wire reinforcement to the base material by means of a sufficient number of nails or screws correctly spaced out, as outlined on Chapter 25. The UBC (1997) requires the stucco/plaster facing be not the main shear resistance element due to its brittle behavior. Lateral resistance is provided directly by masonry or wood lumber in ordinary construction with plaster facings as finishes. In these ordinary types of construction, if failure is observed, it is associated with cracking of the facing.

2.5.3 NATIONAL EARTHQUAKE HAZARD REDUCTION PROGRAM (NEHRP)

The 1997 fifth edition of the NEHRP Recommended Provisions for Seismic Regulations for New Buildings (FEMA 302, 1998) uses a performance based design criteria so that the structure will meet specific performance objectives under specified levels of shaking.

For regular one- and two-family dwellings of light frame construction specific design of the low level seismic zones may be exempt from FEMA 302 provisions. Any other structure may be designed using the recommended provisions. The use of straw-bales is permitted as "an alternative material and method of construction to those prescribed…. (if) Substantiating evidence demonstrates that the proposed alternate, for the purposes intended, will be at least equal in strength, durability and seismic resistance" (NEHRP Section 1.5, 1997).

Under the FEMA 302 provisions, straw-bale structures will generally be contemplated in Seismic Exposure Group I. An analysis procedure is selected for the structure, based on the corresponding Seismic Performance Category.

If the equivalent lateral force procedure is followed, the seismic base shear (V), period (T), vertical distribution of seismic forces (F_x), and horizontal shear distribution of (V_x), as well as torsional, and overturning moments are calculated. FEMA 302 sets the story drift

limitation to $0.025 \cdot h_{sx}$, where h_{sx} is the story height below level *x,* for structures in Seismic Exposure Group I.

The provisions also mention that no drift limit should be set for one-story structures in which the interior walls, partitions and all other structural elements have the capacity to accommodate the story drifts (NEHRP Table 2.2.7, 1997). However, it is not certain that every element in a straw-bale-based structure can accommodate all levels of roof drifts, so it is a conservative approach to limit the story drift to $0.025 \cdot h_{sx}$.

2.5.4 SEISMIC EVALUATION AND RETROFIT OF CONCRETE STRUCTURES (ATC-40)

ATC-40 of the Applied Technology Council (Report No. SSC 96-01) uses a displacement-based approach for structures. The damping used by this approach is related to the energy dissipation of the structure. The spectral acceleration versus spectral displacement capacity spectrum corresponding to a structure's capacity curve is plotted in an Acceleration-Displacement Response Spectra (ADRS) format, and compared with the 5% damped and reduced response spectra. A bilinear representation of the envelope curve, based on the capacity spectrum is required to determine if a performance point exists with respect to the reduced demand spectra. A performance level is established based on meeting determined seismic demands through inelastic structural capacity. The structural design is based on the spectral acceleration and displacement corresponding to the intersection of the bilinear representation of the structure and the reduced response spectra.

CHAPTER 3: MATERIAL PROPERTIES

This chapter describes tests carried out to determine the properties of the materials used for the construction of the straw-bale/facing wall models used for this study.

3.1 STRAW-BALES

The straw for the wall units was obtained from wheat grains. Both two and three polypropylene string bales were used. The three string bales made in eastern Washington State, and had an average density of ρ_{ave}=141kg/m^3 (ρ_{ave} =8.8pcf), while the two string bales came from the Olympic Peninsula area, with an average density of ρ_{ave} = 115kg/m^3 (ρ_{ave} =7.2pcf). The three string bales used were 1% and 23% more dense than the average of those used by Bou-Ali (1993) and White and Iwanicha (1997), respectively. The two string bales were 15% less dense than those used by Stafford and Tichy (1996). The straw-bales were allowed to air out in the University of Washington Structural Engineering Testing Laboratory, prior to construction of the wall units. Only one of the three string bales used was moist at the time of wall construction. The average width and height dimensions of the three string bales were 558.8mm x 419.1mm (22in x 16.5in) while those of the two string bales were 469.9mm x 368.3mm (18.5in x 14.5in).

When half bales were needed, a straw needle was used to insert either polyester or metal packaging straps at the point were the bale was going to be separated. These new ties were tied tightly and secured around the potential half-bale and only then were the original polypropylene ties cut and the bales split. In this manner, half-bales were obtained that replicated as closely as possible the compression and density of the original bale. Some full bales were also retied because the polypropylene ties had lost their tension.

Figures 6 and 7 show an elevation view of the straw-bale in-fill wall, showing the dimensions and density of the bales.

22.5"x28"x16" weight: 47lbs density: 8.0 pcf	45.5"x22"x16.5" weight: 82lbs density: 8.5 pcf	20.5"x22"x15.5" weight: 39lbs density: 9.6 pcf

Approx 8' Straw wall

46"x 22" x16"
weight: 78lbs
density: 8.3 pcf

43"x22.5"x16"
weight: 82lbs
density: 9.1 pcf

23"x22.5"x17"
weight: 48lbs
density: 9.4 pcf

47"x22"x16.5"
weight: 93lbs
density: 9.7 pcf

22.5"x22.5"x16.5"
weight: 46lbs
density: 9.5 pcf

48"x22.5"x17"
weight: 101.5lbs
density: 9.6 pcf   (moist)

47"x22"x16.5"
weight: 78lbs
density: 7.9 pcf

23.5"x22"x16.5"
weight: 44.5lbs
density: 9.0 pcf

46"x22"x16.5"
weight: 87.5lbs
density: 9.1 pcf

23"x 22.5" x16"
weight: 39lbs
density: 8.1 pcf

47.5"x22"x16.5"
weight: 74.5lbs
density: 7.4 pcf

44"x22"x16.5"
weight: 83.5lbs
density: 9.0 pcf

Approx. 8' wall base

Figure 6: In-fill Wall Elevation Schematic (Three-string Bales)
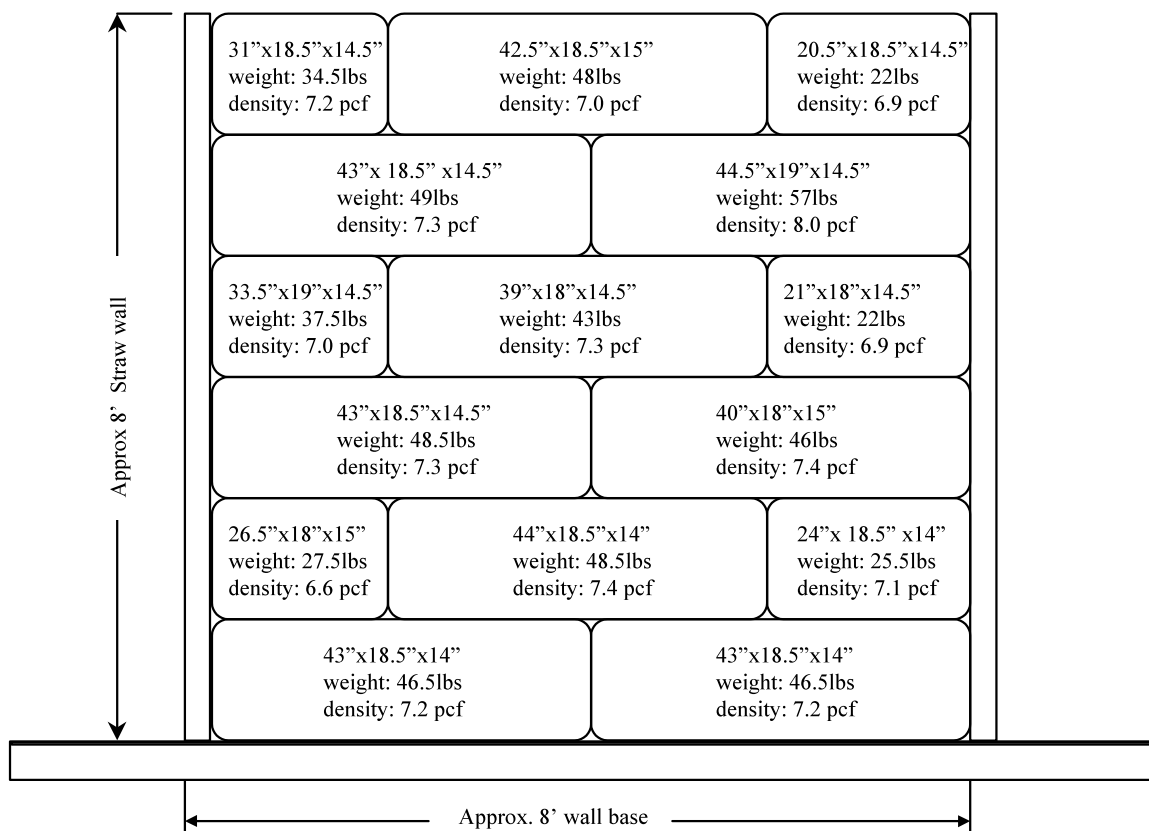
Figure 7: In-fill Wall Elevation Schematic (Two-string Bales)

3.1.1 COEFFICIENT OF FRICTION OF STRAW

A series of 19 tests were performed with two string straw-bales. Two bales laid flat were placed on top of each other, as shown in Figure 8. The lower bale was restricted from moving horizontally, while a horizontal load was applied to the top bale until the friction between the two was overcome and the top bale moved with respect to the lower one. The horizontal load was applied by means of an Enerpac 266.9kN (60kip) capacity hydraulic actuator ram model RCH302 OF6 (Enerpac Hydraulic Equipment, Clinton, WA). The pressure required for the ram was provided by means of a hand pump. The rate of horizontal load application was gradual, but the use of a manual pump prevented the loading rate from being quantified. The maximum load values were read with a voltmeter from the output produced by a 22.24kN (5kip) capacity "S" load transducer cell (Interface Inc. Scottsdale, AZ), previously calibrated (See Appendix A for calibration

curve). Additional vertical loads were applied to the top bale to get more representative values. This added load varied from 0kN to 1.085kN (0lbs to 244lbs). The coefficient of friction was calculated as the ratio of horizontal to vertical load required to slide the top bale.

The test setup avoided miscalculations by using a voltmeter (Fluke Inc.) with a maximum voltage reading function. In this manner, the highest voltage differential from the load transducer cell was recorded and stored. The friction coefficient of straw, (μ_{straw}), was found experimentally as μ_{straw}=0.615. Figure 8 shows a schematic of the test setup, while Figure 9 shows the scatter of voltage maxima scaled to represent the loads. Table A1 in Appendix A tabulates the actual data obtained from the test.
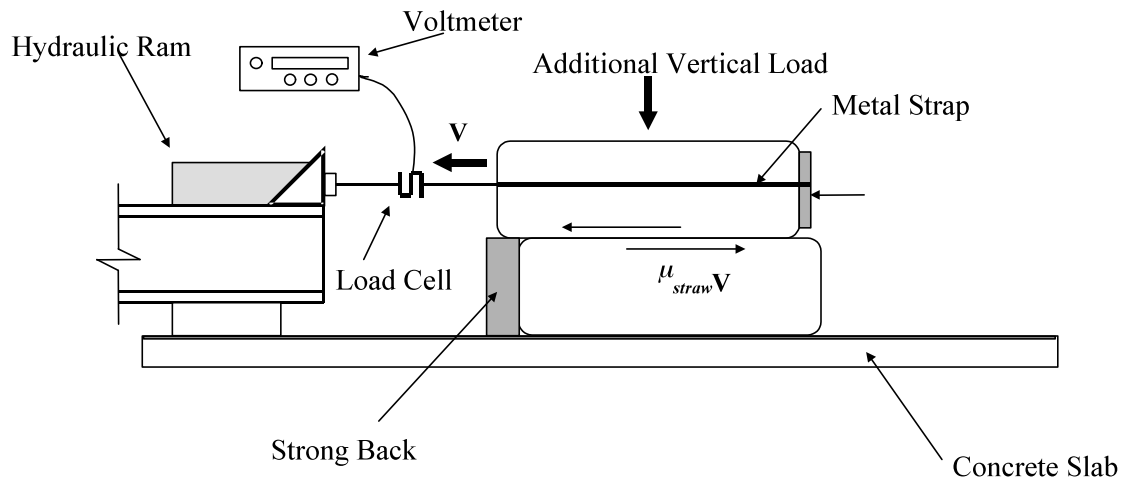
Figure 8: Test Setup for Determination of Coefficient of Friction, μ_{straw}
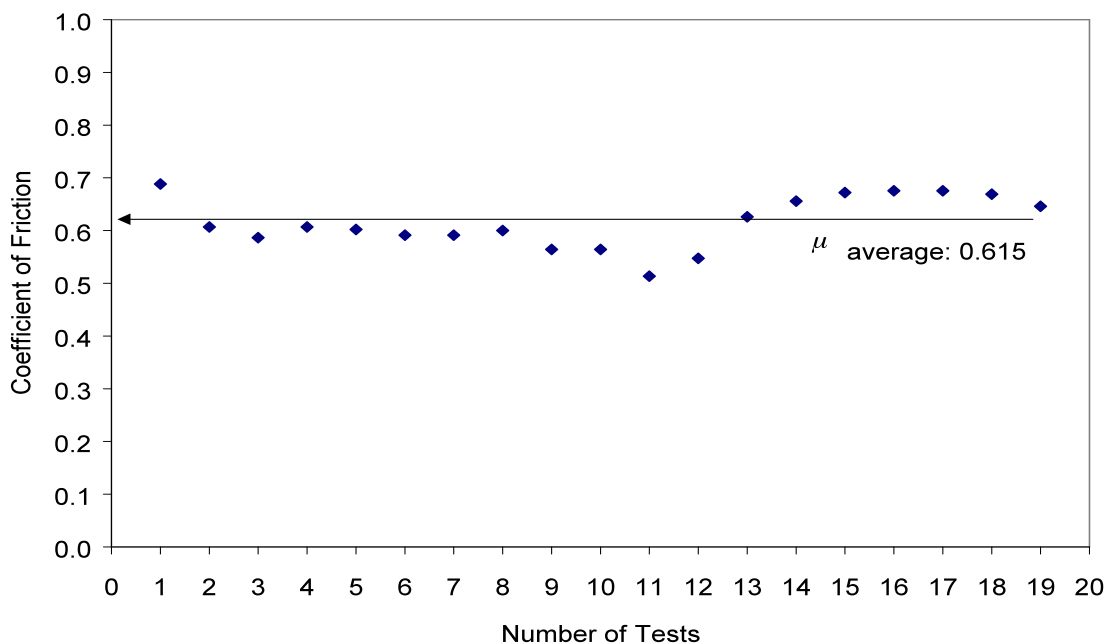
Figure 9: Scatter of Data Obtained from Coefficient of Friction Test

3.2 FACINGS

The facings that were used as confining sides to the straw-bale in-fill in the test units were intended to replicate those commonly used in straw-bale structures. Cement stucco and gypsum-based plaster were selected as the facing materials, represents the typical exterior and interior finishes, respectively. The cement stucco was mixed in a mortar mixer and was made of a mixture of approximately 1 part masonry cement, 3 parts sand and enough water for a proper consistency, adjusted by the plasterer. The plaster mixture consisted of approximately 1 part gypsum based plaster, 2 parts sand and sufficient water for the correct consistency. Approximately 10g (0.02lbs) of 25.4mm (1in) chopped polypropylene fibers was added to both mixtures for crack control. The mixing proportions conform to those specified in Chapter 25 of the 1997 UBC. Even though the weights of the solid mixture components were measured before mixing, the volume of water added varied by as much as 7.570l (2gal), as requested by the master plasterer for

appropriate application consistency. Confining plaster facings are commonly applied to the straw-bale/woven wire surface either by hand application or machine sprayed-on. The wall units had facings applied by hand, the more traditional method used in the field.

The thickness of the facings varied throughout the wall due to the non-planar surface area and dissimilar dimensions of the straw-bales on which it is applied. Thickness measurements were obtained during the demolition process of the test walls, and it was observed to vary from 50 to 100mm (2 to 4in) for both of the coats applied, dependent on the width dimension of the straw-bales at that particular section of the wall. For calculation purposes, an average thickness of 50.8mm (2in) was assumed for both facings on both wall units.

3.2.1 COMPRESSIVE STRENGTH AND THICKNESS OF FACINGS

Sample 50 x 50mm (2 x 2in) cubes of the stucco and plaster mixtures used for the facings were obtained at the time of their application to the wall units. They were allowed to cure for the same time as the wall units (10days) before testing and in the same ambient conditions. The cubes were tested in compression with a 1334kN (300kip) capacity Baldwin universal hydraulic testing machine to obtain the effective compressive strength of the materials. The compressive force was applied to the cubic samples at a rate of 22.2kN/min (5000lbs/min). Table 2 summarizes the compressive strength of the facings applied on both wall units. Since there was a variation in the volume of water added to the mixtures, the values shown in Table 2 represent an upper bound of the actual strength of the facings.

Table 2: 10 Day Compressive Strength of Facings

	Three String Bales Unit 1	Two String Bales Unit 2
Facing Applied	f'_c MPa (psi)	f'_c MPa (psi)

Stucco, Layer 1	14.5 (2100)	13.4 (1950)
Stucco, Layer 2	17.9 (2600)	9.7 (1400)
Plaster, Layer 1	7.4 (1075)	6.8 (990)
Plaster, Layer 2	No Sample Taken	4.8 (700)

Facing thickness values were obtained during demolition of the walls. The values varied randomly along the length of the wall, due to the uneven vertical surface of the straw-bale in-fill wall. Because of this variability, an average thickness value of the stucco facing for both walls, approximately 35mm (1.4in), will be used for calculation of the area of the facings, A_{wf}, in Chapter 8.   Figure 10 shows an elevation schematic of approximately where thickness readings were obtained and Table 3 tabulates the values from each unit.

Figures A7, A8 and A9 in Appendix A are photographs of several of these measurements taken during demolition of the test units.
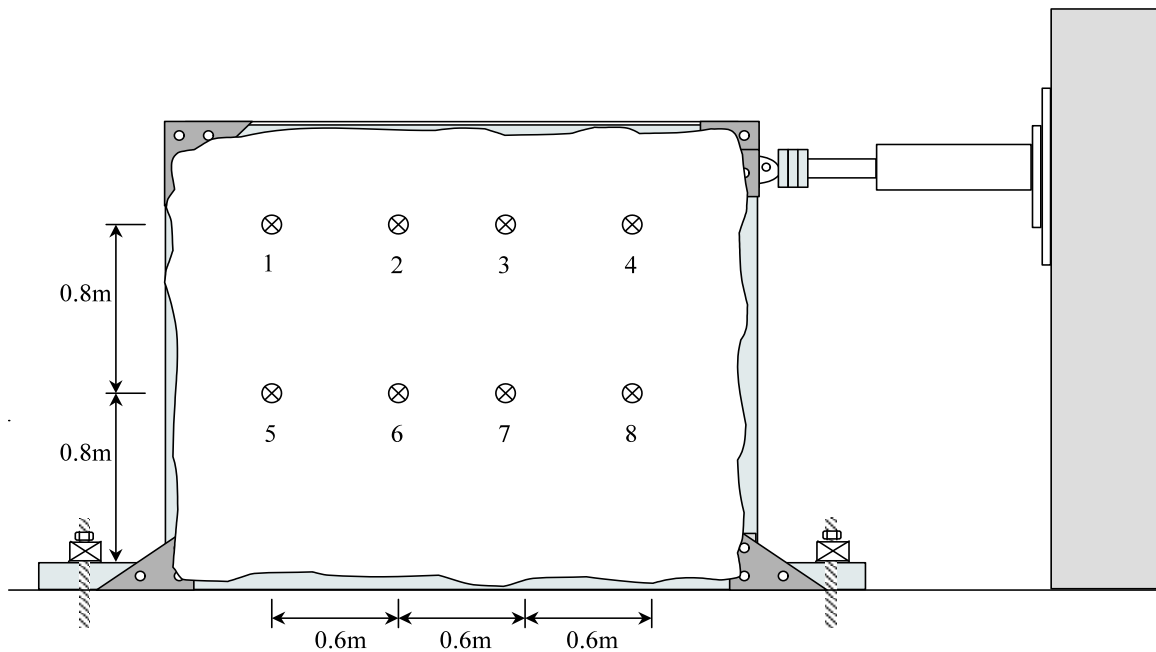
Figure 10: Elevation Schematic of Test Unit

Table 3: Thickness of Facings for Test Units

	Test Unit 1	*Test Unit 2*
Measurement Point	Stucco Facing Thickness (mm)	Stucco Facing Thickness (mm)
1	19	25
2	25	19
3	62	40
4	20	51
5	50	32
6	38	67
7	45	19
8	19	28
Average Thickness-	34.8	35.1

3.2.2 FACING REINFORCEMENT

The main reinforcement used was 17-gauge galvanized woven wire stucco netting reinforcement (ANSI A42.4-1995). A galvanized expanded metal lath (ANSI A42.4-1995) was also used at the connection between bales and columns of the frame. These metal meshes had a tendency to bow away from the straw, so 4, 16-gauge wire ties were passed through each course of straw-bales tying both wall sides of reinforcement together to keep a 6.35mm to 19.05mm (½in to ¾in) distance between the wire and straw (ASTM A 185). The plaster mixtures were applied through the wire and lath and into the straw. The wire could not be seen after the first coat was applied. Attachment of the reinforcement to the perimeter frame was carried out with 38.1mm (1½in) nails at a spacing of 152.4mm (6in), as required in Chapter 25 of the 1997 UBC.

3.3 STRAW/STUCCO FACING SHEAR CAPACITY

The shear capacity of the bond between straw and stucco was also evaluated independently from the full wall unit tests. Stucco facings were individually applied to several two and three string straw-bales. Two application techniques were used to test the variability, if any, of bonding between the two materials due to the application technique. They were "hand-applied" and "machine sprayed-on."

A wooden testing frame was used to apply lateral force to the stucco finishes. Figure A6a in Appendix A shows the test setup, while Figure A6b shows a picture of a test unit ready to be tested. Some of the stucco finishes on the units were sanded down to obtain an almost planar horizontal surface for an approximate distributed loading. Some other more uneven finishes had layers of "hydro-stone" added to create an almost planar surface for an approximate distributed vertical loading along the length of the stucco facing. The shear force was applied in the plane of the stucco/straw bond, replicating the shear load applied to the wall units by means of a 10.68MN (2400kip) capacity Baldwin compression hydraulic testing machine. The compressive plate of the Baldwin machine was fit with two 12.7mm (½in) diameter A36 steel rods, with a 101 by 101mm (4 by 4in) Douglas fir lumber section fitted on these rods for load distribution on to the shear plane (See Figure # in Appendix A). An A36 steel angle section was used to distribute the downward vertical force on the facing. The 22.24kN (5kip) S load transducer cell mentioned previously was used to measure the load values. This load cell was placed on a plate for stability and an MTS swivel (MTS Systems Corp. Minneapolis, MN) was placed on top of the cell to mitigate possible eccentricities as the load was applied. The frame was fit with two rollers to prevent the facing from being pushed out and away from the straw by the moment caused by the vertical load due to the difference in materials stiffness and possible eccentricities. The use of the rollers therefore allowed the collection of values, which represent the shear capacity of the materials with fewer influences from the eccentricities generated by the load. The rollers were placed at $^2/_3$ the height of the facing face. The straw-bales were impaled on two 12.7mm (½in) diameter

all-threaded mild steel rods protruding from the frame, making sure the facing was in contact with the rollers previous to the load application. The load was applied at rate of 444.8N/min (100lbs/min) and each unit was loaded until appreciable yield in shear was observed. The displacement of the facings relative to the straw-bales was not measured.

The maximum voltage values reported by the load transducer cell were recorded with a voltmeter (Fluke Inc.). The equivalent load values were obtained from the load cell calibration curve (See Figure A3, Appendix A) and the shearing stress was calculated from the approximate facing surface area of each unit. The average shear stress capacities determined experimentally for the two methods of application on the two types of straw-bales is presented on Table 3. The complete list of results is presented in Appendix A. It was noticed that a difference existed associated with the side of the straw-bale to which the facing cover was attached. The number of tests ran, however, were not sufficient to quantify whether the cut or the uncut side offered greater shear resistance. It was observed that the better bonding occurred with the cut side, as the facing covers detached after the tests had a higher quantity of straw bonded to them. However, this could not be correlated as a significant factor in the resistance obtained.

Table 4: Shear Resistance of Straw with Stucco Facings

Facing Application Method	Side of Bale Facing Applied On	Number of Ties per Bale/ Type of Tie	τ_{max} kPa
Sprayed-on	Cut	2/ Polypropylene	14.6
Sprayed-on	Cut	2/ Polypropylene	31.0
Hand Applied	Cut	2/ Polypropylene	27.3
Hand Applied	Cut	2/ Polypropylene	27.2
Sprayed-on	Cut	3/ Polypropylene	23.1
Sprayed-on	Cut	3/ Polypropylene	23.4

| Hand Applied | Un-Cut | 3/ Polypropylene | 30.4 |
| Hand Applied | Un-Cut | 3/ Polypropylene | 42.1 |

From the results obtained it can be concluded that hand applied stucco, worked well into the straw, provides a higher shear capacity than sprayed on stucco.

3.4 PRECOMPRESSION MATERIALS

The weight of the roof box beam, approximately 333.6N (75lbs), was the second form of pre-compression applied to the in-fill wall following the "stomping" procedure after each course was laid (King 1996, Stafford and Tichy 1996).   A12-gauge heavy fencing tie wire (Kiwi Fence Systems Inc. PA) ran from the base box beam and over the roof box beam and fastened to the other end by means of a gripple wire splicer (Gripple Ltd. Sheffield, England). Three of these tie wires were used, and each side was tensioned with approximately 1.1kN (250lbs) of force, applied by means of a tensioning tool compatible with the gripple splicer. Figure 11 shows the placement of these wires with respect to the rest of the wall. The rated strength of the tie wires used is to 2.2kN (500lbs). With these wires tensioned in place, the total precompression applied to the straw-bales was approximately 1.4kN (575lbs).
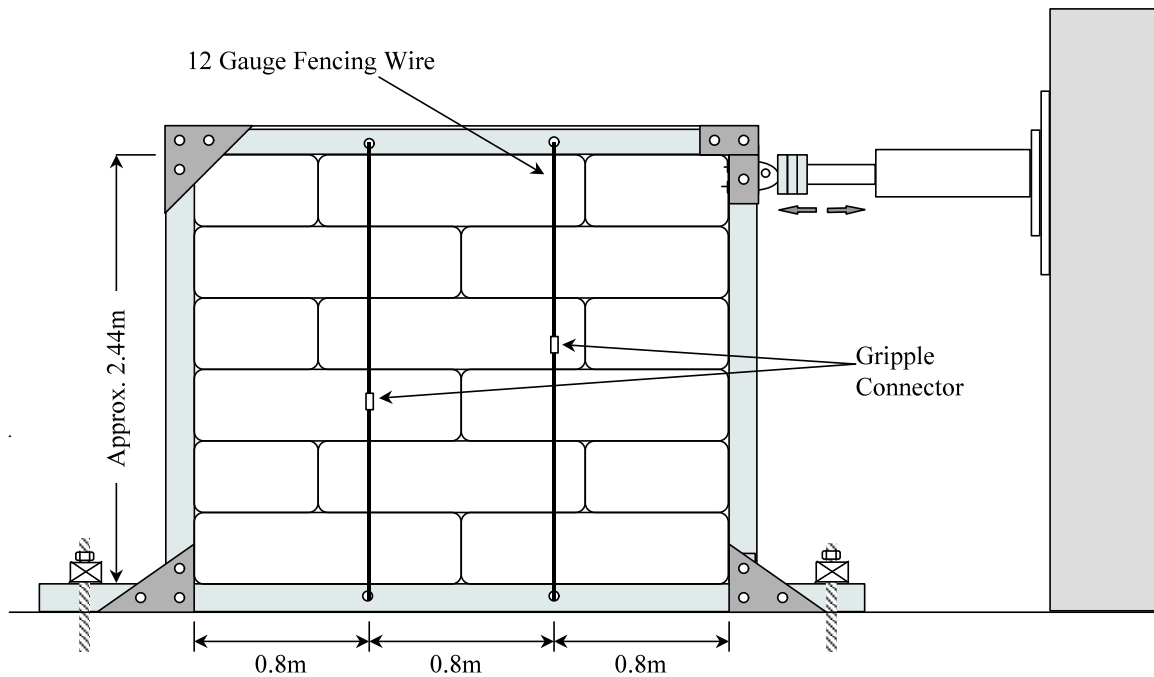
Figure 11: Schematic of Precompression Tie Wire Placement on Straw-Bale In-fill Wall

Several attempts were made to install the smallest strain gauge available to the author directly on the tie wires, which would permit accurate calculation of tensile stress readings before, during and after the tests. The greatest difficulty faced was inadequate bonding: The wire's curved surface did not allow the strain gauge to fully adhere. Secondly, the tie wires' small diameter induced multiple bends along its entire length, which made it difficult to locate almost straight sections to position the strain gauges. A higher level of manual pressure was applied to the gauge installation procedure, in an effort to improve the bonding; however, as a direct result of this increased pressure, the wire length selected for installation would bend and render the gauge installation useless. These factors made the use of strain gauges on the tie wires impossible. At the maximum horizontal roof displacement the wall units were subjected to, 75mm (3in), the corresponding strain in each of the tie wires should have been approximately $8.2 \times 10^{-3}\%$, as calculated from geometry.

3.5 POST AND BEAM FRAME MATERIALS

Timberstrand and Douglas fir lumber were the two types of wood used to construct the post and beam frame. Timberstrand was chosen as the material for the base and roof box beams because of its lack of grain orientation and high shear resistance. These material characteristics were expected to model the rigidity of both typical roofs and, when secured to the floor slab, typical floors used in this type of construction. The box-beams were made of two 367m (12ft) long, 50 by 101mm (2 by 4in) timberstrand lumber stud sections laid on edge and confined on top and bottom by 19.05mm (¾in) thick, 558.8mm (22in) wide and 367m (12ft) long Oriented Strand Board (OSB) sections.

The posts were each made of two 101 by 101mm (4 by 4in) Douglas fir lumber sections, with 558.8mm (22in) wide sections of Oriented Strand Board panels. The OSB panels were secured on the 101 by 101mm (4 by 4in) posts on the side that faced the in-fill material.

The timberstrand and Douglas fir lumber sections were checked for shear capacity both in the perpendicular and parallel direction to the grain. It was determined that the Douglas fir lumber sections had the controlling design shear capacity, V= 26.7kN (6kips).

3.6 POST AND BEAM FRAME ELEMENTS CONNECTIONS

The frame elements were connected using connections different to those commonly used in straw-bale post and beam construction. Pin connections consisting of 12.7mm (½in) thick A36 steel plates and A325 bolts, 152.4mm (6in) long, were designed to allow frame rotation while ensuring a substantial reserve connection capacity. A36 steel has a minimum yield stress, F_y=250Mpa (36ksi) and an ultimate tensile strength range of F_u=400 to 550Mpa (58 to 80ksi), commonly taken as F_u=455Mpa (60ksi) for design. Each 19.1mm (¾in) diameter A325 bolt has a design double shear strength of V=141.5kN (31.8kips) and an ultimate double shear strength of F_v=250Mpa (36ksi), both with the threads in the shear plane (LRFD 1994).

3.7 COMPARISON OF MATERIAL PROPERTIES

The materials used for the construction of the wall units have different material properties, tabulated in Table 5. Their compatibility is necessary to act as a reliable structural system.

Table 5: Properties of the Materials Used for Construction of Test Units

Material	Young's Modulus, E (kN/m²)	Shear Modulus, G (kN/m²)	Poisson's Ratio, v
Cement Stucco	9.7×10^6	4.2×10^6	0.15
Gypsum Plaster	5.1×10^6	2.2×10^6	0.15
A36 Steel	200×10^6	77×10^6	0.29
Wood (Douglas fir)	12×10^6	---	---
Wheat Straw-Bale	$\approx 1 \times 10^3$	≈ 450	0.12

CHAPTER 4: TEST WALL UNITS AND SETUP

This chapter describes how the test wall units were constructed, the setup and the limitations of both. Straw-bale in-fill wall units, with elevation dimensions 2.44m (8ft) long by 2.44m (8ft) high were constructed for this study. Each wall had stucco on one side and gypsum plaster on the other side to model the exterior and interior. The wooden post and beam sizes were representative of actual non-load bearing designs. Figure 9 shows an elevation schematic of the post and beam test frame used. The connections between the posts, floor and roof beam were designed to act as pinned connections so they would not contribute to the lateral force resistance of the wall models.
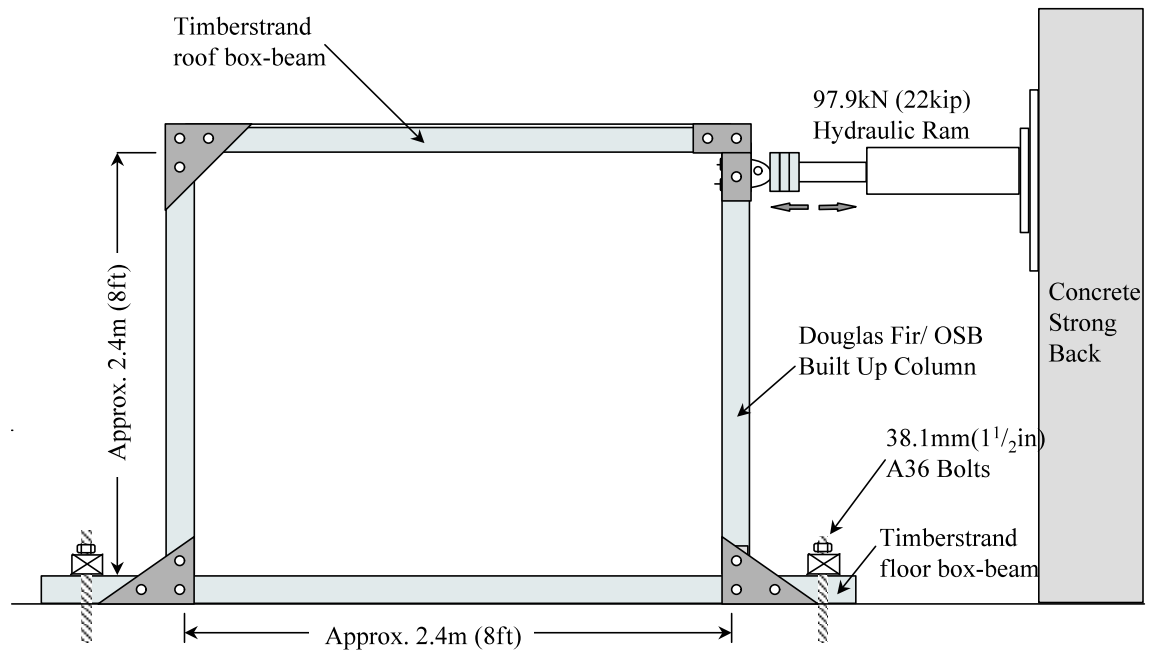
Figure 12: Schematic of Post and Beam Test Frame (Elevation)

4.1 TEST UNIT AND FRAME CONSTRUCTION

4.1.1 FRAME CONSTRUCTION

The post and beam frames were made of a base box beam and roof box beam, and two built-up columns. The thickness of each of these elements was 559mm (22in) and 457mm (18in), or the equivalent width dimension of the three and two string straw-bales, respectively. This replication of the width dimension enabled confinement of only the straw-bales all around the width of the wall units. However, the frame built for unit 1 would also be used to test wall unit 2. The straw-bales used for test unit 1 were 16% wider than those previously used, equivalent to a frame width excess dimension of 89mm (3.5in). It was decided to use the frame constructed for the three string bales for all in-plane tests, as it would expedite the testing program and only minor modifications would be necessary for the proper framing of unit 2.

The base and roof box beams were made of timberstrand lumber. The box-beams were made of two 367m (12ft) long, 50 by 101mm (2 by 4in) timberstrand lumber stud sections laid on edge and confined on top and bottom by 19.05mm (¾in) thick, 558.8mm (22in) wide Oriented Strand Board, or OSB, sections. These OSB sections were secured with wood screws to the timberstrand lumber studs at 152.4mm (6in) off-centers. For the base beam box, 50 by 101mm (2 x 4in) timberstrand lumber section, 381mm (15in) in length, were used as bolt anchors to the 12.7mm (½in) diameter all-threaded mild-steel rods protruding out from the OSB and into the first course of straw-bales as reinforcement. A total of 5 all-threaded rods used as reinforcement for the bottom course of straw-bales. The 5 bolt anchors were secured to the 3.67m (12ft) perimeter studs by means of wood screws, and in between them, shorter timberstrand lumber blocks were screwed on the inside of the 3.67m (12ft) studs for added bending capacity. Figure 13 shows a plan view of the base box beam with a typical cross section and Figure 14 shows an elevation cross section of the base box beam with the reinforcement placing for the bottom course.

381mm (15in) long, 13mm ($^1/_2$in) all thread anchor bolt

50 x 100mm Timberstrand blocking between bolt anchors

Built Up Column

19mm ($^3/_4$in) OSB sections, with 64mm (2 $^1/_2$in) screws 152mm (6in) O.C. top and bottom

Section A

50 x 100mm Timberstrand bolt anchors 406mm (18in) O.C.

50 x 100mm Timberstrand stud on each side of box beam

Section A: Base Beam and Anchor Bolt
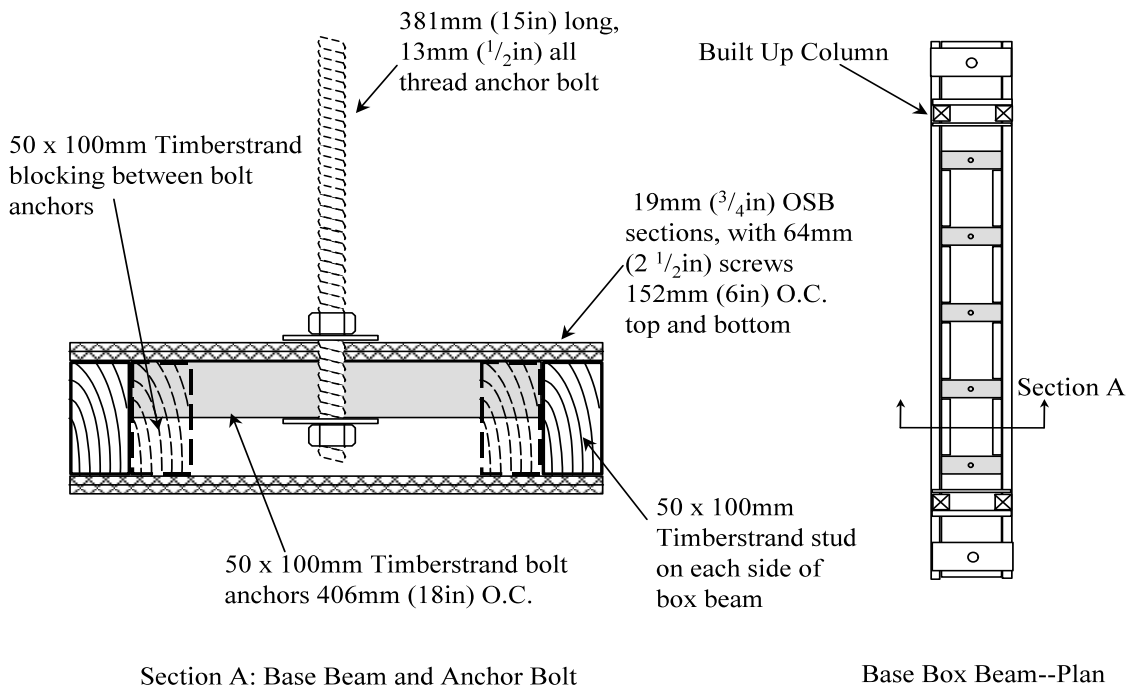
Base Box Beam--Plan

Figure 13: Cross-Section Schematic of Base Box Beam (1)

381mm (15in) long, 13mm ($^1/_2$in) all-thread anchor bolt

19mm ($^3/_4$in) OSB sections, with 64mm (2 $^1/_2$in) screws 152mm (6in) top and bottom

50x 100mm Timberstrand stud
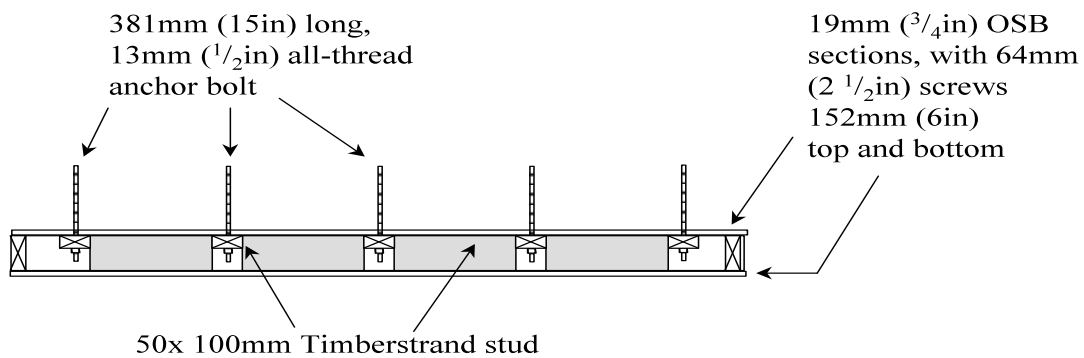
Figure 14: Cross-Section Schematic of Base Box Beam (2)

The roof box beam was built as the base box beam except that: 1) No all-thread rods were used but #4 A615 reinforcing steel bars were hammered in to the top course of straw-bales once erection of the in-fill wall was completed, and 2) There was no need for confinement of the roof box beam, so the top layer of 19.1mm (¾in) Oriented Strand Board was omitted. The straw-bales were pre-compressed by applying a force on the roof box beam by means of 6 tie wires, which were tensioned to the base box beam. These tie wires were placed at a spacing of 1.22m (4ft.).

The built up columns, shown also in Figures 12 and 13, were each made of two 101 by 101mm (4 by 4in) Douglas fir lumber and 558.8mm (22in) wide sections of OSB panels. The panels were secured on the 101 by 101mm (4 by 4in) posts on the side that faced the in-fill material. The OSB sections were screwed the entire height of the posts, providing confinement all around the width dimension of the wall.

Both of the columns were plumbed and secured in a perpendicular position with respect to the base box beam before erection of the in-fill material began. Two 50 by 101mm (2 by 4in) studs were used to provide the bracing needed to keep each of the columns upright. The columns were temporarily connected to the base box beam by means of a thin, galvanized metal connector for stability purposes during construction.

An inner-perimeter frame was constructed for unit 2. It was made of two 50 x 100m (2 by 4in) wood lumber studs firmly attached inside the existing frame by 76.2mm (3in) wood screws spaced out at 76.2 to 101.6mm (3 to 4in).

4.1.2 IN-FILL WALL CONSTRUCTION

The first course of straw-bales was impaled on the all-threaded rods coming out from the base box beam by lifting them over the rods and slowly lowering them to make sure the rods pierced the straw-bale as closely as possible to its half width point. The straw-bales were laid flat, to give the maximum modulus of elasticity (Bou-Ali 1993). The first course consisted of two full bales, which fit exactly inside the frame because of their

longest dimension was approximately 1219mm (48in). The second course consisted of one full and two half-bales. The full bale was placed in the middle of the wall, while the two half bales were placed at the ends. In this fashion, a running bond arrangement was set and the third and fifth courses resembled the first, while the fourth and sixth resembled the second. One person stomped on each course after placement in the frame, to densify and precompress the straw-bales.

4.1.3 IN-FILL WALL REINFORCEMENT

In addition to the all threaded rods protruding from the base box beam and unto which the first course of bales was impaled, additional lateral reinforcement for the wall units was provided by piercing #4 A615 grade 60 steel reinforcing bars (ASTM A615) down through the courses of bales. These 10 re-bars measured 1016mm (40in) long. Two reinforcing bar sections per bale were used, for a total of 15 sections. The first set of 5 re-bars was hammered through the bales after the third course had been set and stomped in the frame. The second set of 5 re-bars was hammered into the wall after the fifth course of bales. The last 5 re-bars were driven through the roof box beam, ending up resembling the base box beam, with the all threaded rods, upside down. These re-bars measured 762mm (30in) and pierced through the sixth and fifth courses. A 4.5kg (10lbs) sledge hammer was used to drive the reinforcing bars in.

4.1.4 FRAME ELEMENTS CONNECTION DESIGN

The connections used for the test frame replaced those used in post and beam frames built to common practice (Steen et al 1994). The connections used in common practice are semi-rigid, metallic connections, capable of yielding to dissipate energy, and which contribute significantly to the stiffness of the system. Even though these characteristics are beneficial to structural systems, these connections are not designed to withstand shear forces comparable to those generated by earthquake loads. In the case of ground acceleration induced shears, the thin metallic plates' capacity would be overcome by the

loading demand, making them the weak link in the system, failing before the wall and frame elements did.

Seismic pin connections consisting of A36 steel plates A325 bolts were designed to allow frame rotation, enabling more representative data of the wall capacity without any additional resistance to be obtained. Each connection consisted of two 12.7mm (½in) plates, and three 152.4mm (6in) long, 19.1mm (¾in) diameter bolts. The bolts were placed in double shear, with the threads in shear planes, and were hand snug tightened. Two bolts secured the connection rigidly to the timberstrand lumber base box beam and the third one was connected it to the column member to represent a pin connection. In this fashion, the third bolt allowed the second member to rotate freely with respect to the first. Figure 15 shows a detail of one of the base beam/column connections.
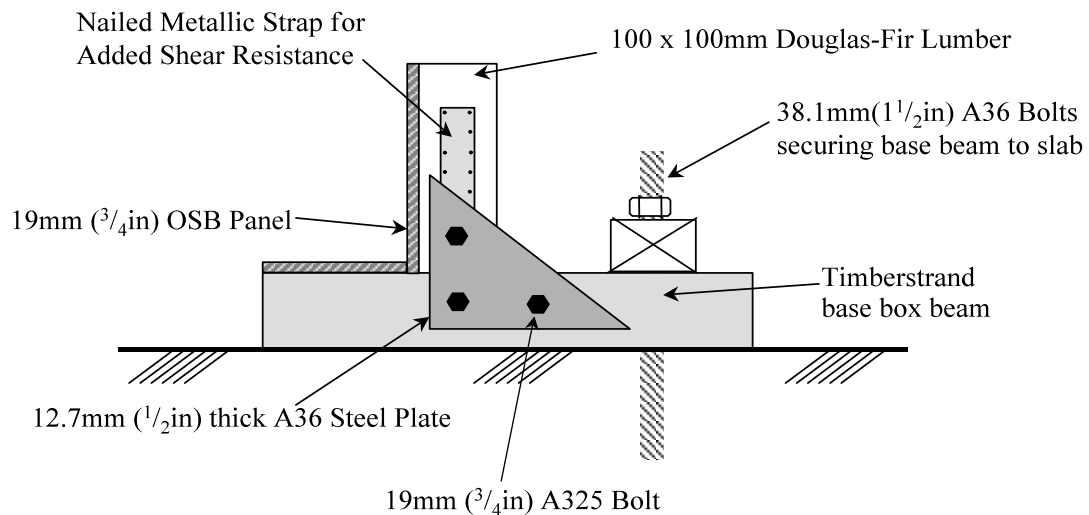
Figure 15: Detail of Seismic Connection for Base Box Beam and Built-Up Column

The plates and the bolts were checked according to LRFD specifications for adequate shear capacity to withstand the full load of the Series 22 MTS hydraulic actuator, or 97.9kN (22kips) (MTS Systems Corp. Minneapolis, MN). The Douglas fir 101mm by 101mm (4 by 4in) lumber column sections were checked for shear capacity both in the perpendicular and parallel direction to the grain. Based on manufacturer specifications, it

was calculated that each column had a shear capacity of 26.69kN (6kips) and this capacity would not be exceeded by the system.

All the required drilling for the installation of the connection components was done with a handheld drill once the frame elements were held in place by non-structural plates. The connections were intended to have a minimal frictional resistance against rotation developed solely from the contact between wood and steel. However, an additional frictional resistance was added to the pin connections from probable angular deviations, or slop, as manual drilling took place. This increased the resistance of the frame to lateral forces. This frictional resistance was not quantified, and its effects are assumed to be negligible to the overall in-plane resistance of the wall. The slop in each drilled hole ranged from 3.2 to 6.3mm ($^1/_8$ to ¼in), therefore a maximum slop of 12.6mm (½ in) in the system could be expected during lateral loading.

4.1.5 CONNECTION OF FRAME TO FLOOR SLAB

The base box beam was secured to the floor slab by means of two 38.1mm (1½in) diameter A36 steel rods. Each rod was checked according to LRFD specifications for adequate shear capacity beyond 97.9kN (22kips). A torque of 292kN·m (2000lbs· ft) was applied to the nuts for securing the wall to the slab to prevent sliding. An oversized 101.6mm (4in) thick A36 steel washer was used at each end. These washers rested on 558.8mm (22in) long, 101 by 152mm (4 by 6in) Douglas fir lumber section supported across the ends of the 3657mm (12ft) long timberstrand lumber sections. Fig. 5 shows this connection at the end of the wall where the ram was connected. The end farthest away from the ram was attached to the slab in the same way.

The units were not held down at the connection centers, and the moment capacity of the timberstrand base box beam was relied on to keep the units flush against the concrete slab. Because of this, there was a possibility of uplift if the base box beam deformed under flexure up from the slab.

4.1.6 FACING REINFORCEMENT PLACING

A 17-gauge, 1inch—25.4mm galvanized woven wire stucco netting (ANSI A42.4-1995) was used as reinforcement for the plaster facings. Three sections of this wire, shown in Figure 16, covered the entire sides of the walls and was secured with roofing nails at approximately 152.4mm (6in) spacing to the perimeter of the frame. Each wire section was nailed first to the top box beam and then stretched by hand and nailed to the base box beam. Tie wire was used to tie the three wire mesh sections together at approximately 304.8mm (12in) vertical intervals, or as deemed needed to keep the mesh flush against the straw. The use of 16-gauge wire provides a vertical reinforcement ratio of 0.0015mm^2 of steel per mm^2 of stucco, which satisfies the minimum reinforcement requirement under the 1997 UBC (Section 1914.3.2).

Expanded metal lath, shown in Figure 16, was used at the ends of the each wall and also fastened to the perimeter with roofing nails. The lath was also tied to the wire mesh as needed. The lath was 610mm (24in) wide and ran the entire height of the wall. It was observed that the mesh and lath tended to bow away by as much as 102mm (4in) from the wall, particularly in the middle. Tie wires passing through the bales secured the lath and mesh from one side of the wall to the lath and mesh of the other, assuring the reinforcement remained stayed in the range of 12.7mm to 19.05mm (½in to ¾in) away from the straw. Four tie wires were passed through each course of bales, totaling 24, and were tied using pliers.

Figure 16: Facing Reinforcement

The firm attachment of the reinforcement to the framing elements is crucial for the transferal of shear load to the facings. The number of nails used for attachment and their correct spacing becomes the most important variable of how effectively the load transferal occurs. If few nails are used, the stiff reinforced facing will pull out the nails from the frame and behave in a ductile manner. Failure in this case would most probably be by buckling when the very thin and flat facing column begins detachment from the straw-bale surface. If sufficiently detached, subsequent loads could even result in total collapse of the facing as a whole panel. On the other side of the spectrum, if a large quantity of nails is used, the facing reinforcement will remain firmly attached to the frame, and thus will behave in a brittle manner, cracking in tension due to forced deformations. Failure in this case is associated with exceeding the shear capacity of the facing column.

Besides the firm attachment of the reinforcement to the framing elements by means of nails, the reinforcing wire need also be attached securely to the straw-bales. The reinforcing wire should be loose enough to permit the stucco/plaster to be thoroughly worked into the straw and remain more or less in the middle of the first layer of stucco/plaster for adequate placement. Attachment of the reinforcement to the straw-

bales is necessary to prevent a possible collapse in the instance the facing becomes detached from the frame due to too few nails, as previously described. The wire ties placed through the courses of bales to attach one side of the reinforcement to that on the other side of the wall act as braces, increasing stability as well as reducing the $^{kl}/_r$ ratio for the thin facing column. The contribution of these ties to the capacity of the straw-bale/plaster facing system may be compared to that offered by plate stiffeners used in W-shape steel beams (King 1999).

4.1.7 PLASTER FACING APPLICATION

The plaster was mixed and applied by plasterer apprentices, familiar with the application on straw-bales, and closely supervised by a master plasterer. The application of the facings was carried out in two steps:

a) First, a base coat, known as "scratch" coat, was applied to the wall, thoroughly working it through the reinforcement and into the straw. This first coat was left with a rough finish to help adhesion of further layers (Steen et al 1994, King 1996).

b) A second coat, known as "brown" coat, was applied on 24 hours later and smoothed out, to resemble as much as possible the finish given to typical walls.

The usual third coat was not applied because it is generally used for aesthetic purposes (Such as for giving the wall a specific color or texture) and too thin, providing no structural contribution. The facings were allowed to cure for 10days before loading the wall units. No moisture enhancing procedures were used during curing. An elevation schematic of the wall constructed as described is shown in Figure 17. Figure 18 shows a cross section of the three string straw-bale wall with the facings applied to it and Figure 19 shows a cross section of the two string straw-bale wall with facings.

97.9kN (22kip)
Hydraulic Ram

Concrete
Strong
Back

Approx. 2.4m (8ft)

Approx. 2.4m (8ft)

Figure 17: Elevation Schematic of Wall with Facings

1st Straw-Bale Course

2-coat Gypsum
Plaster Facing

Straw-Bales

Section B

152.4mm (6in) Nails
Securing 17-gauge
Wire Stucco Netting to
Frame

2-coat Cement
Stucco Plaster
Facing

Section B: Base beam and 1st Course Straw-Bales

Base Box Beam-- Plan

Figure 18: Typical Cross Section of Three String Straw-Bale Wall with Facings
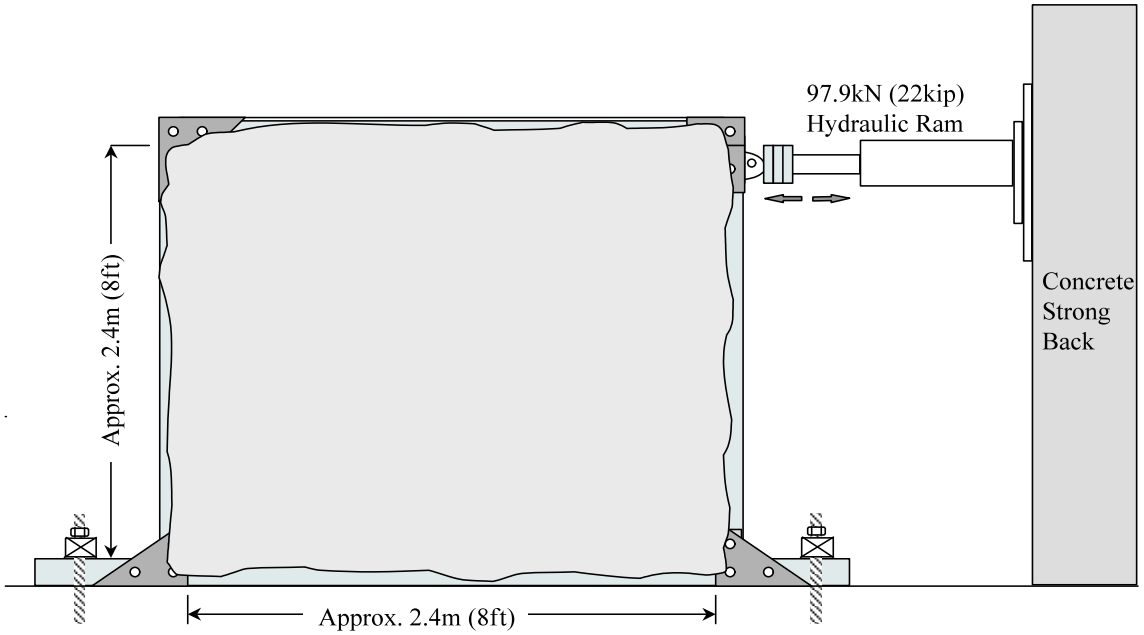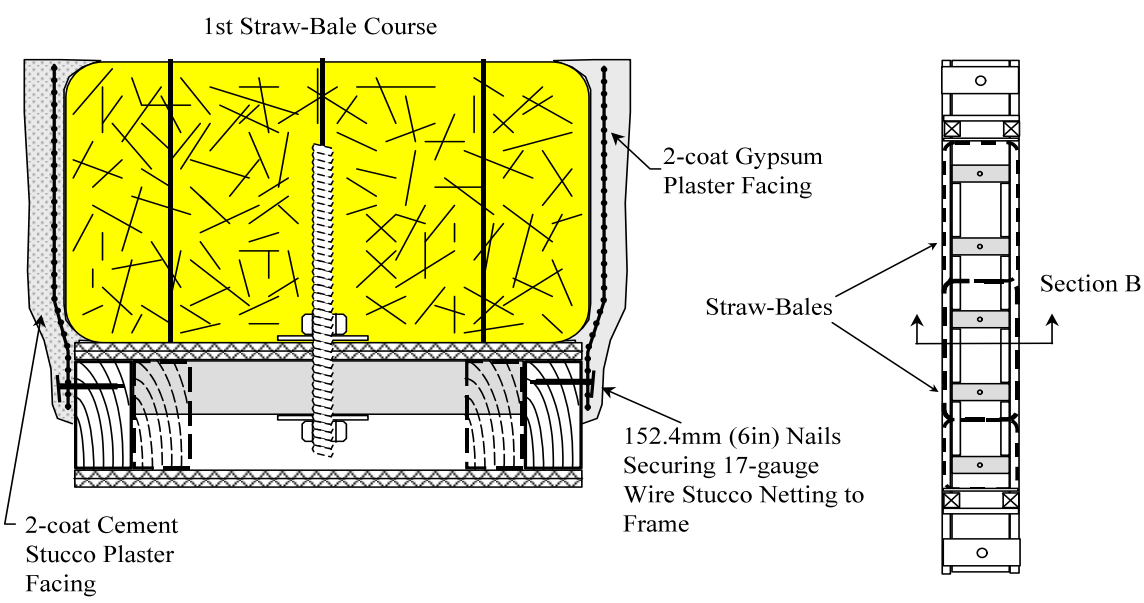
Section C: Base beam and 1st Course Straw-Bales

Base Box Beam-- Plan
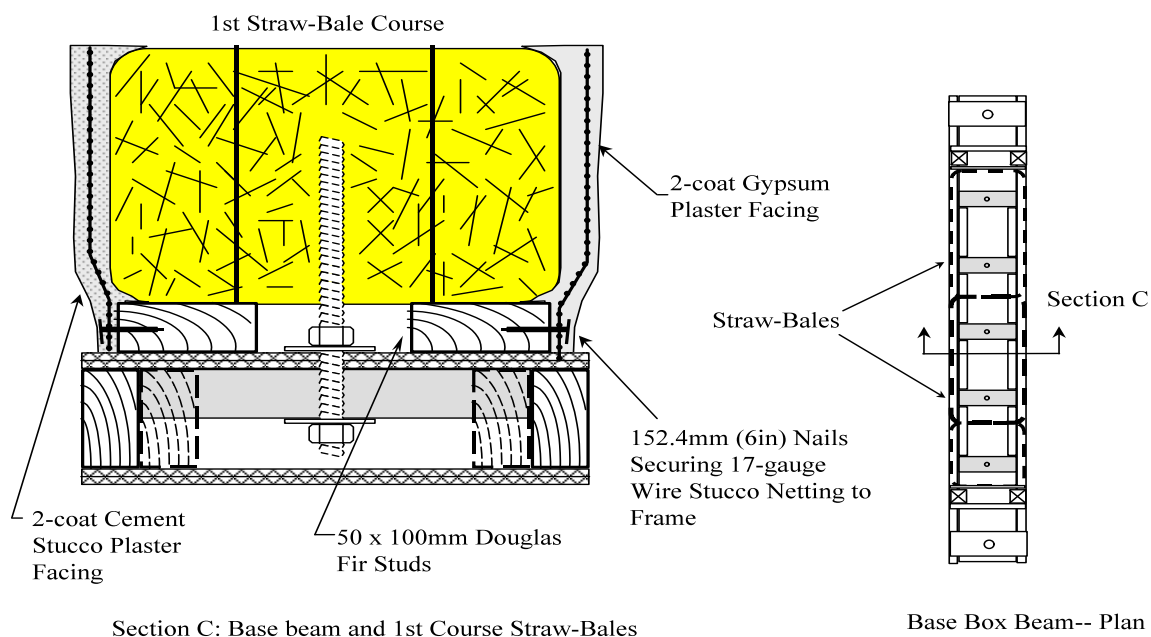
Figure 19: Typical Cross Section of Two String Straw-Bale Wall with Facings

4.2 UNIT AND SETUP RESTRICTIONS

The 97.9kN (22kip) MTS hydraulic actuator that was used has a maximum displacement capacity of (10in). After the plates for its attachment to the strong back were set in place, the ram's piston was extended approximately 76.2mm (3in) to reach the built-up column of the wall. Therefore, the frame had a horizontal displacement range of 76.2mm (3in) in the direction towards the hydraulic ram and 177.8mm (7in) away from it. The hydraulic ram used for applying the in-plane load was attached to the frame as shown in Figure 20. A 97.9kN (22kip) capacity load cell was placed at the end of the ram piston by means of a threaded rod to measure the load values. An MTS swivel (MTS System Corp. Minneapolis, MN) was attached to the load cell by means of another threaded rod section to enable continuous loading as the wall system deformed parallelogram-wise. MTS spiral washers (MTS System Corp. Minneapolis, MN) were installed on this second threaded rod to prevent a fatigue failure due to cyclic loading.

12 by 25mm, 6mm thick
A36 Steel Rectangular Tubing

12mm thick
A36 Steel Plates

97.9kN (22kip)
Hydraulic Ram

A

A

MTS Load Cell

19mm A325 Bolts   MTS Swivel

Section A-A

Elevation Ram Connection
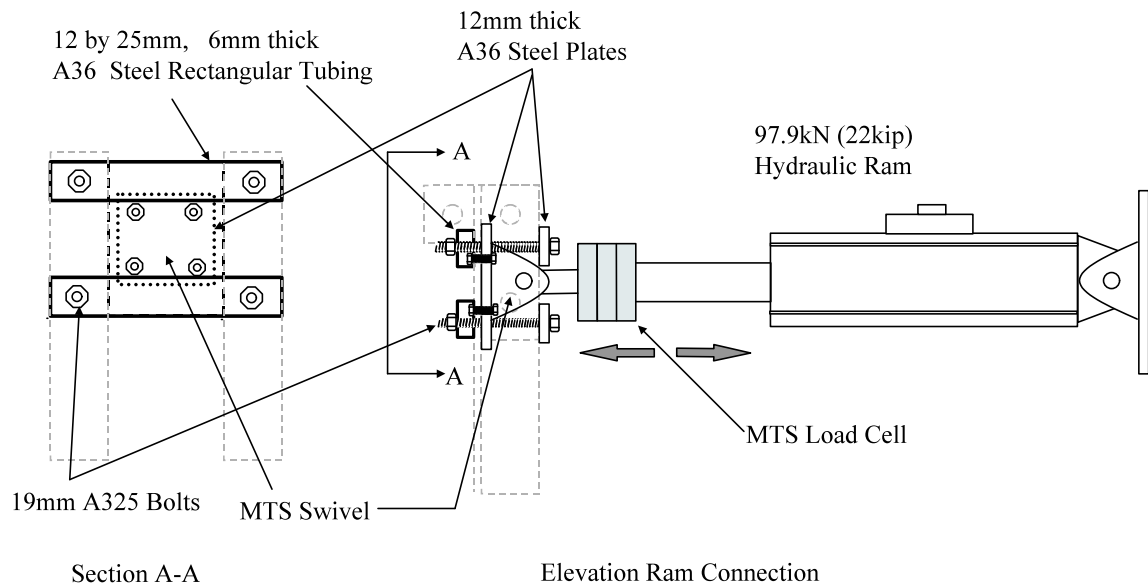
Figure 20: MTS Hydraulic Ram/Frame Attachment Schematic

The ram was braced against horizontal rotations, but was allowed to rotate vertically, with a maximum rotation angle of ±3.0° with respect to the horizontal. The angular variations in the load applications were too small to make the load unrepresentative of an earthquake shear. The deformation of the wall height was controlled by the displacement capacity of the ram piston: The maximum reduction in wall height, as the frame deformed into a parallelogram, was restricted to 12.7mm (0.5in) by the maximum angle of vertical rotation of the hydraulic actuator.   Figure 21a shows a schematic of the horizontal bracing used, while 21b shows the vertical rotation permitted.

A36 Steel Welded Angle

A36 W6x16
Steel Section

3°

a) Lateral Bracing Against
Horizontal Rotation
(Plan View)

b) Allowed Angle of
Vertical Rotation
(Elevation View)
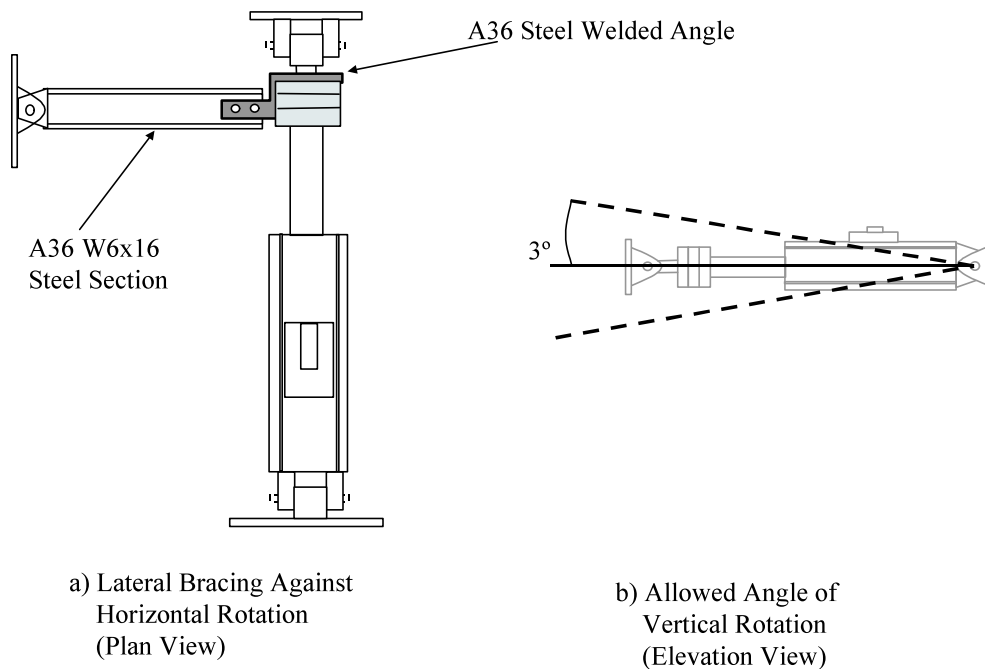
Figure 21: Lateral Bracing Against Horizontal Rotation and Allowed Angle of Rotation

The wood frame used for the testing of the wall was not tested quantitatively for in-plane resistance. The frame was seen to deform with negligible resistance in a parallelogram shape, until a horizontal displacement of approximately 381mm (15in). At this displacement, the right angles of the Douglas fir/OSB built up columns met sharply with the horizontal plane of the OSB on the timberstrand base box beam, and resistance was observed. Within the stroke displacement of the ram, equal to 178mm (7in), the pin connections allowed the frame elements to rotate easily and offer only frictional resistance.

CHAPTER 5: INSTRUMENTATION AND LOADING REGIME

5.1 INSTRUMENTATION

Voltage-differential instruments were used to measure deformations of the wall units. The instruments used were 7 linear motion position transducers, commonly known as potentiometers, and 1 linear variable differential transformer, known as LVDT. Figure 22 shows the location of the instrumentation used with respect to the wall.
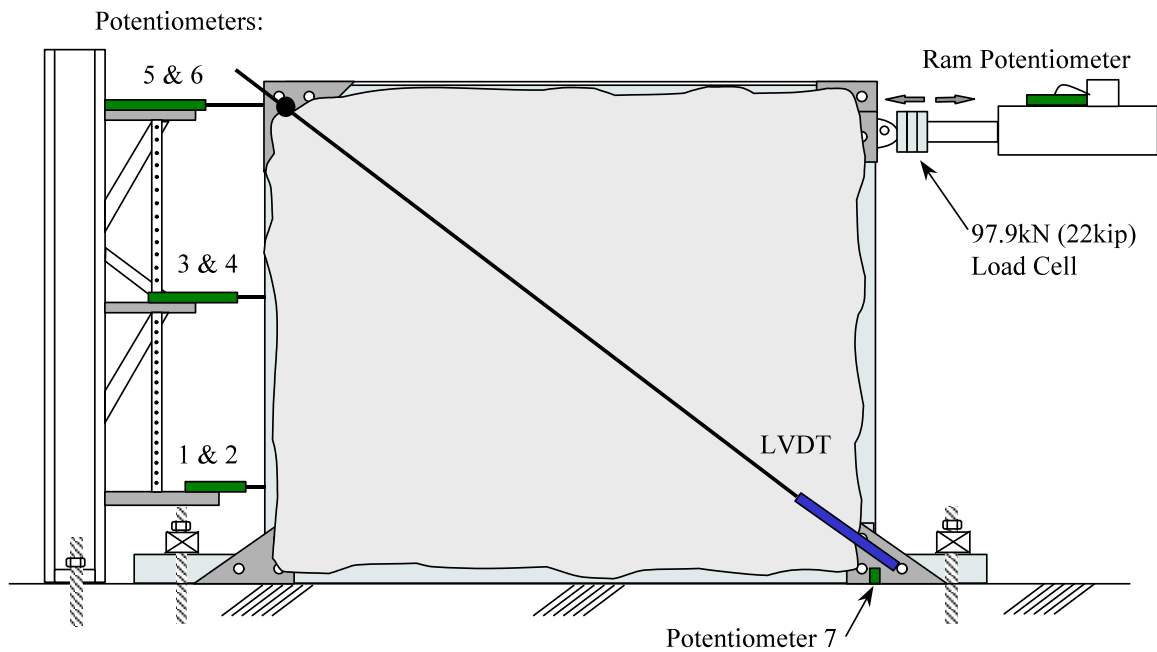
Figure 22: Wall Unit Instrumentation Setup

Four different types of potentiometers were used. Potentiometers 1 and 2, as shown in Figure 22 are a pair SLF-S-050-OB with an extension of 57mm (3in) (Waters Manufacturing Inc., Wayland MA). Potentiometers 3 and 4, SLF-S-150-OB, have a 103mm (6in) stroke.   Numbers 5 and 6 are two LFS-12/300-OD5 with a 305mm (12in) extension (Waters Manufacturing Inc., Wayland MA).   The potentiometer used to measure uplift was a Series 9605 linear potentiometer with a maximum displacement of

12.7mm ($^1/_2$in) (Duncan Electronics, Tustin, CA). The LVDT used to record diagonal measurements has an extension limit of 103mm (6in) (Lucas Schaevitz, Pennsauken, NJ).

It was decided that no instruments were needed to measure the sliding of the wall with respect to the slab because the 38.1mm (1½in) A36 steel diameter rods were sufficiently tightened to prevent any slipping. Visual inspection during the course of the test attested to the wall remaining fixed to the slab.

Potentiometers 1 through 6 obtained displacement readings with respect to a steel column fixed to the slab, used as reference point. A light galvanized metal frame was attached to the steel column, extending the potentiometers to the wall (See Figure 22).

Potentiometers 2, 4 and 6 measured the bottom, middle and top horizontal displacement, respectively, of the frame's column at the end of the wall opposite the load application end. A nut with a closed, rounded tip was fit at the end of these potentiometers' rods to rest directly on a small plastic strip glued to the frame column. Silicone lubricant was sprayed on the plastic strip to enable the potentiometer rod tips to slide without being subjected to any rotational effects. The wall could then deform while the potentiometers' rods remained horizontal and in contact to obtain readings, independent of any wall distortions. Potentiometers 1, 3 and 5 measured the horizontal displacement at the bottom, middle and top, respectively, of the vertical plane formed inside the frame by the actual straw-bales. These three potentiometers were attached to the straw-bales by embedding a threaded rod with an "arrow" like head until the rod could not be pulled out by hand. Bending a small dry wall anchor into a triangular shape until it resembled the head of an arrow made the arrow-shaped anchor. A small swivel was used to attach these anchoring rods to the potentiometer rods to mitigate possible bending moments as the wall deformed. Placement of these potentiometers was chosen to enable a direct comparison between the displacements of the framing elements to those of the vertical plane of straw inside one of the column frame elements. These six potentiometers were installed in pairs, as shown on Figure 22.

The hydraulic ram has an integrated potentiometer to measure the displacement of the piston. Potentiometers 5 and 6 were positioned to read displacements at the same height the load was applied. Potentiometer 7 was used to measure vertical uplift of the test frame with respect to the slab at the end of the wall were the load was applied. This potentiometer was attached to one of the A325 bolts that remained fixed at one of the seismic connections on the base box beam. The LVDT was used to measure the change in the diagonal dimension of the wall units and was attached to seismic connections on opposite corners with magnetic clamps, fitted with a uniaxial swivel. Each clamp was free to rotate in the plane of the wall, minimizing bending moments induced by the wall deformations and allowing the LVDT rod extension to remain as close to straight as possible.

A 97.9kN (22kip) capacity MTS load transducer cell, model 661.20A-03 (MTS Systems Corp. Minneapolis, MN) was placed at the end of the ram to measure the load values. The load cell, LVDT, and potentiometers were all calibrated prior to the tests, using a 1334.4kN (300kip) capacity Baldwin universal hydraulic testing machine, adequate voltage sources and a voltmeter. Data points were obtained which enabled the generation of calibration curves for each of the instruments. Calibration factors were taken from the curves obtained and are included in Appendix A.

5.2 DATA ACQUISITION SYSTEM SETUP

Voltages of 10 or 12Vwere applied to the potentiometers. Voltage differentials were sent to Metrabyte EXP 16/A 16-channel multiplexer and Metrabyte STA-U units (Keithley-Metrabyte) to generate digital readings. The data was modified using version 6.1.2 of LabTech software (Laboratory Technologies Corp & Kiethley-Metrabyte), with a model 5170 IBM computer system with a 286 processor (IBM, Armonk, NY). Load and displacement readings were taken every ½ second. For a qualitative interpretation of the behavior of the wall units during the tests, a window was setup to graphically display load versus roof-displacement values as well as the numerical values of the displacements

being recorded by the LVDT and each of the potentiometers to show unit behavior and to check the proper functioning of the instruments.

5.3 LOADING REGIME

One monotonic and two cyclic in-plane load tests to quantify the shear resistance of the straw-bale in-fill wall units were carried out. For this study, the in-plane lateral loads were applied at the roof level of the wall units and set by drift, rather than load control. The application of loads was carried out manually on the MTS hydraulic ram controller, allowing brief pauses during loading cycles to permit visual evaluation of damage to the wall units.

A preliminary test, Test 0, was used to obtain the performance of a full-scale straw-bale in-fill wall with no plaster facings. This was carried out in order to quantify the shear resistance that straw had by itself without plaster facings. Loading was stopped when the lateral resistance of the wall stopped increasing. This also ensured that the in-fill wall maintained its structural integrity, in order to apply plaster facings to it and use it as a full model with plaster facings.

The two subsequent wall units, wall units 1 and 2, were full-scale models of walls with facings and were loaded with a lateral in-plane force at the roof level to previously established drift levels. The load application continued until the target displacements were reached or until significant strength degradation to the in-plane loads was evident. When diagonal tension cracks appeared, or a drop in resistance was observed, the load was released and reapplied for three or four consecutive cycles at that particular displacement. This was done in order to examine the degradation of the system's capacity at that particular drift.

Figure 23 shows the in-plane roof level load applied to wall unit 0. Figures 24 and 25 show the in-plane cyclic roof level load applied to wall units 1 and 2.
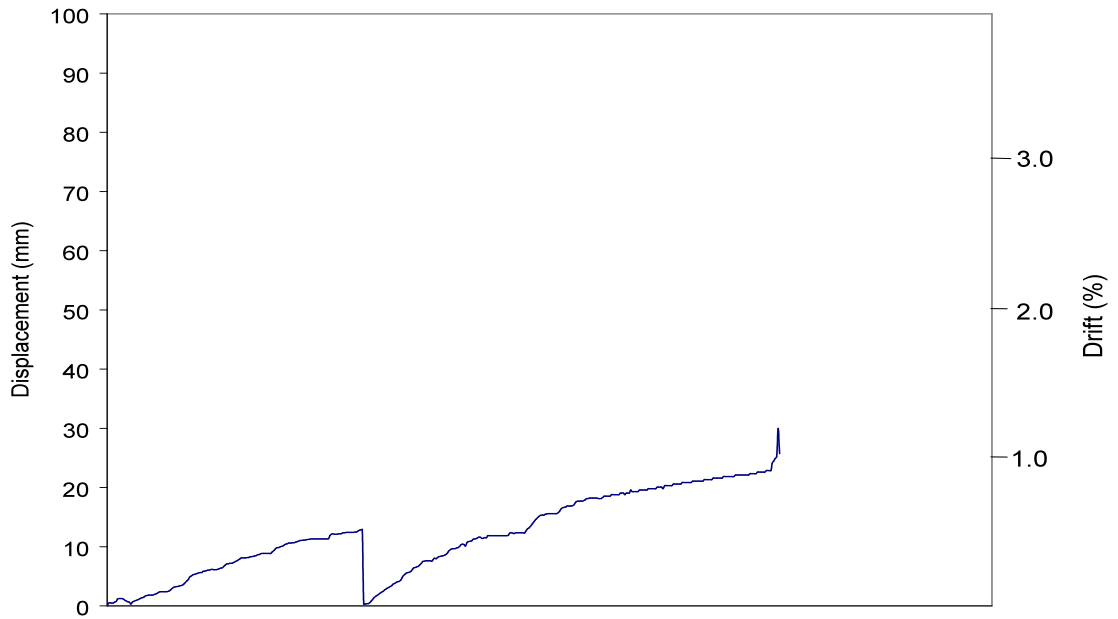
Figure 23: Monotonic In-plane Load Regime for Wall Unit 0 (Three-string bales, no facings)
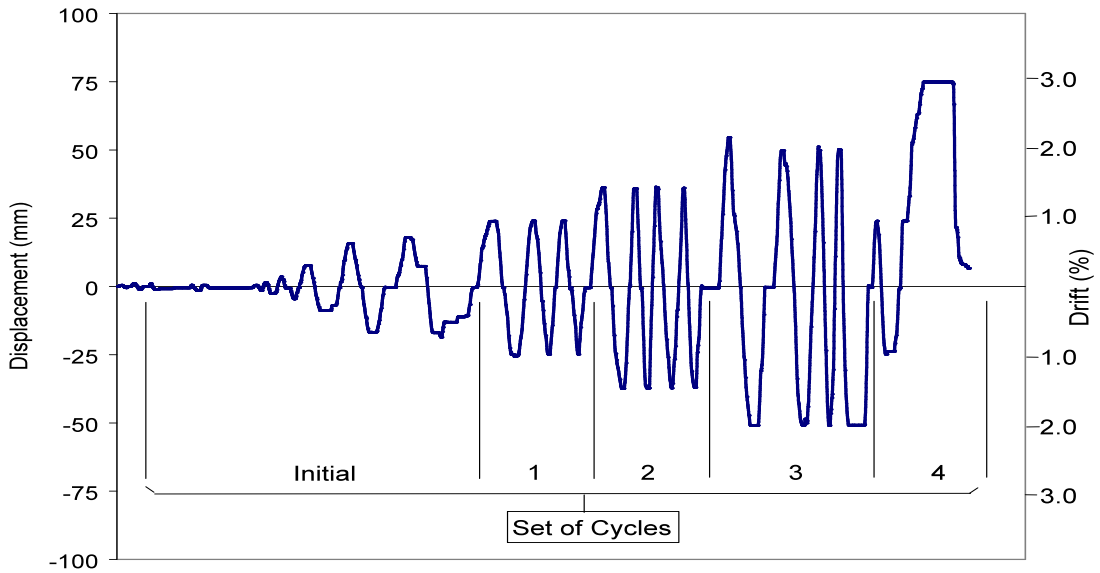
Figure 24: Cyclic Load In-plane Load Regime for Wall Unit 1 (Three-string bales, with plaster facings)
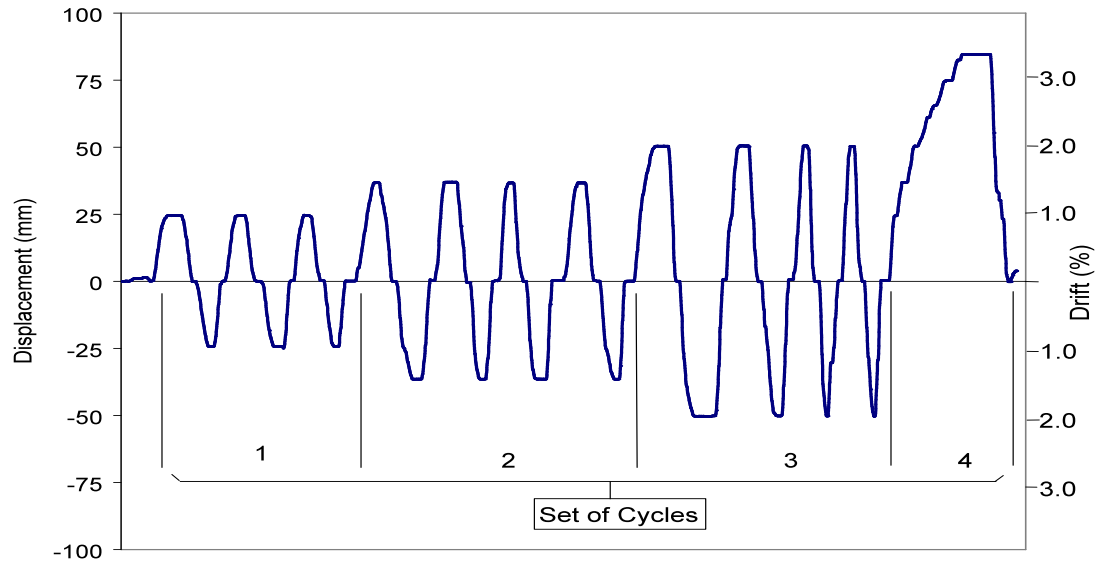
Figure 25: Cyclic Load In-plane Load Regime for Wall Unit 2 (Two-string bales, with plaster facings)

CHAPTER 6: BEHAVIOR OF IN-PLANE LOAD TESTS ON WALL UNITS

6.1 TEST UNIT 0

6.1.1 OBSERVATIONS

A straw-bale in-fill wall without facings was subjected to in-plane lateral loading to obtain the strength and stiffness. Limited lateral resistance was obtained, with inelastic deformations observed once the frictional resistance, denoted by courses of bales moving with respect to each other as the frame displaced.

The column element where the load was applied pushed on the straw-bale vertical plane at that end, and deformed it with a straight-line geometry. The vertical plane of the wall opposite the load application deformed with the curve like shape. This observed behavior is represented by the schematic in Figure 26.

Figure 26: Predicted Behavior of Post and Beam Straw-Bale In-fill Wall w/out Facings, Subject to Monotonic In-plane Loading

The load carrying mechanism was the straw itself, entirely dependent on Young's Modulus, E, friction, μ, and stiffness, k. The frame, as mentioned in Section 4.2, offered negligible lateral resistance due to its pin connections.

Neither uplift nor slip occurred during Test 0. Position markers were set on each course of straw-bales, and elevation pictures taken before the test and at 2% drift. Superimposing these pictures on one another demonstrates the bulging effect the straw-bale vertical plane farthest from the point of load application, represented by Figure 26. These pictures are shown in Figure 27.
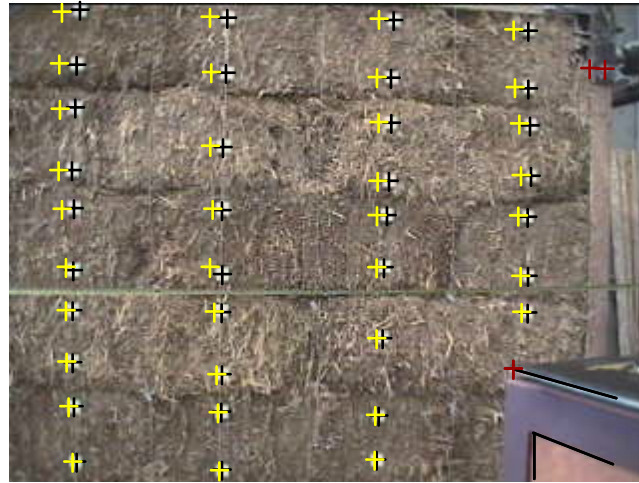
Figure 27: Observed Deformations at 2% Drift, Test Unit 0

6.1.2 FORCE-DISPLACEMENT BEHAVIOR

The loading regime used for wall unit 0 is shown in Figure 23, Section 5.3. Load and lateral displacement values were recorded throughout the test.

The hysteretic force-versus-displacement loops incurred by the monotonic loading are shown in Figure 28. Figure 29 shows the envelope curves related unit 0. The unit behaved elastically during the first load application, up to 0.35kN (79lbs) and a 0.05%drift, showing no degradation in strength.

During the second load application, up to 1.25kN (281lbs) at a 0.5%drift, there was marked degradation in strength, and the response became more inelastic. The unit stiffened up unexpectedly on the third loading, as can be seen in Figure 29.

The wall unit had a maximum lateral resistance of approximately 1.9kN (427lbs), at approximately 0.4% drift. The test was halted at this point, as load resistance was constant with increasing lateral strain.
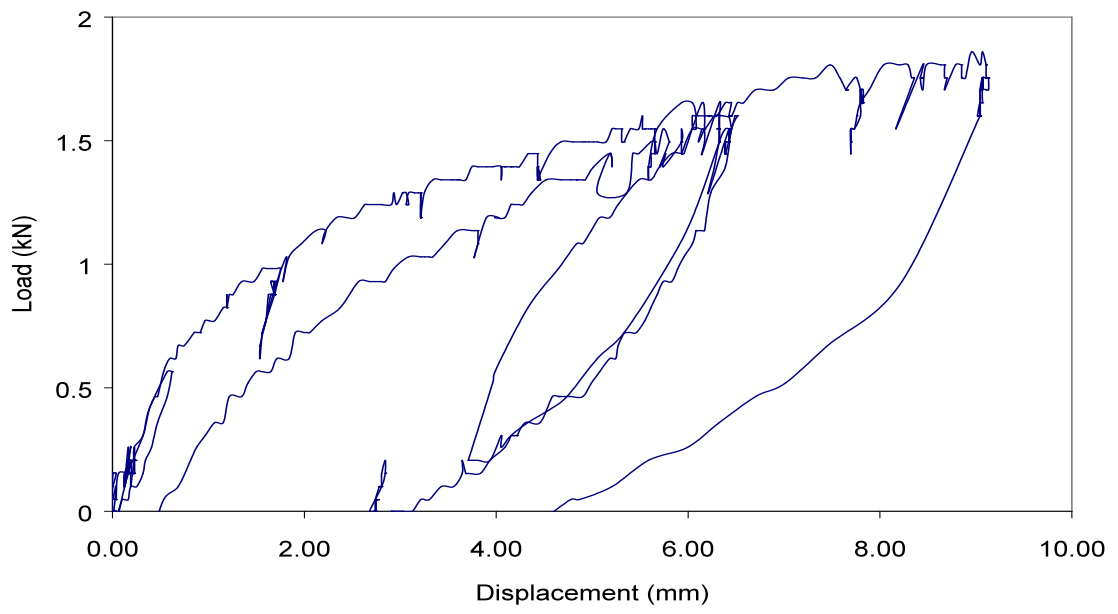
Figure 28: Load versus Displacement, Test Unit 0
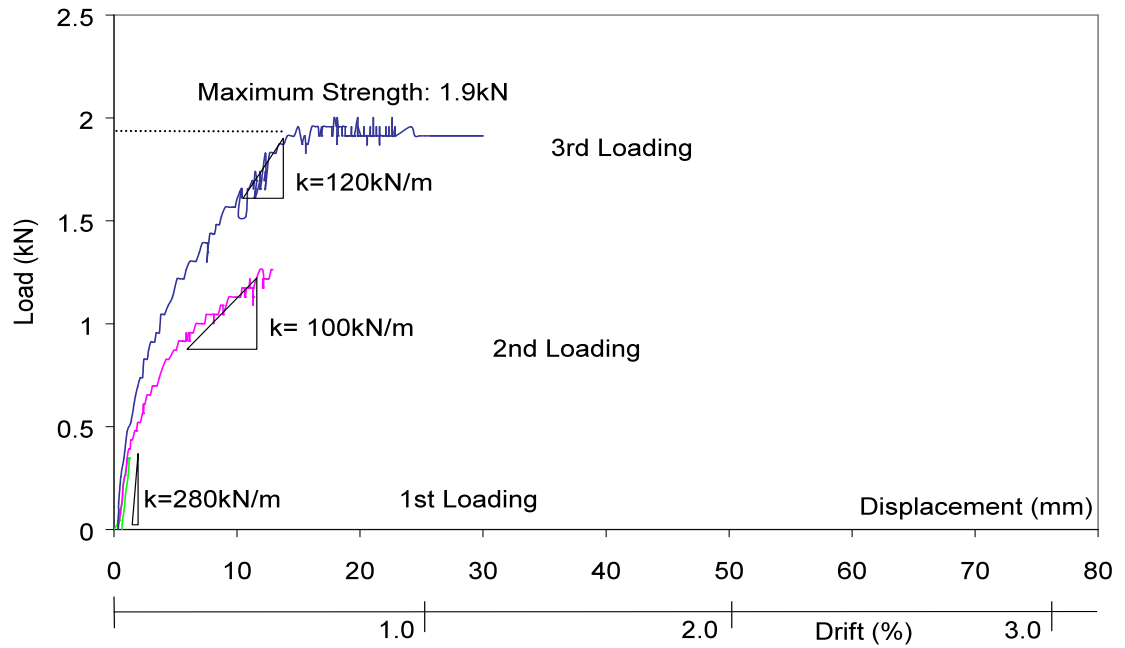
Figure 29: Envelope Curves, Test Unit 0

6.1.3 STIFFNESS DEGRADATION

The first loading of Test 0 had a tangent stiffness, k, of 0.3kN/m (1.6kips/in). The second loading showed a stiffness degradation of 65% from the first loading. A stiffness degradation of 55% is associated with the third loading when compared to the initial stiffness, as seen in Figure 30. Oddly, the stiffness related to the third loading is 17% higher than that of the second loading. Hence, it may be said the unit stiffened at the third loading.
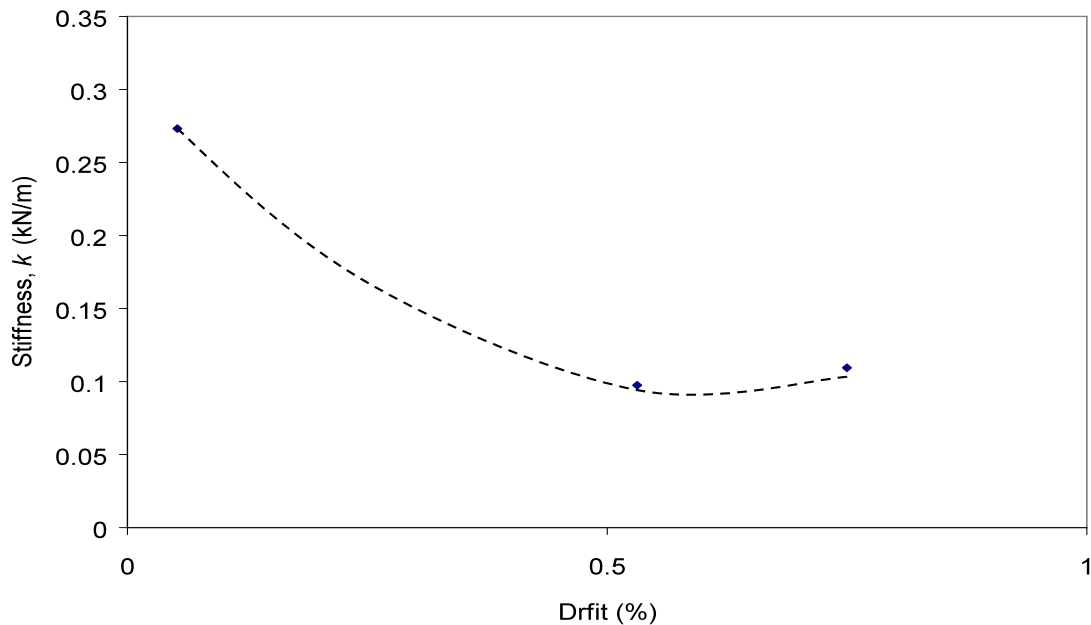
Figure 30: Stiffness Degradation Test Unit 0

6.2 TEST UNIT 1

6.2.1 OBSERVATIONS

Facings were applied to test unit 0 and subjected to the repeated cyclic in-plane loading regime shown in Figure 24, Section 5.3. The load carrying mechanism was directed towards the facings, the material with the higher shear modulus, G. Appearance of diagonal tension cracks on the facings of the straw-bale/facing system was expected to signal excess to the in-plane lateral capacity of the wall.

Tension cracks were observed only at the corners of the facings, with some measured uplift as the frame deformed. Figure 31 shows a schematic of the observed behavior of test unit 1.
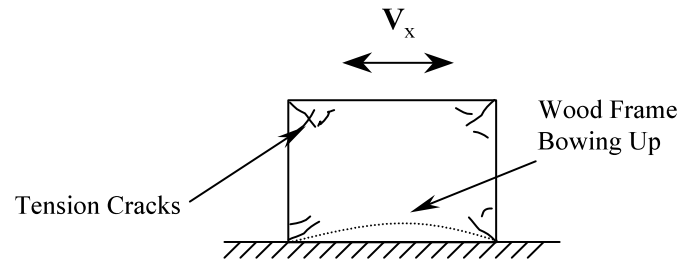
Figure 31: Schematic of Observed Behavior for Test Unit 1

The first diagonal cracks that were observed appeared at the top corners of the wall, approximately at roof displacements of ±19.05mm (0.75in), ±0.75% drift, associated to the set of cycles of the loading regime labeled as "initial" in Figure 24, Section 5.3. Figure 32a and b show pictures of the cracks on the stucco and plaster facing at the mentioned drift. No cracks were visible at this drift level on the plaster facing. No diagonal tension cracks appeared at the middle of the wall on either facing at this drift level. Neither uplift nor sliding occurred up to this drift level.

a) Plaster Facing   b) Stucco Facing

Figure 32: Damage to Test Unit 1 at ±0.75%
Drift

At ±1% drift, more tension cracks developed on the corners of the stucco facing and the existing ones propagated further, as shown in Figure 33. This drift level is associated with the 1st set of cycles of the loading regime (See Figure 24, Section 5.3). At this drift level, a maximum uplift of 8mm ($^1/_3$ in) was recorded at the middle of the base box beam. Slip of the wall with respect to the floor slab, approximately 12.7 (½in), was observed, as shown in Figure 34. This was corrected by re-tightening the bolts that held the unit down to the slab. Visual inspection confirmed no further sliding of the unit during the remainder of the tests. Figure 35 is a plot showing the uplift levels at ±1% drift.

Figure 33: Damage to Test Unit 1 at ±1% Drift   Figure 34: Slip of Unit 1 at ±1% Drift
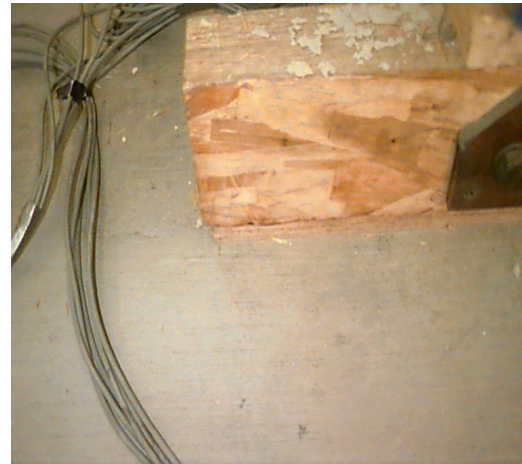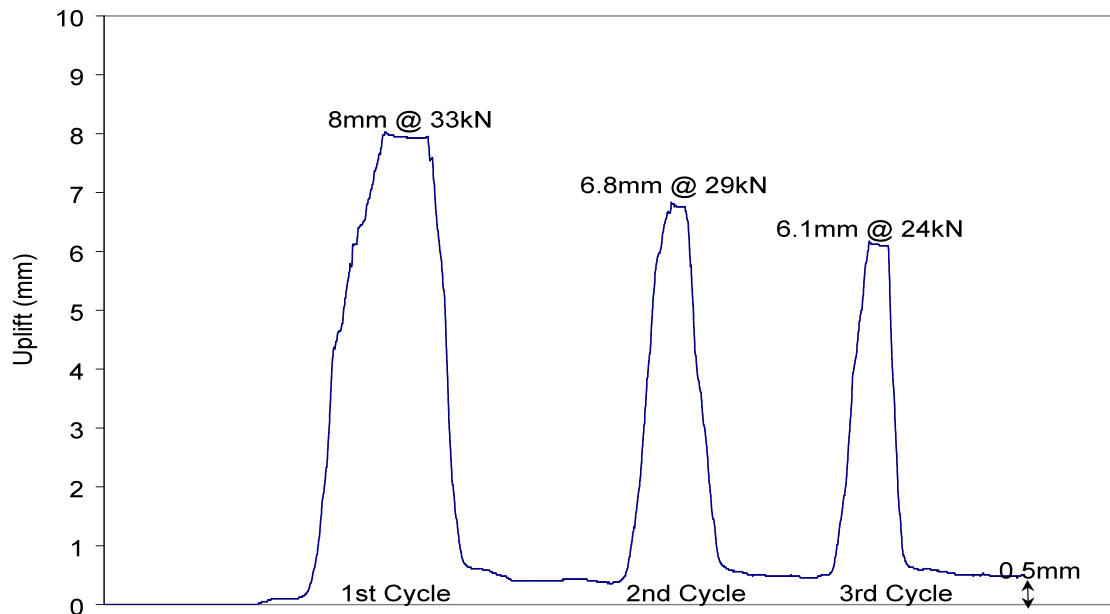
Figure 35: Uplift for Test Unit 1 at ±1% Drift

At 1.5 to 2% drift, equal to roof displacements between 38.1 and 50.8mm (1.5 and 2in), separation of the facings from the straw-bale surfaces and frame elements was visible, as shown in Figure 36. This drift level corresponds to the 2nd and 3rd set of cycles of the loading regime, Figure 24 of Section 5.3. Cracks propagated further at the corners, but no cracks were visible in the middle of either facing, as shown in Figure 37. The plaster facing began spalling at both of the top corners, particularly where the steel connection plates were located. The uplift recorded at the middle of the base box beam is shown in Figure 38. No further slip of the wall with respect to the floor slab was observed at this drift level.

a) Plaster Facing   b) Stucco Facing

Figure 36: Facing Separation at ±1.5 to 2% Drift

Figure 37: Damage to Stucco Facing, Test Unit 1, at ±1.5 to 2% Drift
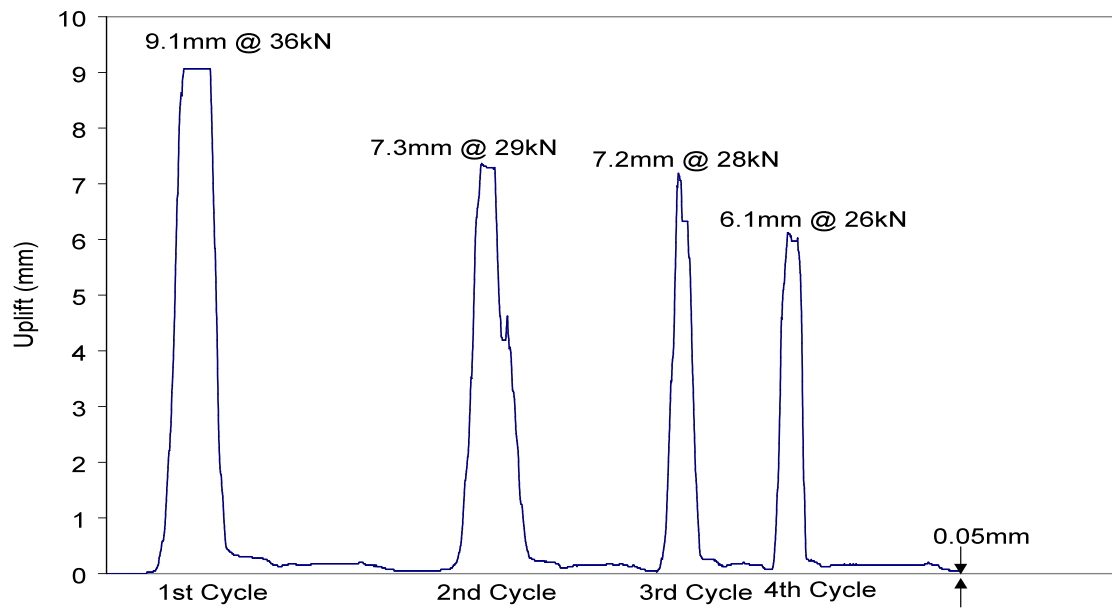
Figure 38: Uplift for Test Unit 1 at ±1.5 to 2% Drift

At a +3% drift, tension cracks did not visibly propagate further. The 4th set of cycles of the loading regime, Figure 24, Section 5.3, is associated with this drift level. Detachment of the facings from the straw-bales was visible, as shown in Figure 39. Further spalling continued on both facings, particularly on the plaster one. No further slip was observed at this drift level. The stroke capacity of the potentiometer (Potentiometer 7) used to measure uplift was exceeded, and maximum uplift recorded at the middle of the base box beam was 9.1mm, as shown in Figure 40.

Figure 39: Facing Separation at +3% Drift
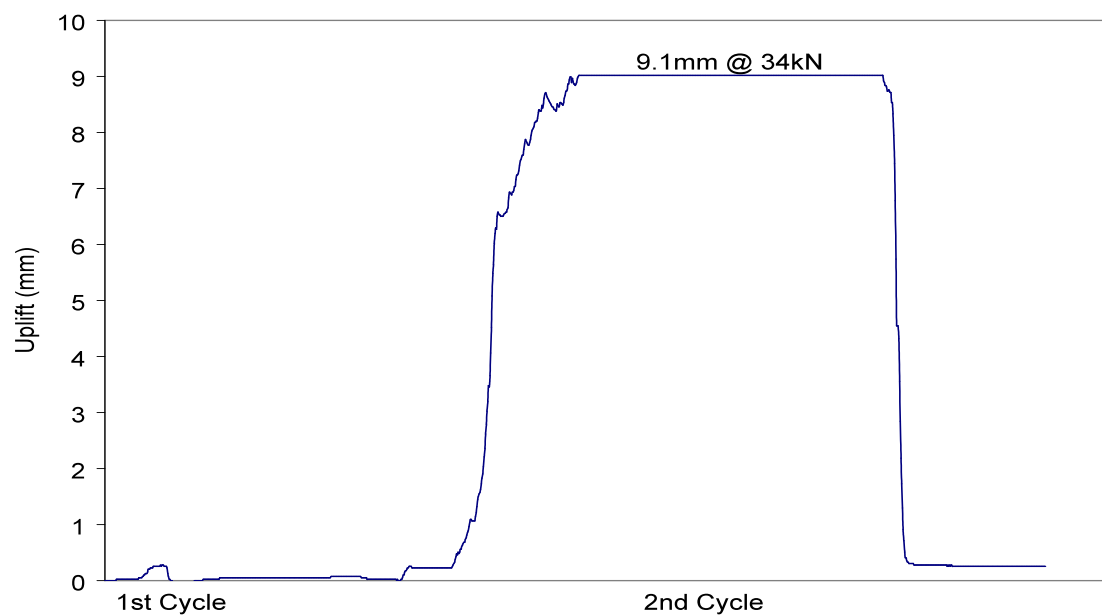
Figure 40: Uplift for Test Unit 1 at +3% Drift

6.2.2 FORCE DISPLACEMENT BEHAVIOR

The cyclic loading regime shown in Figure 25, Section 5.3 was applied to unit 1.

The lateral strength at roof displacements of ±19.05mm (0.75in) or ±0.75% drift was equal to approximately 31.6kN (7.1kips).   The hysteretic load displacement loops associated with the initial set of cycles of the loading regime are shown in Figure 41.

At ±1% drift, the lateral strength of test unit 1 was 39.1kN (8.8kips). The force displacement hysteretic loops shown in Figure 42 have been corrected for both uplift and slip. These loops are associated to the 1st set of cycles of the loading regime.

At ±1.5% drift, the maximum in-plane load applied was approximately 41.8kN (9.4kips). Figure 43 shows the hysteretic loops at this drift level and associated with the 2nd set of cycles of the loading regime.

At ±2% drift, unit 1 had a strength of approximately 44.4kN (9.9kips). This was the maximum lateral in-plane force the wall was subjected to. Figure 44 shows the hysteretic loops at this drift level and associated with the 3rd set of cycles of the loading regime.

At +3% drift, the maximum lateral strength dropped by approximately 20% from the previous value.   Structural failure is identified with this decrease in strength level (Park and Paulay, 1974). The force displacement hysteretic loop for a +3% drift is plotted in Figure 45, and is associated to the 4th set of cycles applied in the loading regime. The test was halted at this drift level to preserve the integrity of the frame for further tests.
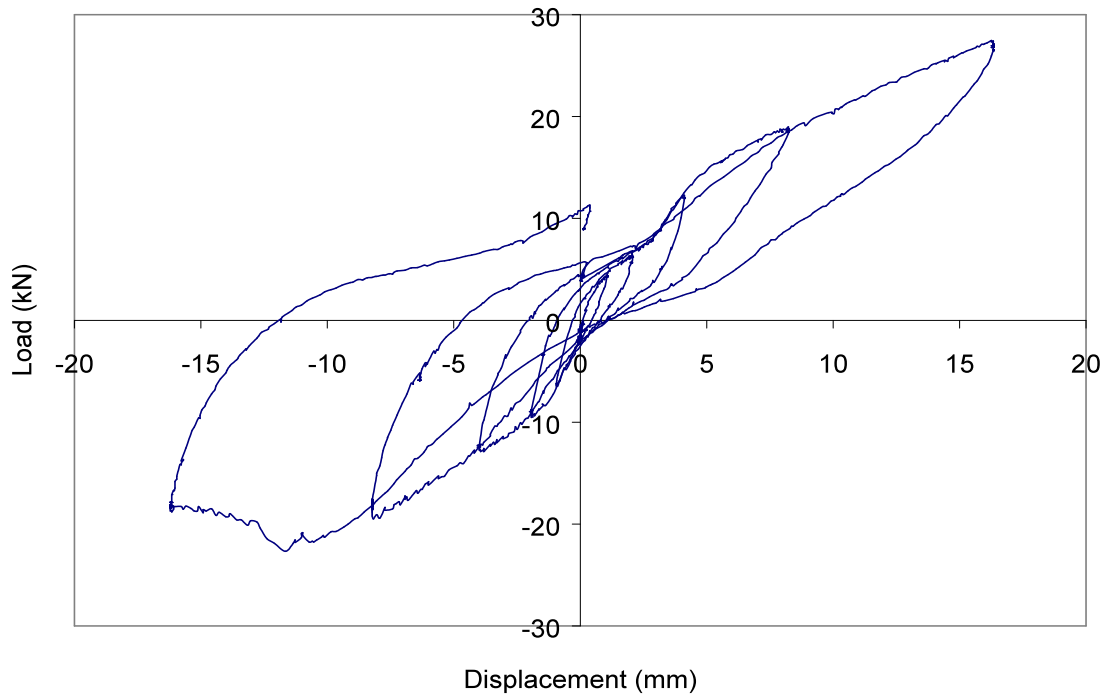
Figure 41: Hysteretic Load Displacement Loops for Test Unit 1 (±0.75% Drift)
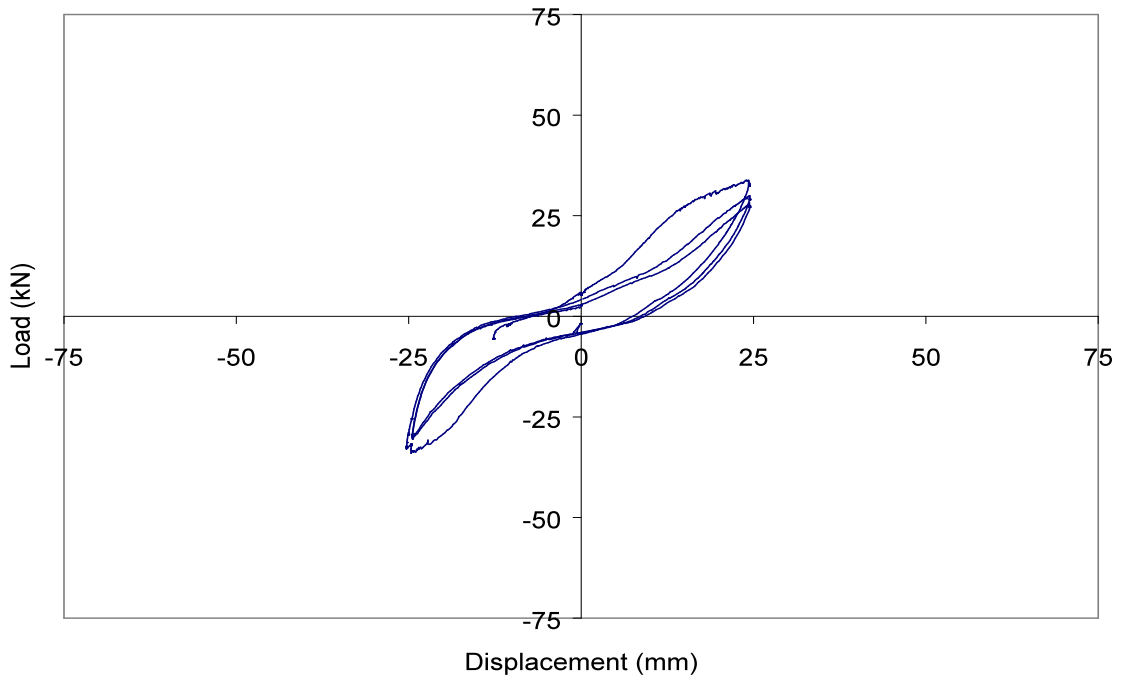
Figure 42: Hysteretic Load Displacement Loops for Test Unit 1 (±1% Drift)
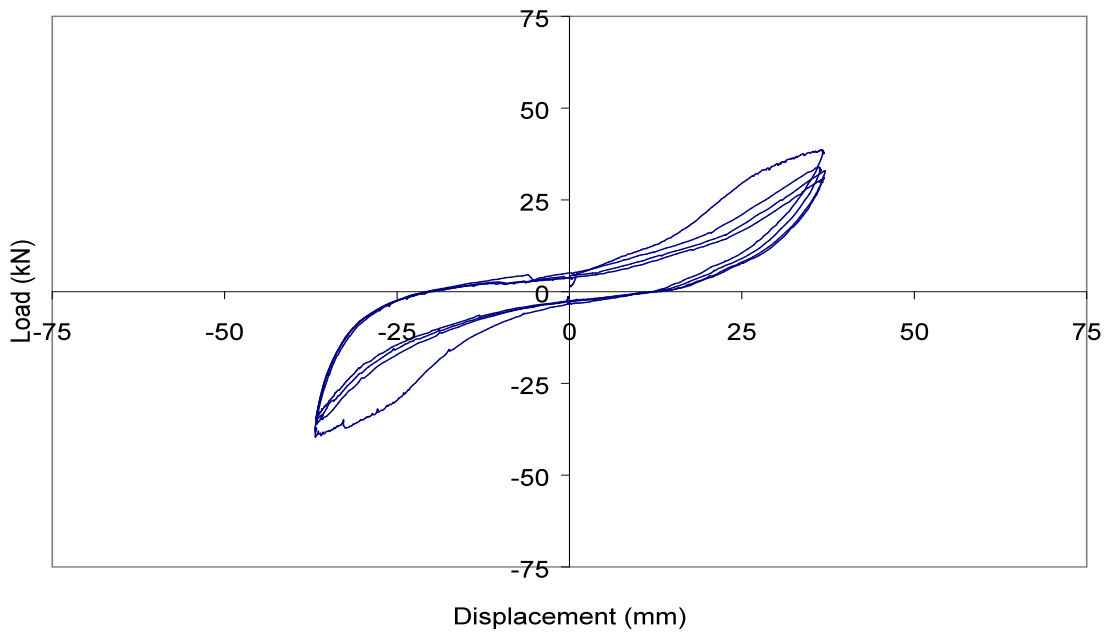
Figure 43: Hysteretic Load Displacement Loops for Test Unit 1 (±1.5% Drift)
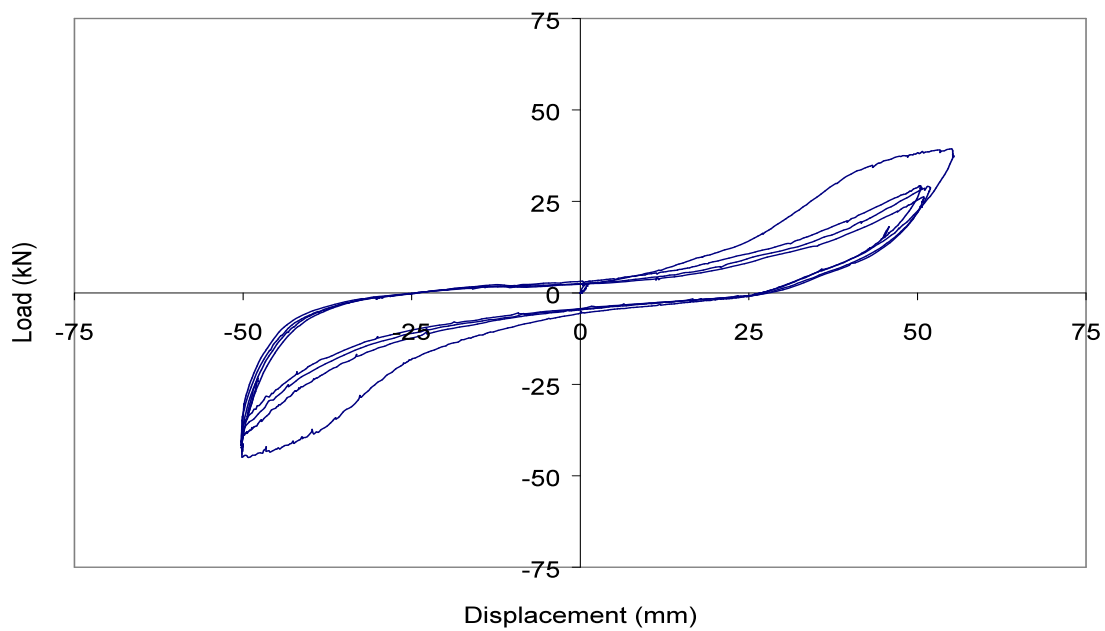
Figure 44: Hysteretic Load Displacement Loops for Test Unit 1 (±2% Drift)
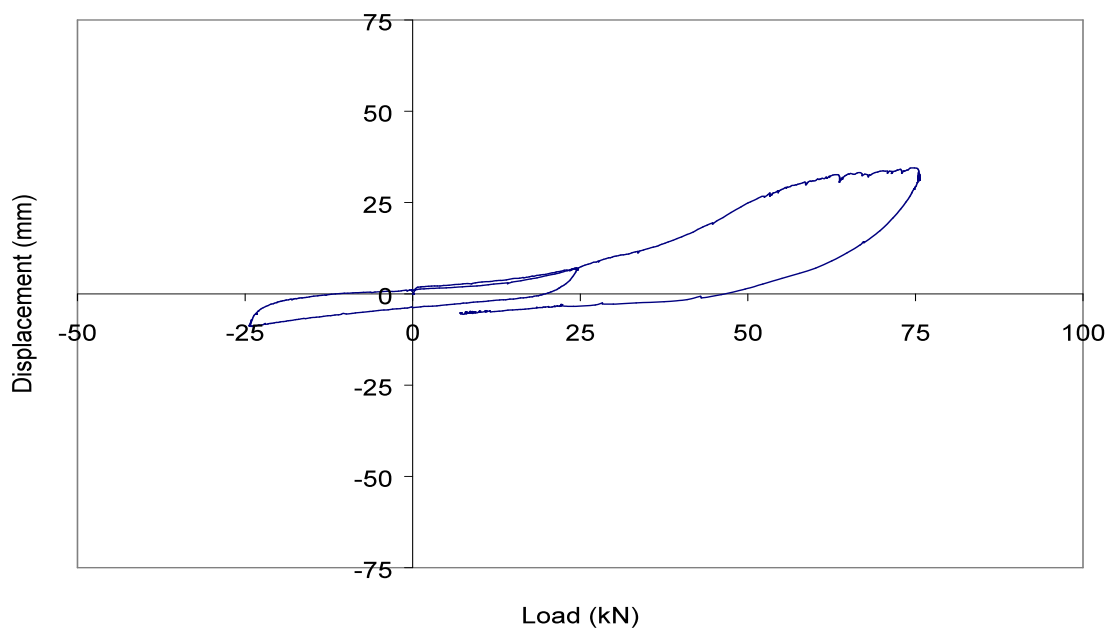
Figure 45: Hysteretic Load Displacement Loops for Test Unit 1 (+3% Drift)

Envelope curves were generated for unit 1 from the complete set hysteretic load displacement loops as presented in Figures 46 and 47. The curves represent the capacity of unit 1 in opposite directions.
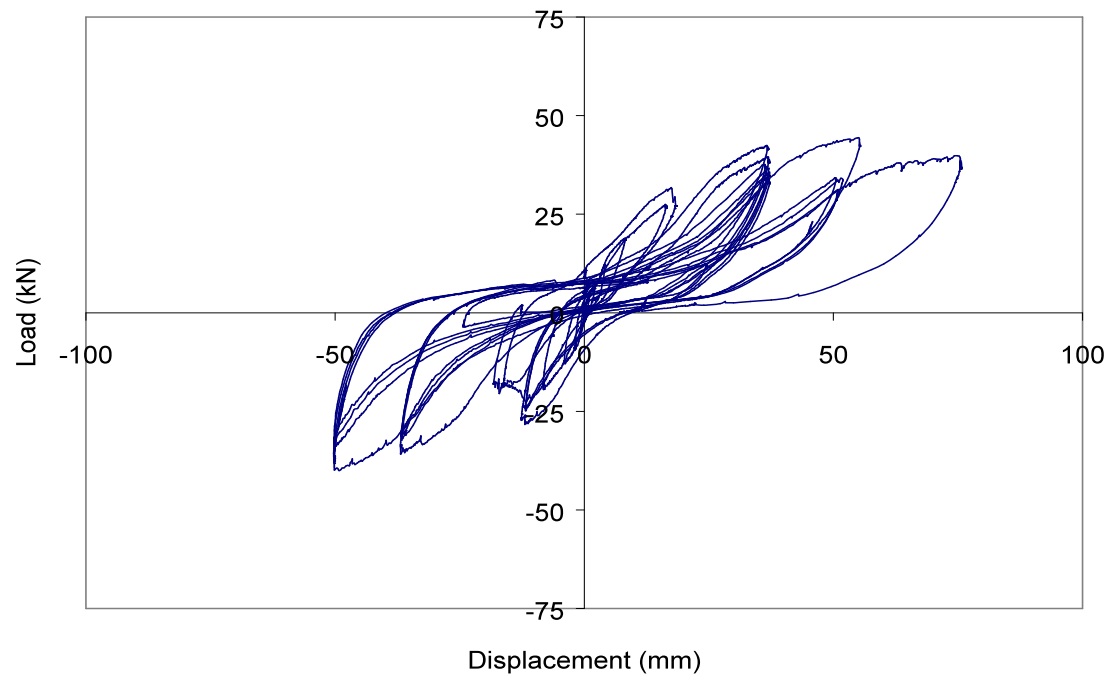
Figure 46: Complete Set of Hysteretic Load Displacement Loops for Test Unit 1
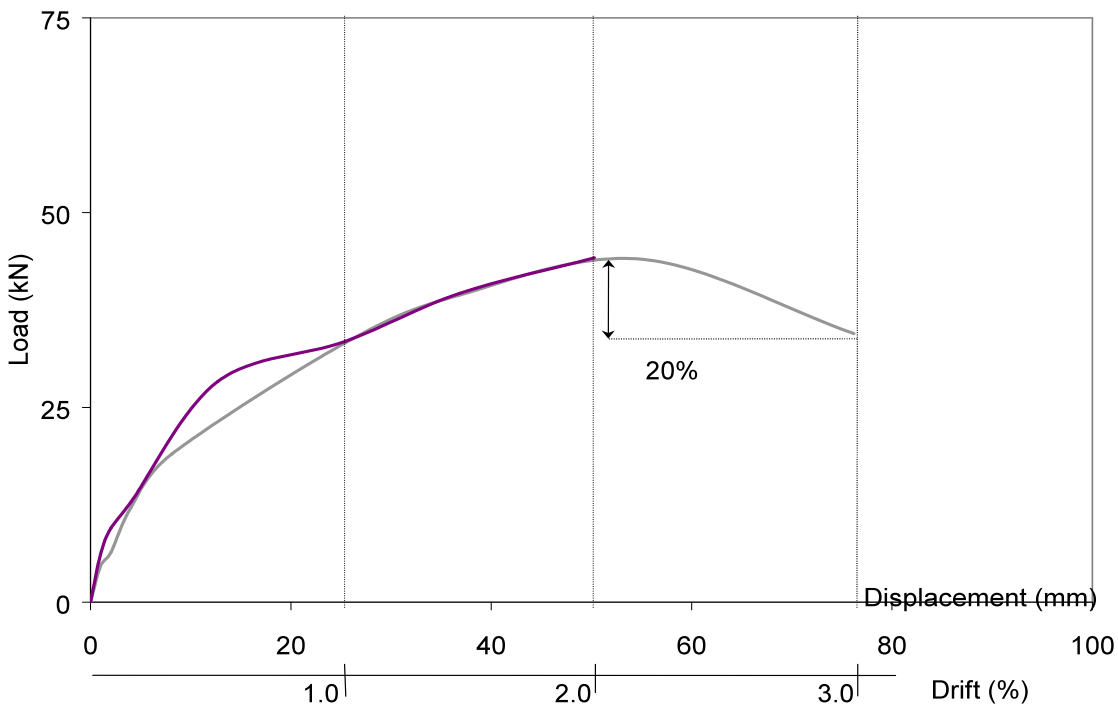
Figure 47: Envelope Curves for Test Unit 1

The energy dissipated by unit 1 was approximately 11.9kJ (105k·in). The individual and cumulative energy absorbed by each of the loops is presented in the following table. *ΣEnergy* represents the summation of the energy after every set of cycles from the loading regime. The last value in the column *ΣEnergy* represents the total energy absorbed by the wall unit.

Table 6: Energy Absorbed by Test Unit 1

Displacement / Drift	Energy Absorbed after n^{th} set of cycles from the Loading Regime	Σ Energy
<±25.4mm / <±1%	1.0kJ after initial set	1.0kJ
±25.4mm / ±1%	1.6kJ after 1st set	2.6kJ
±38.1mm/ ±1.5%	3.3kJ after 2nd set	5.9kJ
±50.8mm / ±2%	4.8kJ after 3rd set	10.7kJ
+76.2mm / +3%	1.3kJ after 4th set	11.9kJ

6.2.3 STIFFNESS DEGRADATION

The initial stiffness, $k_{initial}$, was obtained as the tangent to the unloading force displacement loop as depicted by the dashed line in Figure 48, shown as the ratio:

$$k_{initial} = \frac{LateralForce}{Displacement} = \frac{F}{\Delta} \ldots\ldots\ldots\ldots\ldots\ldots\ldots\ldots\ldots.(7.1)$$

The initial stiffness of unit 1 was equal to approximately 10.1MN/m (57.7kips/in). The area enclosed in the dashed circle represents an unusual behavior, since the increasing slope of the loop represents stiffening of the system. This effect may be attributed to the slipping of the unit with respect to the floor slab and once slippage stopped, the unit was able to develop more lateral resistance, represented by the steepening of the curve slope. The phenomena may also be attributed to the excessive oversizing of the A325 bolt holes, as they were done with a manual drill. The unit may have moved, represented as the decreasing slope of the loops. When the bolts finally hit the oversized hole perimeter, the slope becoming very similar to the initial stiffness slope, stiffness continued degrading.
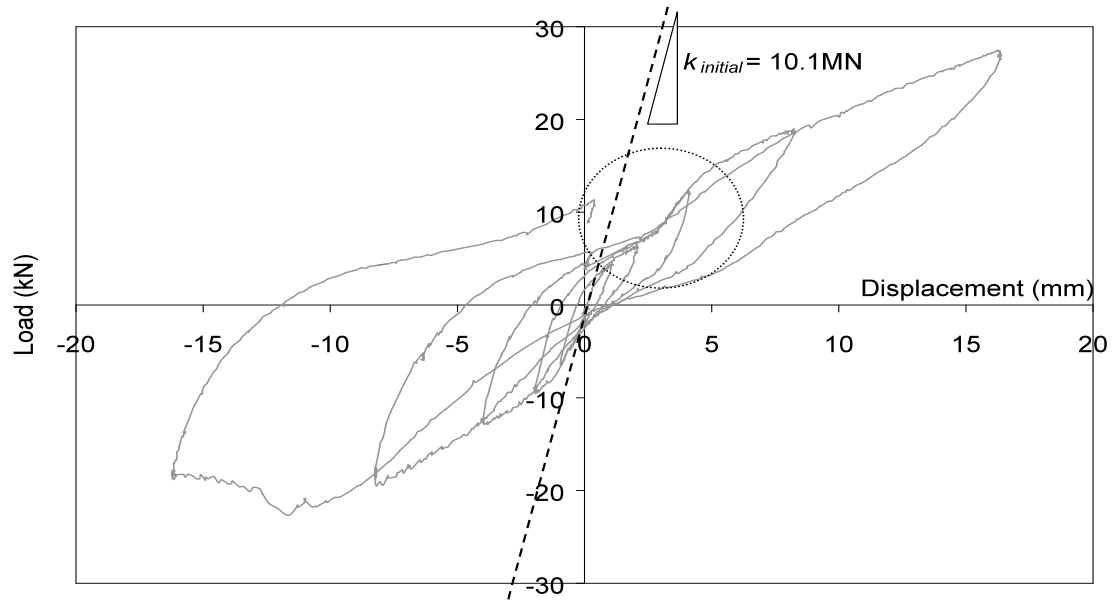
Figure 48: Initial Unit Stiffness, based on Force-Displacement Linear Relationship

At 0.05% drift, the stiffness dropped to a value of approximately 4.6MN/m (26.25kips/ft) when taken as the secant to the unloading portion of the force-displacement loop. Subsequent loading degraded the unit stiffness approximately 95% to a final secant stiffness of 0.5MN/m (3.4kips/in) at a drift of 3.1%. The progression of lateral stiffness degradation, k, of unit 1 is plotted in Figure 49 as a function of drift.
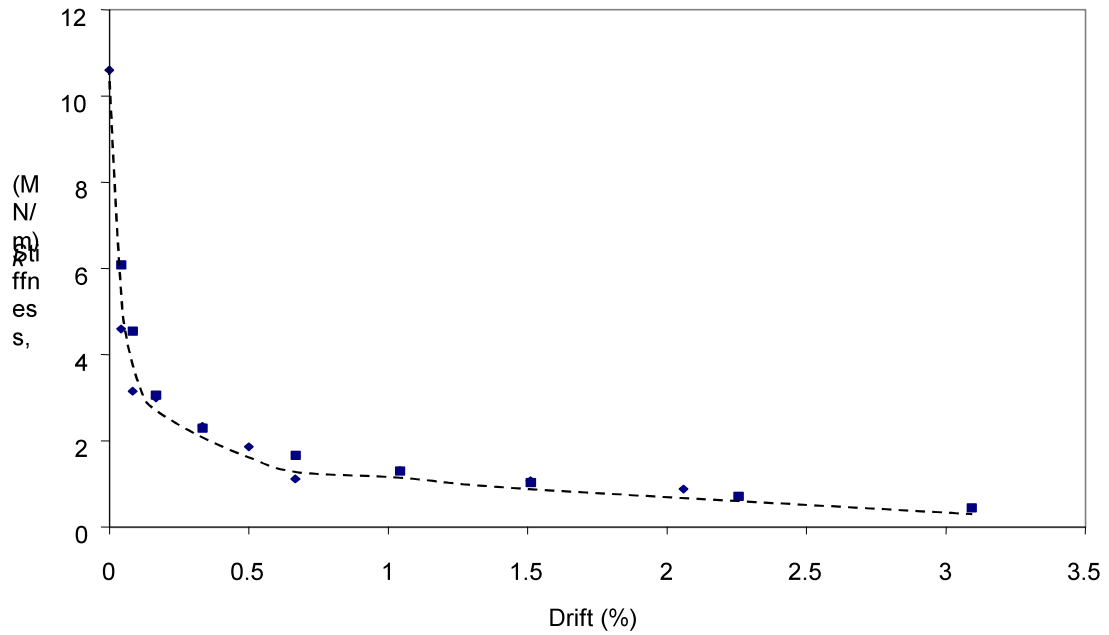
Figure 49: Stiffness Degradation, Test Unit 1

6.3 TEST UNIT 2

6.3.1 OBSERVATIONS

Test unit 2 was subjected to the repeated cyclic in-plane loading regime shown in Figure 25, Section 5.3. The load carrying mechanism was directed towards the facings, the material with the higher shear modulus, G. Tension cracks were observed only at the corners of the confined facings, with some measured uplift as the frame deformed throughout the test. Figure 50 shows a schematic of the observed behavior of test unit 2.
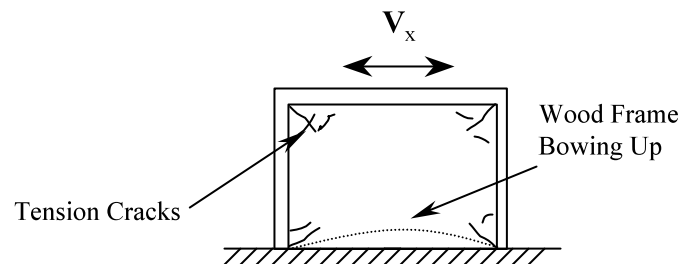
Figure 50: Schematic of Observed Behavior for Test Unit 2

The first diagonal cracks that were observed appeared at the top corners of the wall, approximately at roof displacements of ±25.4mm (1in), ±1% drift, associated to the 1st set of cycles of the loading regime in Figure 25, Section 5.3. No diagonal tension cracks appeared at the middle of the wall on either facing at this drift level. No slip occurred at this drift level. A 2mm (0.1in) maximum uplift at the middle of the base box beam was recorded at this drift level, shown in Figure 51.
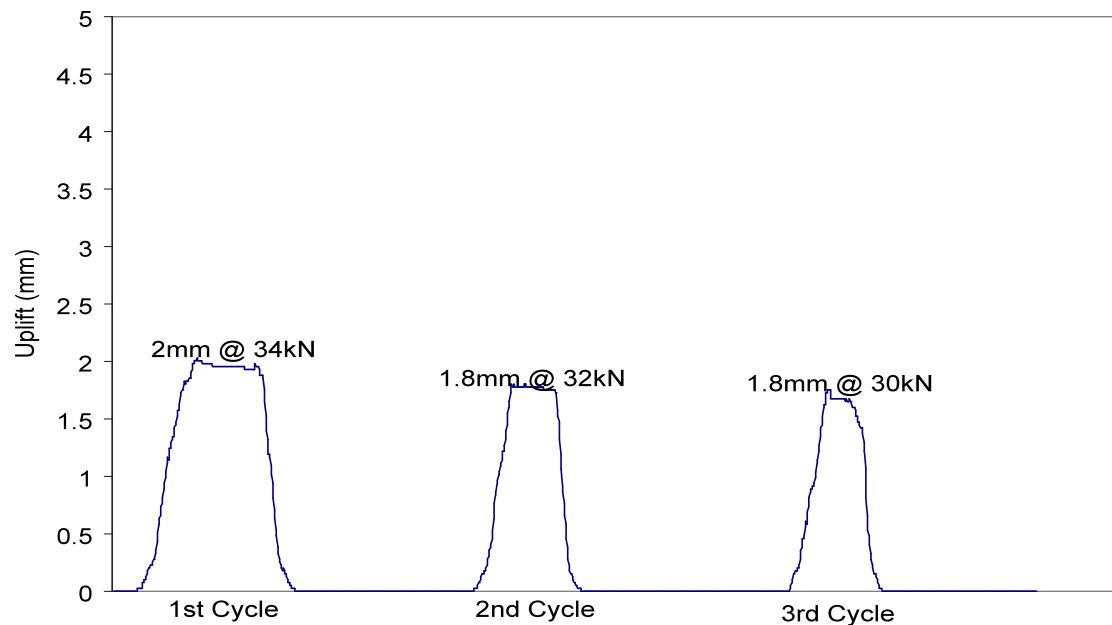
Figure 51: Uplift for Test Unit 1 at ±1.0% Drift

At ±1.5% drift, more tension cracks developed on the corners of the stucco and plaster facings and the existing ones propagated further. The plaster facing spalled considerably, as shown in Figure 52. This drift level is associated with the 2nd set of cycles of the loading regime (See Figure 25, Section 5.3). At this drift level, a maximum uplift of

3.4mm (0.13in) was recorded at the middle of the base box beam. No slip occurred at this drift level. Figure 53 is a plot showing the uplift levels at ±1% drift for unit 2.

Figure 52: Damage to Plaster Facing, Test Unit 2, at ±1.5% Drift
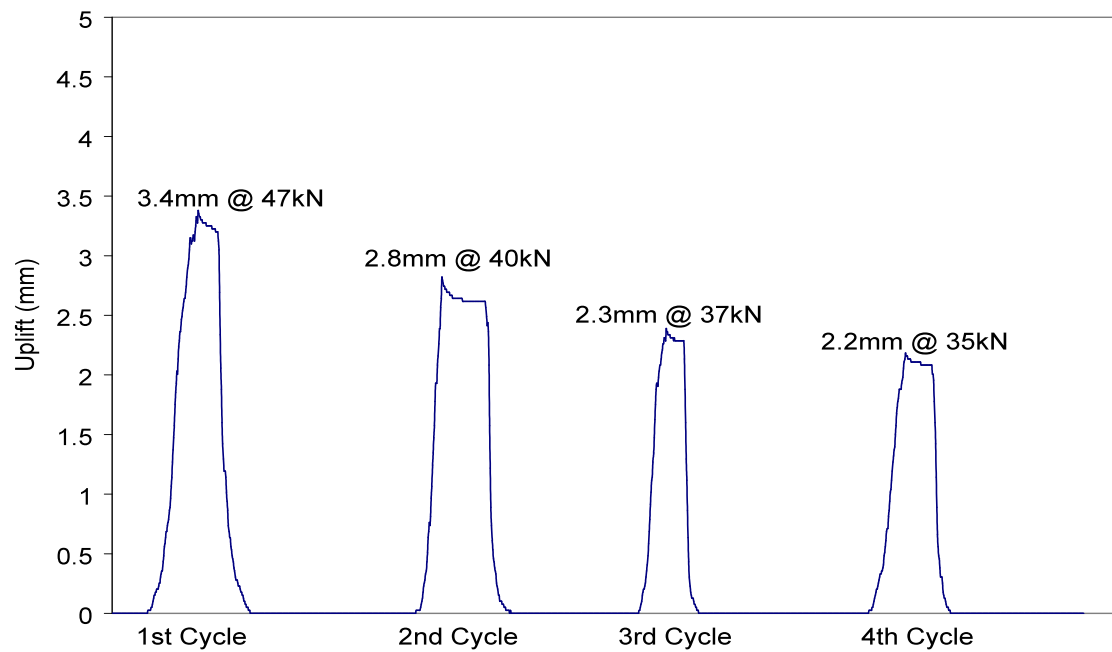
Figure 53: Uplift for Test Unit 1 at ±1.5% Drift

At 2% drift, equal to roof displacements of 50.8mm (2in), both facings began spalling due mainly to the confinement provided by the frame. This drift level corresponds to the 3rd set of cycles of the loading regime, Figure 25 of Section 5.3. Separation of the facings from the straw-bale surfaces and frame elements could not be observed because of the confinement. The maximum uplift recorded at the middle of the base box beam was 3.7mm (0.15in) as shown in Figure 54. No slip of the wall with respect to the floor slab was observed at this drift level. Spalling of both facings at the top corners continued until a +3% drift was achieved
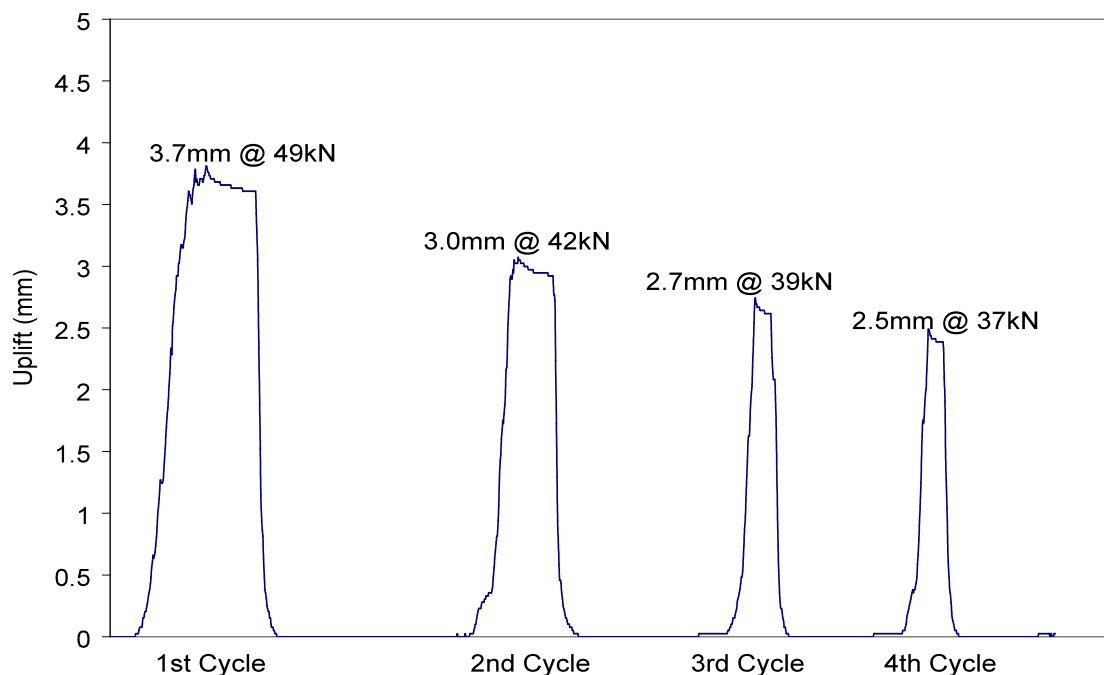
Figure 54: Uplift for Test Unit 2 at 2% Drift

At a +3% drift, the 101 by 101mm (4 by 4in) Douglas fir member of the built up column cracked in shear at about $^4/_5$ of its height, as shown in Figure 55. The 4th set of cycles of

the loading regime, Figure 25, Section 5.3 corresponds to this drift level. No slip was observed at this drift level. A maximum uplift of 5.3mm (0.2in) was recorded at the middle of the base box beam as shown in Figure 56. The test was stopped when the frame element cracked.
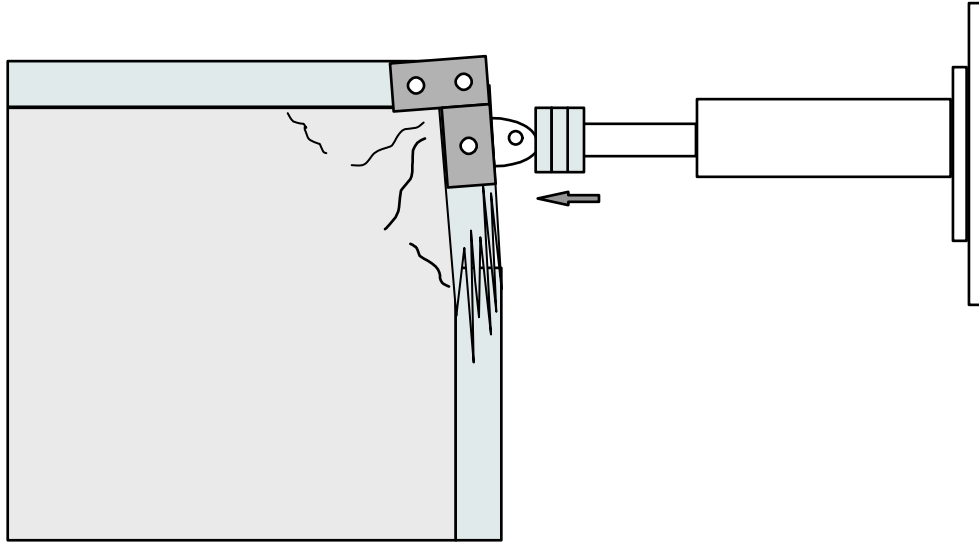
Figure 55: Schematic of Damage to Unit 2 at +3% Drift
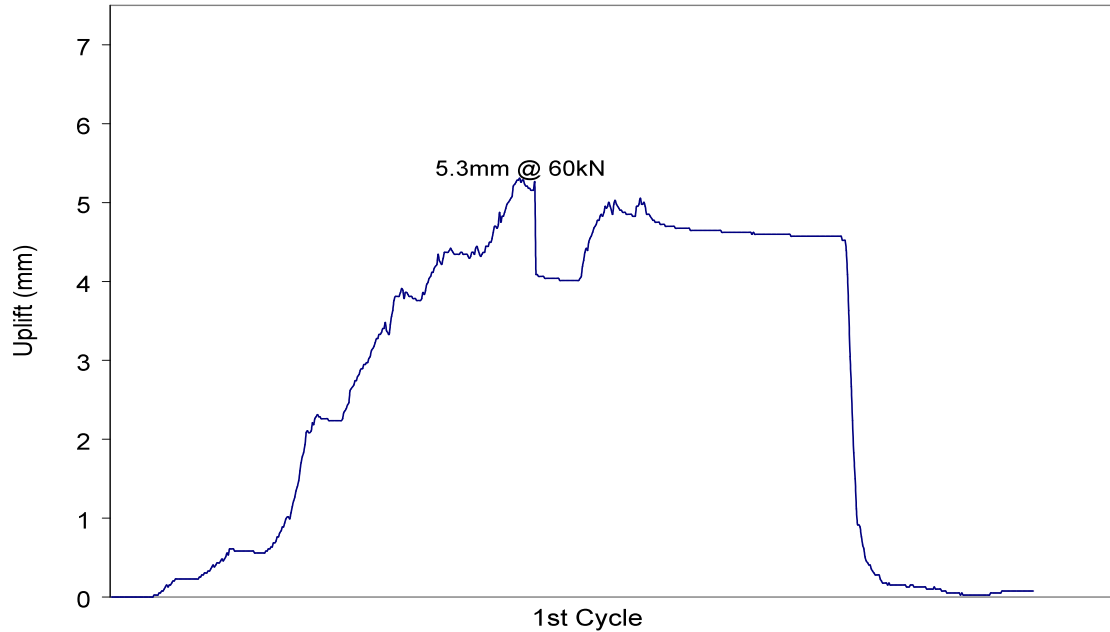
Figure 56: Uplift for Test Unit 2 at +3% Drift

6.3.2 FORCE DISPLACEMENT BEHAVIOR

The lateral strength at roof displacements of ±19.05mm (0.75in) or ±0.75% drift was approximately equal to 31.6kN (7.1kips).

At ±1% drift, the lateral strength of test unit 1 was 33.8kN (7.6kips). The force displacement hysteretic loops shown in Figure 57 have been corrected for both uplift and slip. These loops are associated to the 1st set of cycles of the loading regime.

At ±1.5% drift, the maximum in-plane load applied was approximately 47.2kN (10.6kips). Figure 58 shows the hysteretic loops at this drift level and associated with the 2nd set of cycles of the loading regime.

At ±2% drift, the maximum in-plane load applied was approximately 48.9kN (11kips). Figure 59 shows the hysteretic loops at this drift level and associated with the 3rd set of cycles of the loading regime.

At +3% drift, the maximum lateral strength recorded was 50.8kN (13.6kips). This strength dropped approximately 20% almost instantaneously when the frame element failed. The force displacement hysteretic loop for a +3% drift is plotted in Figure 60, and is associated to the 4th set of cycles applied in the loading regime. The test was halted at this drift level since the frame was no longer structurally sound and the subsequent values would not be representative.
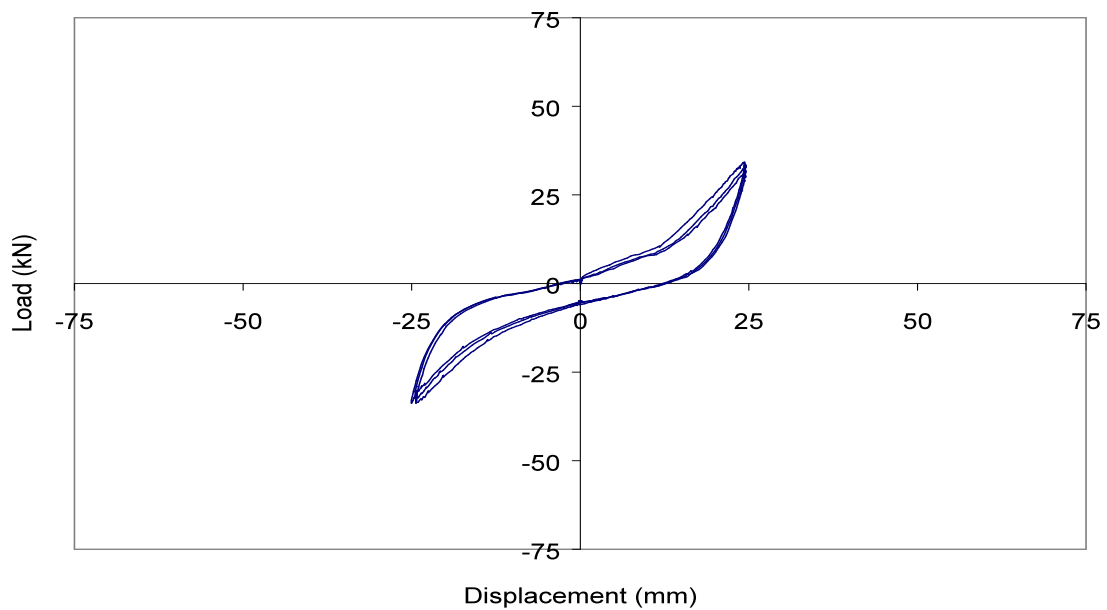
Figure 57: Hysteretic Load Displacement Loops for Test Unit 2 (±1% Drift)
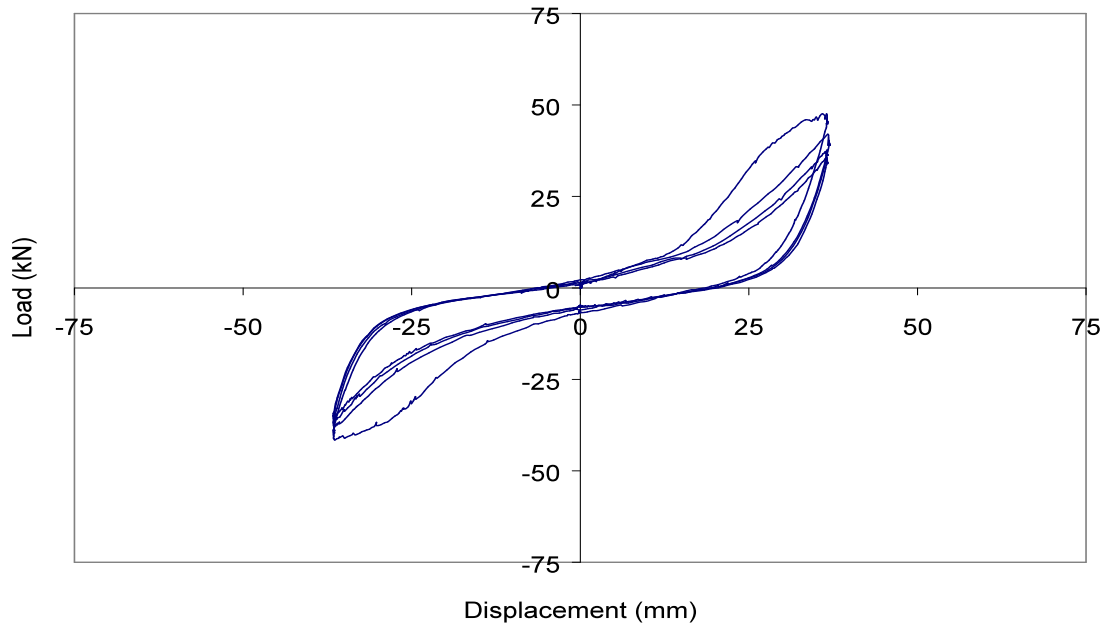
Figure 58: Hysteretic Load Displacement Loops for Test Unit 2 (±1.5% Drift)
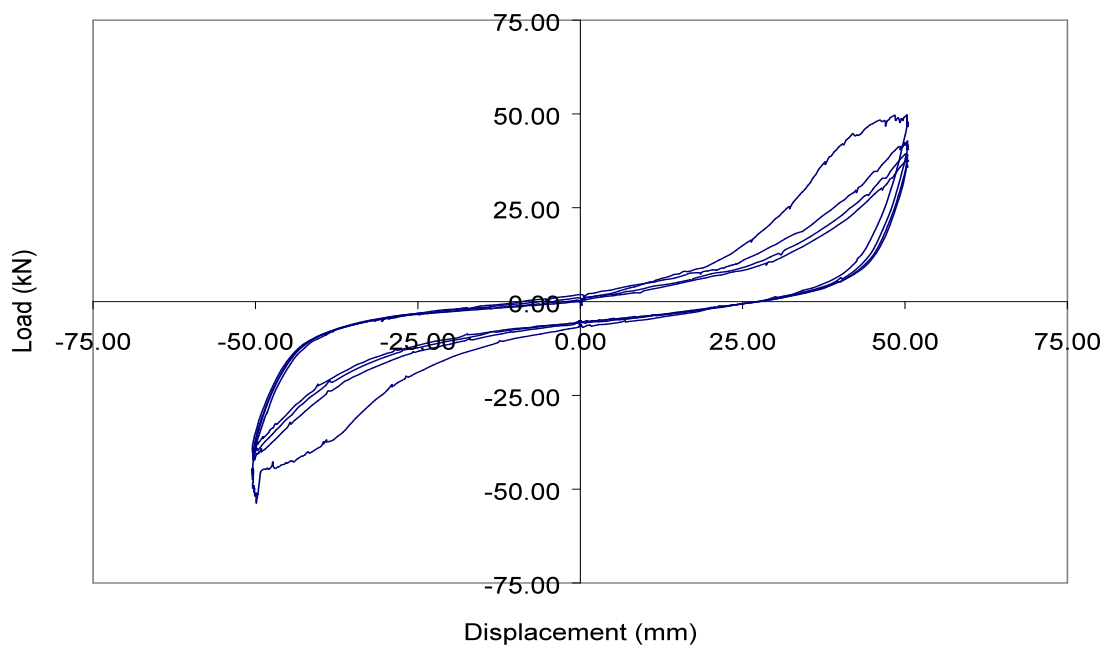
Figure 59: Hysteretic Load Displacement Loops for Test Unit 2 (±2% Drift)
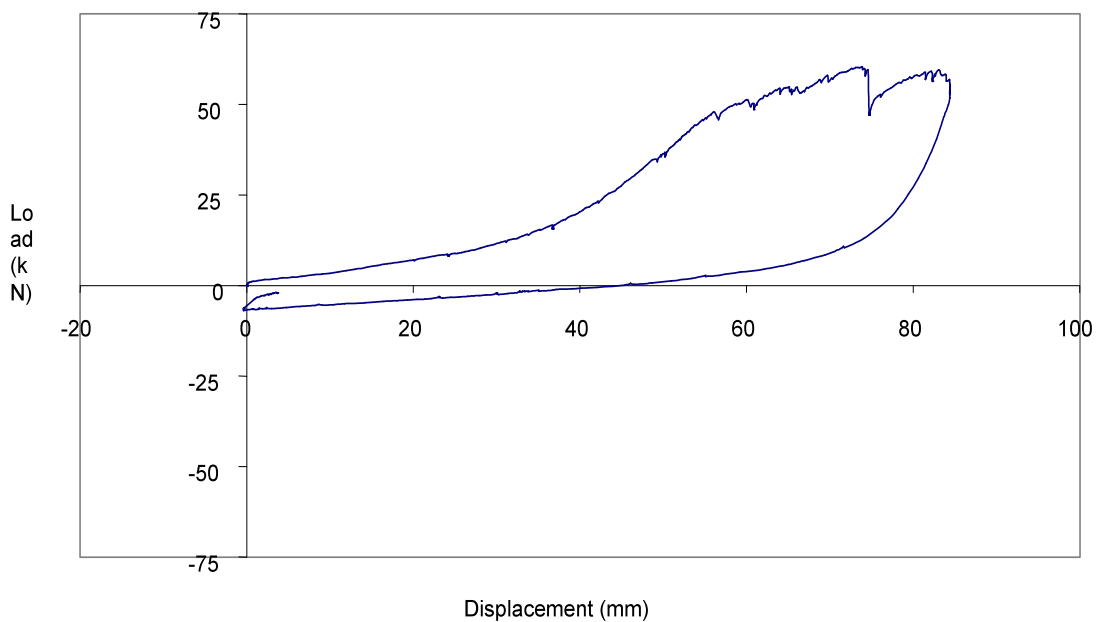
Figure 60: Hysteretic Load Displacement Loops for Test Unit 2 (+3% Drift)

Envelope curves, as presented in Figures 61, were generated for unit 2 from the complete set hysteretic load displacement loops, shown in Figure 62. The curves represent the capacity of unit 2 in opposite directions.
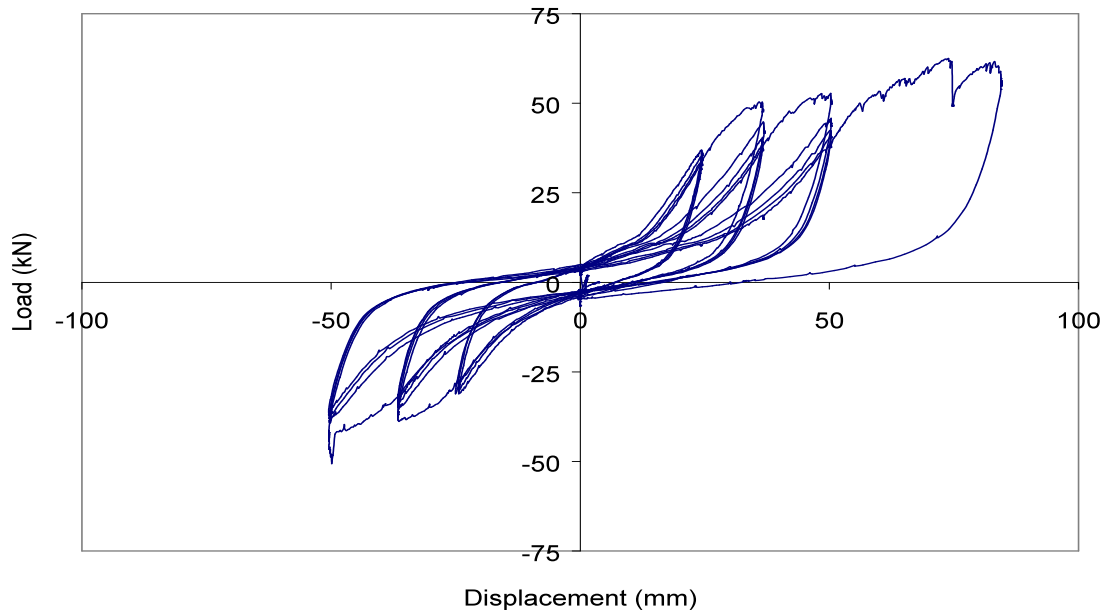
Figure 61: Complete Set of Hysteretic Load Displacement Loops for Test Unit 2
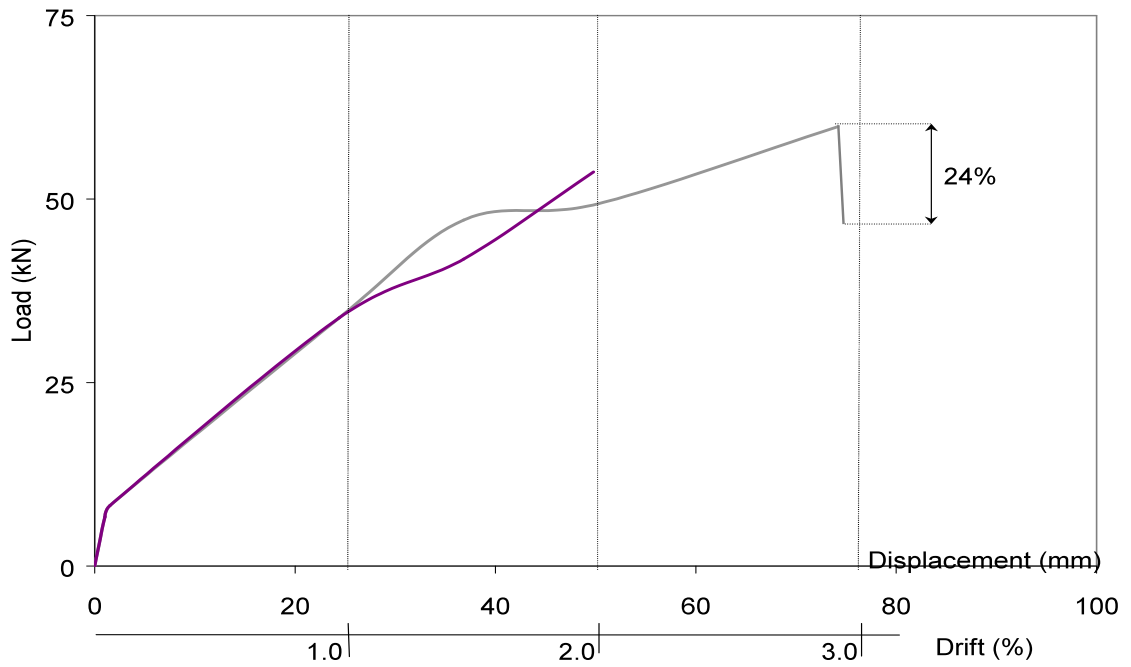
Figure 62: Envelope Curves for Test Unit 2

The energy dissipated by unit 2 was approximately 12.1kJ (107k·in). The individual and cumulative energy absorbed by each of the hysteretic loops is presented in Table 7. *ΣEnergy* represents the summation of the energy after every set of cycles from the loading regime. The last value in the column *ΣEnergy* represents the total energy absorbed by the wall unit.

Table 7: Energy Absorbed by Wall Units

Displacement / Drift	Energy Absorbed after n^{th} set of cycles from the Loading Regime	Σ Energy
±25.4mm / ±1%	1.4kJ after 1st set	1.4kJ
±38.1mm/ ±1.5%	3.6kJ after 2nd set	5.0kJ
±50.8mm / ±2%	4.9kJ after 3rd set	9.9kJ
+76.2mm / +3%	2.2kJ after 4th set	12.1kJ

7.3.3 STIFFNESS DEGRADATION

The initial stiffness of unit 2 was assumed to be 10.1MN/m (57.7kips/in). It degraded to approximately 6.6MN/m (30.8kips/in) at approximately 0.05%drift. Subsequent loading degraded it approximately 92%, to a final stiffness of 0.8MN/m (4.7kips/in) at a 3.0% drift, moments before the 101 by 101mm (4 by 4in) Douglas Fir section failed. Immediately after failure of the wood section, it degraded an additional 2%, to a final stiffness of 0.6N/m (3.6kips/in) at a drift of 3.1%. The progressively degrading lateral stiffness, k, of unit 2 is plotted in Figure 63 as a function of drift.
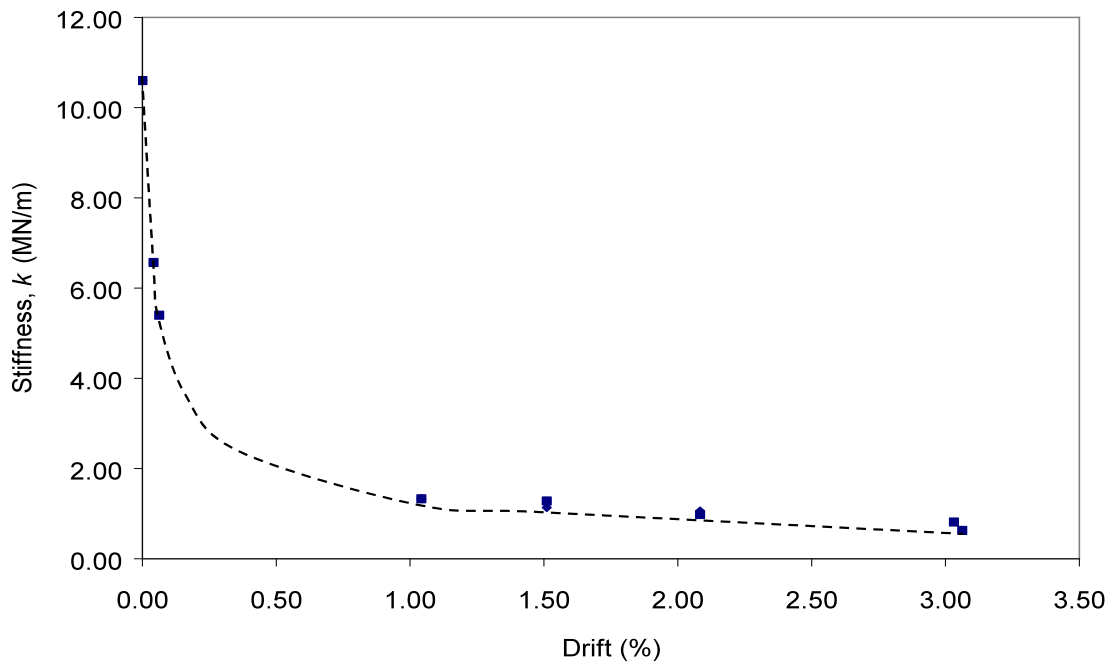
Figure 63: Stiffness Degradation, Test Unit 2

6.4 COMPARISON OF TEST UNITS AND BEHAVIOR

6.4.1 DIFFERENCES IN CONSTRUCTION

Unit 0 was an in-fill wall made with three string straw-bales, with two #4 A615 steel reinforcing bars per bale as vertical reinforcement, erected inside the post and beam frame with width dimensions proportional to those of the three string straw-bales.

Unit 1 was the same in-fill wall with wire mesh and expanded lath placed and attached to the frame and straw-bales to provide reinforcement for the stucco and gypsum-based plaster facings to be applied, as described in Section 4.1.3.

Unit 2 had the in-fill wall made with two string straw-bales. The frame constructed for unit 1 was used to unit 2, and was 16% less wide than the width dimension of the two

string bales. As a result, unit 2 was confined inside the original test frame. A new inner-perimeter frame was constructed with 2 wood lumber studs firmly attached inside the existing frame. The stucco netting reinforcement and lath was nailed to this inner-perimeter in order to provide the appropriate reinforcement for the facings.

The mass of the wall units varied by 9.5%, test unit 1 having a larger mass equal to 19.7kN (4.4kips) compared to a mass equal to 17.8kN (4.0kips) for unit 2.

6.4.2 DIFFERENCES IN OBSERVED BEHAVIOR

Unit 0 was observed to displace easily. Neither changes in uplift nor sliding of the unit with respect to the slab were recorded throughout the application of the monotonic loading.

Tension cracks on the facings applied on Unit 1 were observed at lower drift levels than with unit 2. Detachment of facings from the straw-bale plane and wood frame was clearly visible in unit 1, but could not be observed in unit 2 because of the frame confinement. Spalling was particularly visible in unit 1 around the location of the steel plate connections. The excessive spalling and cracking observed in unit 2 were influenced by the contributory compressive stresses from the confining frame. Unit 1 was seen to slide with respect to the floor slab at a drift level of +2%. With the anchoring bolts re-tightened, no further slip was observed. Unit 2 had no appreciable slip. Greater uplift was observed for unit 1 than for unit 2, in the order of 2½:1. The effect of slip and uplift on units 1 and 2 is shown in Figures 64 and 65. The frame used during the testing of unit 1 maintained its structural integrity, where one of the column elements cracked during the testing of unit 2.
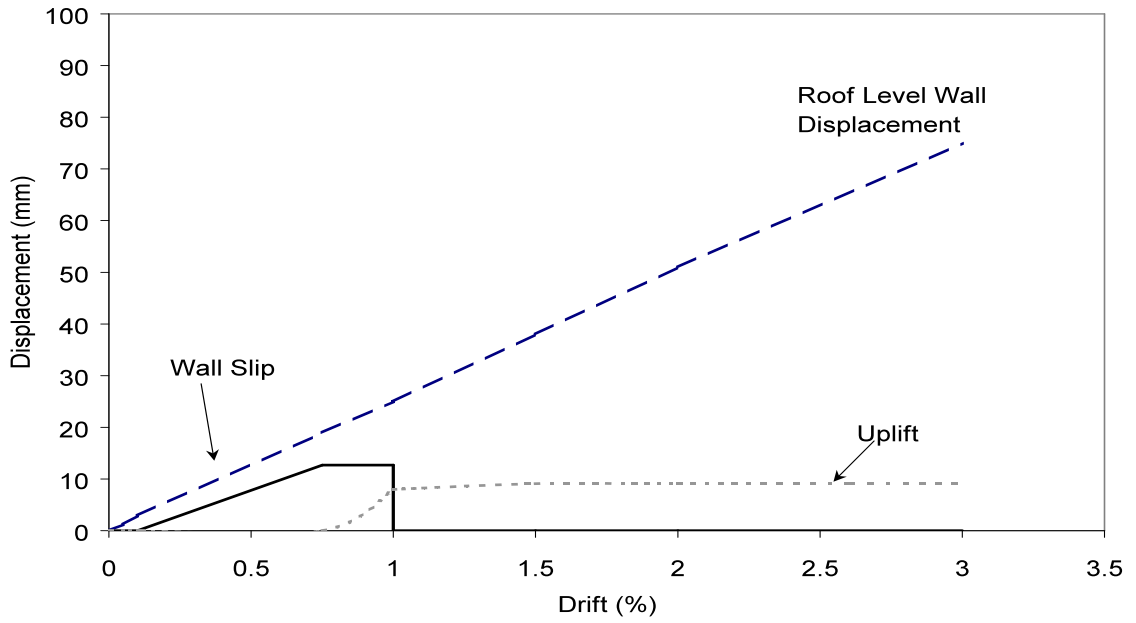
Figure 64: Uplift, Slip and Roof Level Displacement, Unit 1
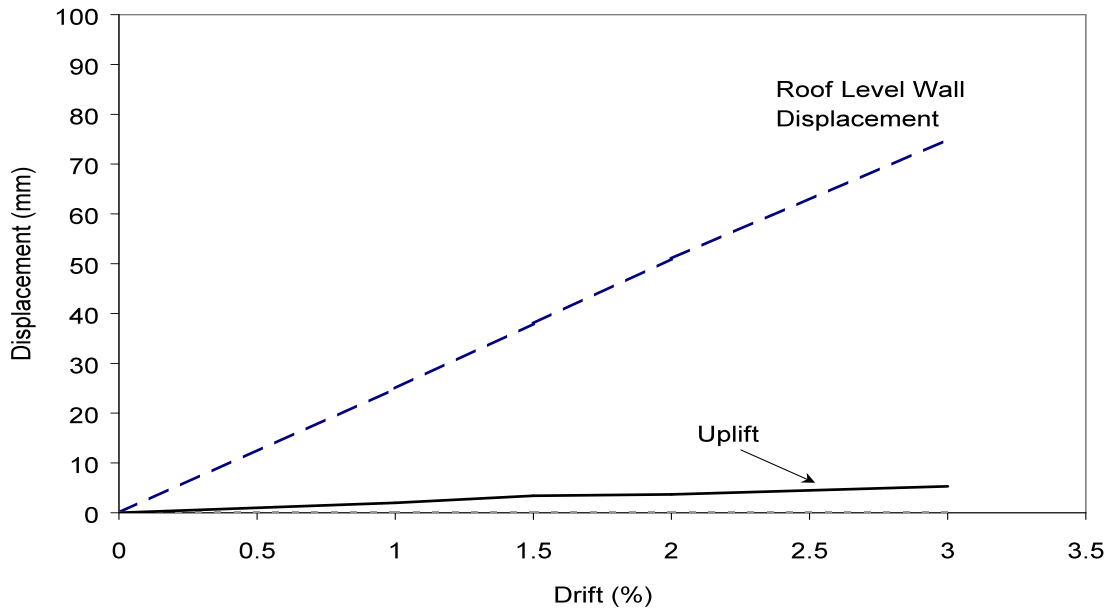
Figure 65: Uplift, Slip and Roof Level Displacement, Unit 1

6.4.3 DIFFERENCES IN FORCE-DISPLACEMENT BEHAVIOR

Unit 0 was loaded until the load resistance ceased increasing with subsequent lateral displacements. The test was promptly stopped to preserve the structural and geometric integrity of the bales. Although the three string wall unit's monotonic in-plane lateral load capacity was substantially less than Bou-Ali's (1993) units', the vertical plane's curved shape deformations observed appear to be very similar. The difference in resistance is attributed to higher pre-compression levels used by Bou-Ali (1993), as well as the longer wall dimensions of his units (2440mm (8ft) versus (3660mm (12ft)). Furthermore, Bou-Ali's (1993) units are representative of load bearing walls, and hence the construction technique varies from the one used for this study, representative of non-load bearing walls.

Since the response of straw-bale/facing walls to cyclic in-plane loading had not been quantified previously, the initial set of cycles of the loading regime used for unit 1 consisted of very small drift increments. The regime used for unit 2 consisted of larger initial drift increments, displacing directly to 1% drift on the first loading.

The maximum lateral resistance of unit 1 was approximately 44.2kN (9.9kips) and occurred at 2%drift. At +3%, unit 1 had lost 20% of this capacity.

Unit 2 had a lateral resistance at 2% drift of 53.7kN (12.1kips), 18% higher than unit 1. Unit 2 had a maximum lateral resistance of 60.4kN (13.6kips), at 3% drift. At a 3.1% drift, the frame cracked and the resistance of unit 2 dropped almost instantaneously by 20%. Both units were displaced to a drift level of 3%, at which, the resistance capacity was 80% of the maximum resistance recorded. Unit 2 had a maximum recorded lateral strength 27% higher than unit 1

Figure 66 shows a comparison of the envelope curves obtained for units 1 and 2 as a function of drift.
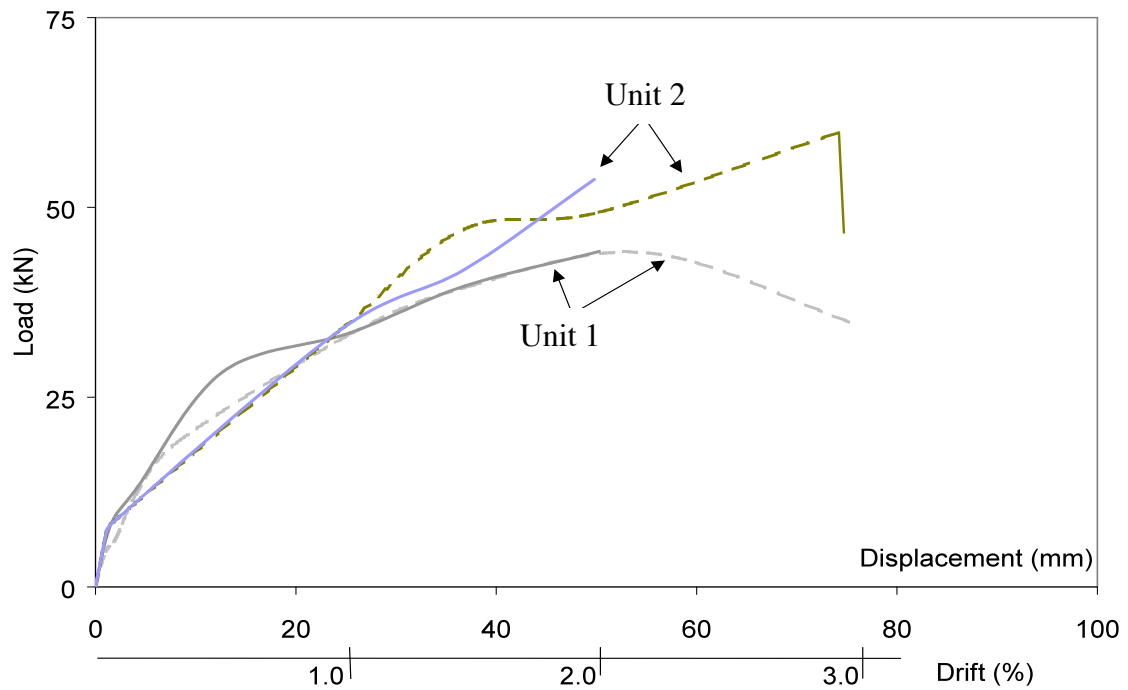
Figure 66: Envelope Curves for Units 1 and 2

6.4.4 DIFFERENCES IN ENERGY DISSIPATION CAPACITY

Unit 2 dissipated approximately 12.1kJ (107k·in) after application of the loading regime. This value was less than 2% greater than the amount of energy dissipated by unit 1, approximately 11.9kJ (105k·in). Figure 67 shows a comparison of the energy dissipation capacity of both units as a function of drift.
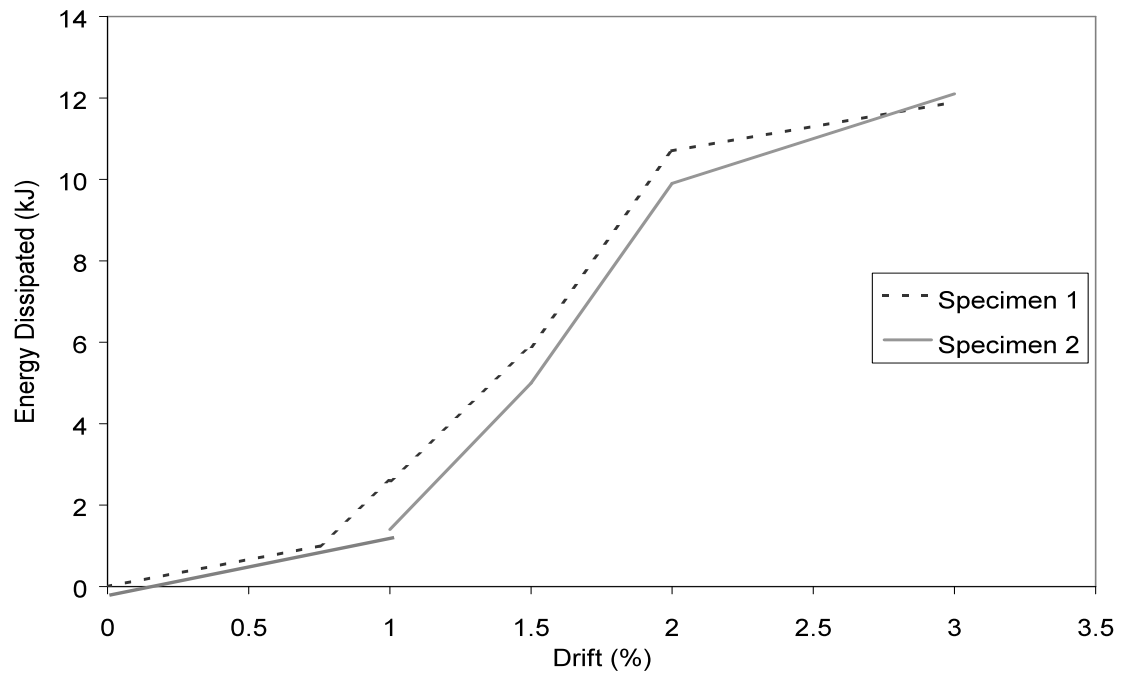
Figure 67: Energy Dissipation Capacity of Units 1 and 2

7.4.5 DIFFERENCES IN STIFFNESS

At a 0.05% drift, unit 2 had a lateral stiffness 7% greater than unit 1. After the cyclic loading, the stiffness degraded 95 and 94% for units 1 and 2, respectively, with unit 1 having a final stiffness 28% lower than the final stiffness of unit 2.   The progressive degradation of lateral stiffness, k, for both units can be seen in Figure 68.
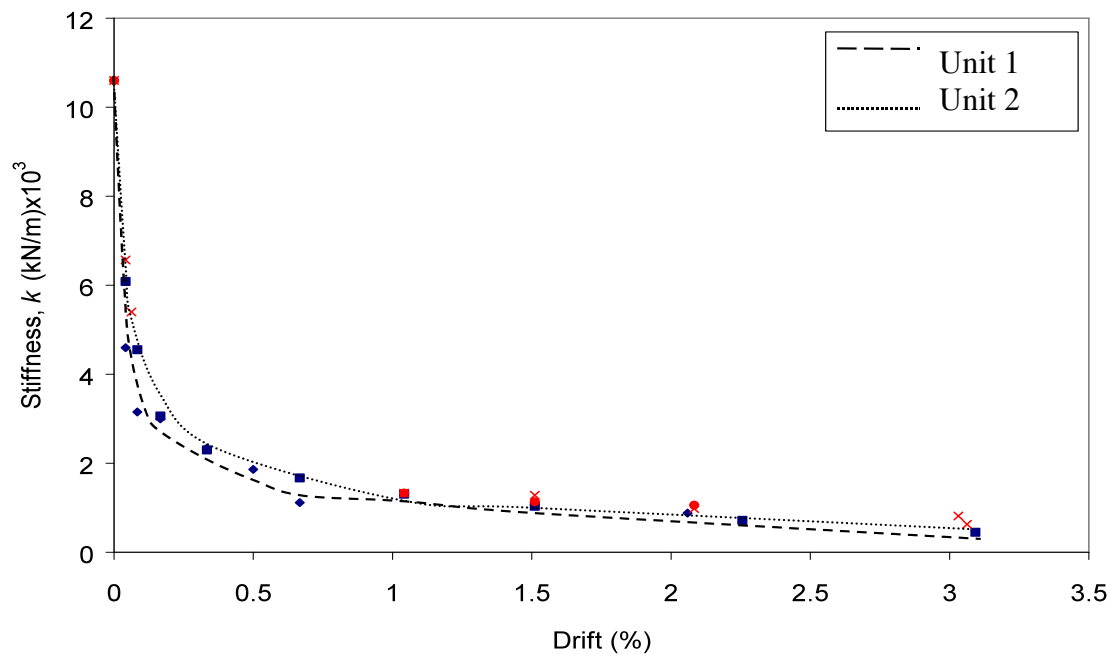
Figure 68: Stiffness Degradation for Units 1 and 2

CHAPTER 7: ANALYSIS OF RESULTS

The test data will be interpreted to allow useful design expressions to be developed as follow:

7.1 DESIGN STRENGTH

The strength of the walls should be developed using known material properties, so that design according to codes may be carried out. The design strength, V_y, should also be selected to represent the behavior of the structure represented as a bilinear oscillator as shown in Figure 69, with a Factor of Safety included in the selection of the strength.

Figure 69: Typical Force Displacement Curve
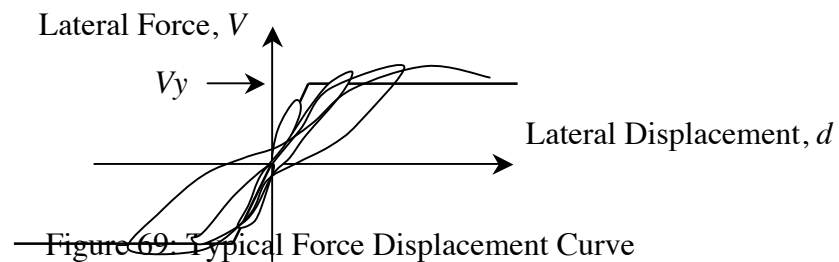
Since the shear modulus, G, times the width, w, of straw-bales is approximately 1/7 as stiff as the facings, then the facings are likely to carry the majority of the load at small drifts. It is assumed, probably conservatively, that the maximum strength may not exceed that predicted by ACI 318 (1995), $V = 0.1667\sqrt{f'_c}\,b_w d$ (MPa) (equivalent to $2\sqrt{f'_c}\,b_w d$ (psi) in English Units) for reinforced concrete members, due to the variability in stucco and plaster.

If the facings are inside the frame and confined by the frame, as was the case in unit 2, then the strength of the system is determined by the shear strength of the facings. Since

these facings are made from cementitious materials, a lower bound on the strength of the system is described as:

$$V = \alpha \cdot d(b_p \sqrt{f'_{cp}} + b_s \sqrt{f'_{cs}}) \ldots\ldots\ldots\ldots\ldots\ldots\ldots.(7.1)$$

Where f'_{cp} is the compressive strength of the plaster, f'_{cp} is the compressive strength of the stucco, b_p is the average thickness of plaster facing, b_s is the average thickness of stucco facing, d is the wall length, and α is a coefficient which will be found from the experimental work.

If the facings are outside the frame, as was the case in test unit 1, then the strength of the system is determined by the shear strength of the facings if the connection of the facings to the frame is good. However, the connection generally consists of nails continuously placed around the perimeter frame. When tensile stresses become large at the facing-frame connection, the facing fails in brittle manner. This will reduce the strength.

The 17-gauge stucco wire reinforcement also contributes to the strength. If only 17-gauge stucco wire was applied to the frame, and there was no straw or facing, then the stiffness would be expected to be low as a result of the initial flexibility of the 17-gauge stucco wire. The facing stiffens the 17-gauge stucco wire and the strength of the system is increased. However, at the nail connections, facing will often be between the wire and the nails. This facing may spal before the strength in the wires is activated. Because of the complexity of the behavior, this strength is not treated directly in this thesis.

The strength of this second type of unit will be more dependent on the type of connection. An upper bound on the strength may be obtained from Equation 7.1, but the strength will be reduced in proportion to the stress at each nail connection. A bolted connection torsional shear analysis is probably what is needed to find the demand resistance at each bolt. The resistance can be found by experimental work and depends on the strength of the facing, the stiffness of the nail connector and the edge distance.

Furthermore, during cyclic loading, slop develops in the facing beside the nails as the hole size increases. Since this experimental work was not carried out in this thesis, a lower bound design equation of the form shown below in Equation 7.2 will be used. It is expected that β will be less than α in Equation 7.1 if the compressive strengths of the facings, f'_{cp} and f'_{cs} are equivalent.

$$V = \beta \cdot d(b_p \sqrt{f'_{cp}} + b_s \sqrt{f'_{cs}}) \dots\dots\dots\dots\dots\dots\dots\dots\dots(7.2)$$

7.2 DESIGN STIFFNESS

If the materials wee to remain linear until failure, then the stiffness of the system would be constant and could be determined by standard means. However, for reasons described above, non-linearity occurs in the system and the stiffness is likely to decrease. For design, the stiffness of the units is required so that the structure may be analyzed as a bilinear oscillator.

Since the shear force (V)-shear angle (γ) equation of an elastic structure is given as:

$$V = GA\gamma = GA\delta/L \dots\dots\dots\dots\dots\dots\dots\dots\dots\dots\dots(7.3)$$

where the shear stiffness, V/δ, is given as GA/L. Since the system is not linear, the stiffness may be described as:

$$k = \kappa GA/L \dots\dots\dots\dots\dots\dots\dots\dots\dots\dots\dots\dots\dots(7.4)$$

where κ is a factor obtained from experimental results to account for non-linearity and is less than unity. To minimize subjectivity in the selection of stiffness from the data, it will be determined at a displacement of $0.75d_y$ where $d_y = H_y/k$ as shown in Figure 70.
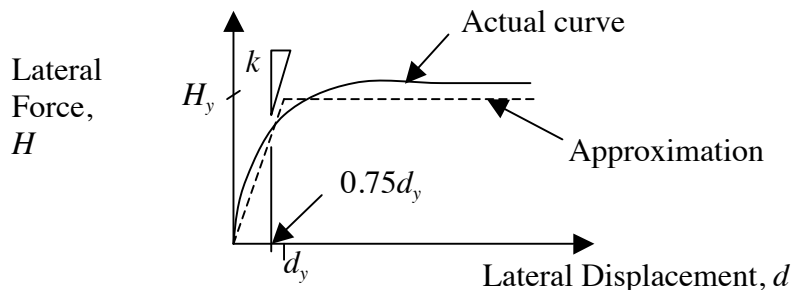
Figure 70: Schematic of Actual Load Curve and Bilinear Approximation

7.3 ENERGY DISSIPATION

Energy dissipation is required in the ATC-40 to determine the demand spectra. This energy dissipation is written as a ratio, R, of the energy absorbed to the energy of an equivalent rectangle with the same force and displacement peak values as shown in Figure 71. This energy ratio is converted into an equivalent damping ratio, ζ, as shown in Equation 7.5, which is defined as for each ductility, $\mu = d/d_y$. Assuming an initial viscous damping, $\zeta_o = 5\%$, then the total damping, ζ_{tot}, is given in Equation 7.6.

$$\zeta = R \text{ x } 2/\pi \ldots\ldots\ldots\ldots\ldots\ldots\ldots\ldots\ldots\ldots\ldots\ldots\ldots.(7.5)$$

$$\zeta_{tot} = \zeta + \zeta_O \ldots\ldots\ldots\ldots\ldots\ldots\ldots\ldots\ldots\ldots\ldots(7.6)$$
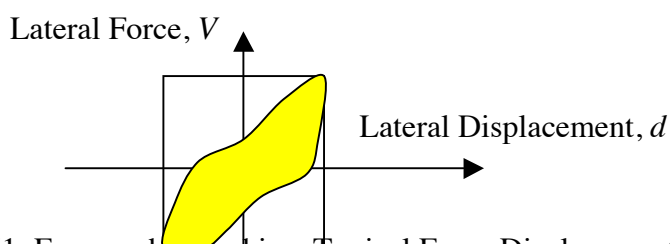
Figure 71: Energy absorbed in a Typical Force Displacement loop
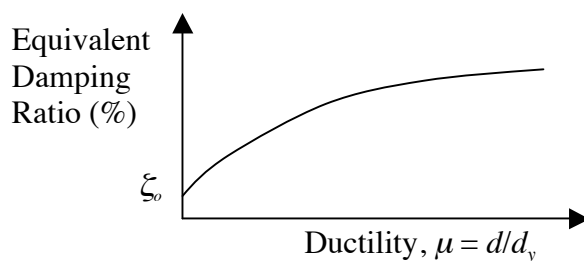
Figure 72: Energy absorbed in a Typical Force Displacement loop

If the equal displacement principle (Newmark and Hall, 1982) holds then the ductility factor, μ, is equal to the lateral force reduction factor which is described as R in the UBC (1997) or FEMA 302 (1998) Provisions.

The energy dissipation ratio, R, was calculated by using a mathematical function in MatLab, Version 5 (The Math Works Inc. Upper Saddle River, NJ) using the experimental load and displacement hysteretic loop data. Programming of the MatLab function was done previously by Jared M. Nelson of the University of Washington (PEER A2 Project, 1998).

7.4 ENVELOPE CURVES

An envelope curve is a representation of the lateral displacement as a function of the force applied to a structure. An envelope curve is obtained by plotting force displacement values related to significant strength degradation. Envelope curves are generated in order to approximate how a structure will behave after exceeding its elastic limit. From a envelope curve, a capacity spectrum and an acceleration-displacement response spectra are obtained to determine how a structure handles a seismic demand, or its performance, under ATC-40. Figure 73 shows a envelope curve generated from force displacement hysteretic loops.
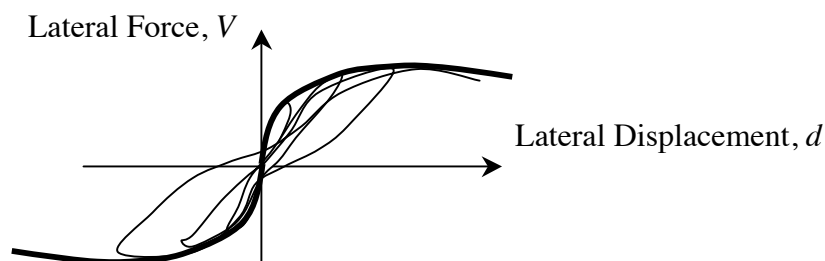
Figure 73: Generation of Envelope Curve based on Force
Displacement Hysteretic Loops

7.5 DEFINITION OF FAILURE

Failure is defined as being the point at which the strength decreases to less than 80% of the peak strength obtained (Park and Paulay, 1974). This is represented in Figure 74, where d_u is the failure displacement at 80% of the yield load, v_y.
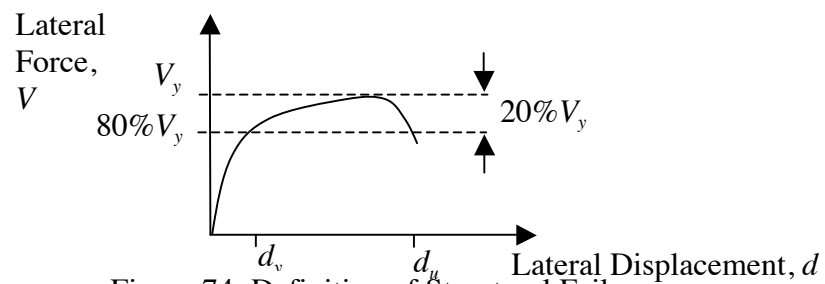
Figure 74: Definition of Structural Failure

CHAPTER 8: DEVELOPMENT OF DESIGN RECOMMENDATIONS

8.1 DEVELOPMENT OF MODEL

A computer model of the wall units was developed using an elastic analysis program (IES, 1998). The model is represented by Figure 75. Each of the materials used in the wall units can be represented by different elements in the model to better understand their contribution to the resistance of lateral forces. The model can also illustrate the load transfer mechanism in a simple way. The parameters used to develop the model elements were correlated to the experimental data.
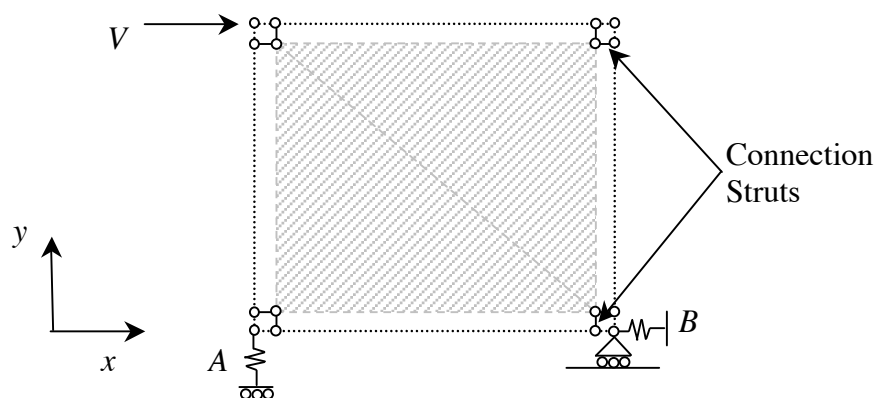
Figure 75: Schematic of Model of Test Developed for Linear Analysis Program

The model of the wall was analyzed at different drifts, and compared with the data obtained experimentally. The design parameters described in this chapter were used in the development of the model for better correlation with obtained data. The results of the linear analysis for a range of drifts between 0.05 and 2% are included in Appendix B.

8.2 DESIGN STRENGTH

As described in Section 7.1, the facings are likely to carry the majority of the lateral load. The facings are represented in the model by the hatched gray truss element.

However, other factors such as the 17-gauge reinforcement in the facings, the connection between the facing and the frame, and any moment resistance in the frame add to the ultimate strength of the wall units. Therefore, the design strength selected needs to represent the contribution of each of these elements. The model elements need to also represent the contribution of each so the behavior may be modeled more accurately.

The design strength, V_y, is defined as 80% (Park and Paulay, 1974) of the maximum lateral strength of the weaker test unit. This occurred at approximately 2% drift for test unit 1. The minimum of the two test strengths was used because the author did not want to rely on the effect of frame confinement on the test unit strengths unless more experimental data is available. This design strength is based only on these two units and engineering judgement should be used before applying these strengths to design of actual structures which may have different properties that those tested here.

The average compressive strength of the facings, f'_{cp} and $f'_{cs,}$ of unit 2 are 11.6 and 5.8MPa, (1050 and 845psi) respectively. The facings have an average thickness of 34.8mm (1.4in), and a horizontal dimension of 2.44m (8ft). Equation 7.1 is then equal to the following:

$$V = a \cdot 2.44m(\sqrt{11.6MPa} \cdot 0.0348m + \sqrt{7.4MPa} \cdot 0.0348m) \ldots\ldots\ldots\ldots.(8.1)$$

Equation 8.1 is equal to $V = \alpha \cdot 520.2$kN, and coefficient α may be calculated as $^1/_{15}$.

The average compressive strength of the facings, f'_{cp} and $f'_{cs,}$ of unit 1 are 7.4 and 16.2 MPa, (1075 and 2350psi) respectively. The facings have an average thickness of 34.8mm (1.4in), and a horizontal dimension of 2.44m (8ft). Equation 7.2 is then equal to the following:

$$V = \beta \cdot 2.44m(\sqrt{16.2MPa} \cdot 0.0348m + \sqrt{7.4MPa} \cdot 0.0348m) \ldots\ldots\ldots\ldots.(8.2)$$

Equation 8.2 is equal to $H_y = \beta \cdot 620.0$kN, and coefficient β may be calculated as $^1/_{17}$.

The values obtained from Equations 8.1 and 8.2 are to be considered lower bounds of the strength of the units tested. The contribution of the frame-facing connection is not considered in either equation due to the lack of information regarding its behavior.

8.2 DESIGN STIFFNESS

The stiffness of the test units was dependent on the shear deformation of the facing panel, and the stiffness of the frame-facing connection. If the materials had remained linear up until failure, then the stiffness would be constant and could be determined by standard means. However, for reasons described above, non-linearity occurred in the system and the stiffness decreased. This non-linearity was taken into consideration when developing the stiffness of the model elements and were adjusted for degradation according to drift.

The stiffness, k, of a structural system expressed as V/δ for linearly elastic materials, where V and δ are the lateral force and displacement at the top of the structure respectively. In order to model the actual behavior by a bilinear curve, the stiffness was characterized as the secant value to 75% of the design strength obtained on the first loading cycle, as shown in Figure 76. The initial stiffness of the test units, k_d, was equal to 4.6MN/m (26.25kips/ft).
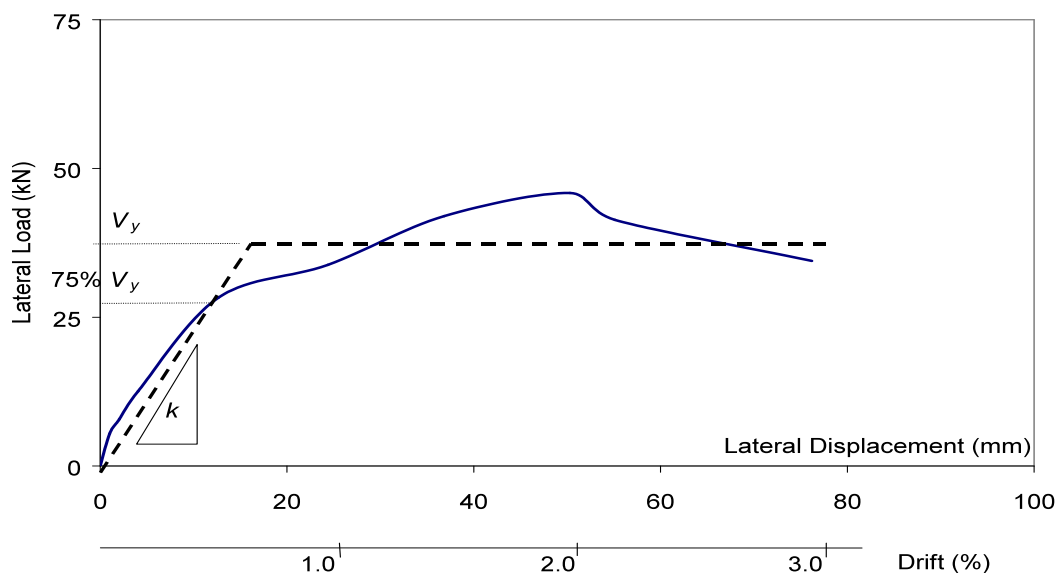
Figure 76: Schematic of Actual Load Curve and Linear Approximation

Equation 7.4 relates the actual measured stiffness, k, to that of an elastic structure, $GA_{To}t/L$, where κ is a modifier for non-linearity.

$$k = \kappa GA_{Tot} / L \dots\dots\dots\dots\dots\dots\dots\dots\dots\dots\dots\dots\dots(8.3)$$

Therefore, at a design strength, V_y, of 36kN (8.1kips), the representative stiffness, k, is equal to 4.6MN/m (315.1kips/ft). This can be expressed in terms of the properties of the materials used for the units as:

$$4.6\text{MN/m}=\kappa \, GA_{Tot}/L\dots\dots\dots\dots\dots\dots\dots\dots\dots\dots\dots\dots(8.4)$$

In this equation GA_{Tot} is the shear moduli and area of the structural system. Therefore, it may be written as:

$$GA_{Tot} = G_{Stucco}A_{Stucco} + G_{Plaster}A_{Plaster} + G_{Straw}A_{Straw}\dots\dots(8.5)$$

Based on the material properties values shown in Table 5, Section 3.7, and on the corresponding areas, Equation 8.5 becomes:

$$GA_{Tot}= 195.6MN + 100.1MN + 0.6MN = 295.7MN……(8.6)$$

As seen from Equation 8.6, the lateral resistance provided by the straw-bale in-fill wall is very small and may be neglected. Therefore, GA_{Tot} will be dependent only on the shear moduli, G, and area, A, of the stucco and plaster facings only. Equation 8.4 is therefore equal to

$$4.6MN = \kappa \cdot 295,700kN / 2.44m ……………………….(8.7)$$

Coefficient κ is calculated as 0.038 based on the material properties.

The design strength and stiffness are plotted as a function of drift in Figure 77 alongside the envelope curves obtained experimentally for both test units.

The stiffness previously obtained can be related to the contributing stiffness of each of the model elements, $k_{element}=AE/L$, by checking that the relationships between force and displacement in the model as a system and of the test units are equivalent, as seen in Figure 78. This was done by statics and geometry and checked at different drift levels on the model.
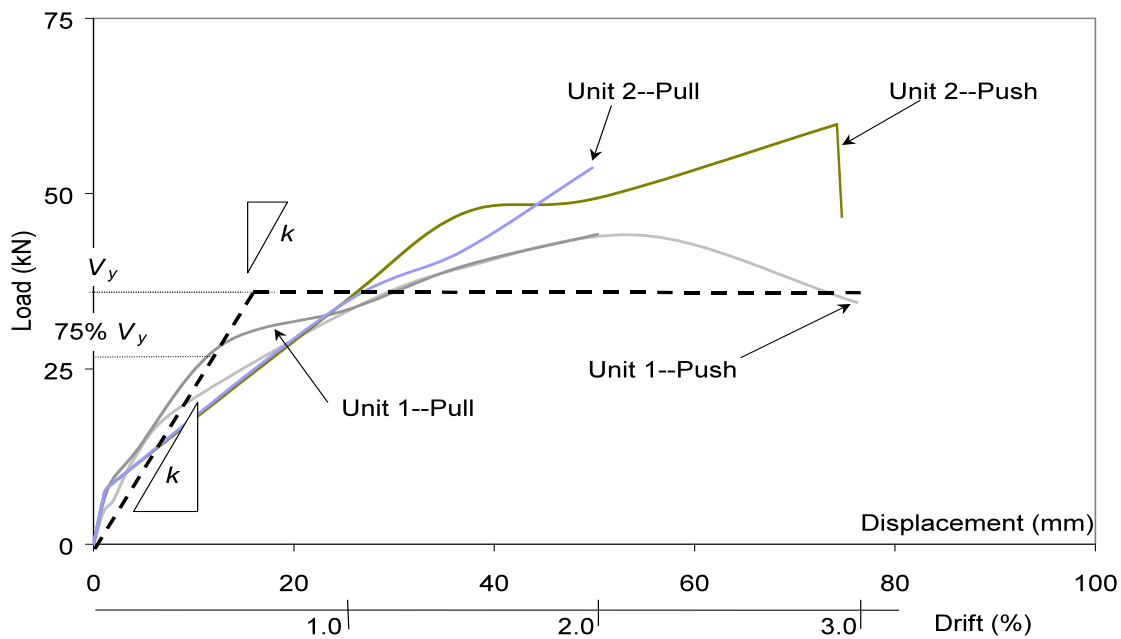
Figure 77: *Hy*, and *k*, as an Equivalent Bilinear Curve, and Envelope Curves for Test Units 1 and 2 versus Drift

a) Linear Model   b) Test Unit
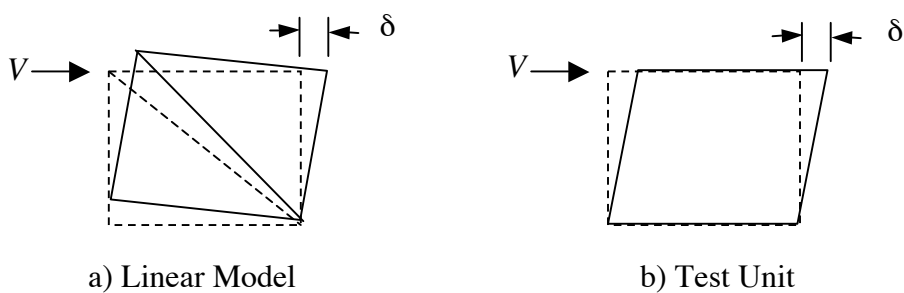
Figure 78: Schematic of Equal Force-Displacement Relationship between Model and Test Unit

The facing stiffness may be modeled by assigning properties to the strut in the truss element of the model related to the stiffness based on the material properties of the test units. In Equation 6.4, G is obtained from E, which is obtained from Equation 8.5.1 of ACI 318 (1995), $E = (w_c)^{1.5} 33\sqrt{f'_c}$, where w_c is the average of the density of the stucco/plaster, assumed to equal 100pcf, and f'_c, 1.7ksi, is the average of the compressive strengths obtained from compressive cube tests on the facings, shown in Table 2, Section 2.1. The force and displacement values obtained for the test unit 1 at 0.05% drift were used to determine the AE/L value for the strut, equal to 93.5x10^{6}kN/m.

The stiffness of the connection struts at the four corners represent the connections between the facings and the frame. These connections are continuous along the perimeter of the test units and since limited information is available on the behavior of this connection, the modeling technique used is approximate, as shown in the detail of one of the corners of the model on Figure 79. Further refinements based on better understanding of the complexities involved with the behavior of the connections could enable modeling of other structures.
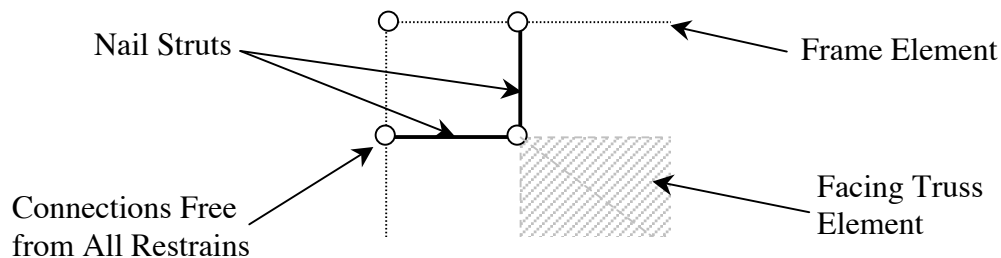
Figure 79: Nail Strut Model Connections

The connection struts modeled the reduction in stiffness due to the effects of degrading of the edges of the corner of the facings, as shown in Figure 80a. The high compressive stress concentrations caused by the confinement of the facings in unit 2, which would be expected to increase the strength as shown in Figure 80b, were ignored when modeling the frame-facing connections. The confining may cause higher facing forces but this

was not critical in the behavior of test unit 2 due to the facing degradation caused by the reverse cyclic loading applied.
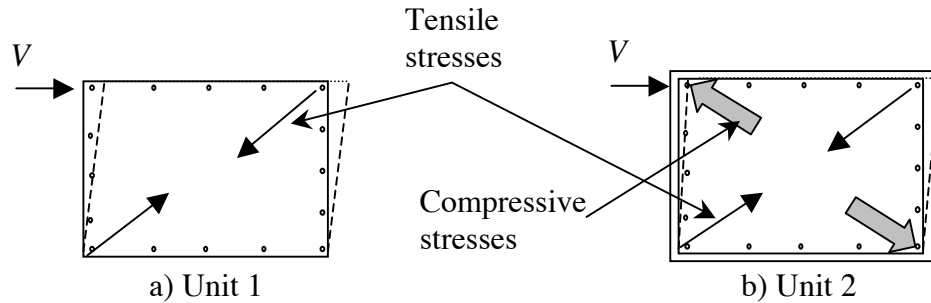
Figure 80: Deformations of Test Units

Attributing the stiffness of the test units to the frame-facing connection, the stiffness of the test units could be modeled at different drifts, as degradation of the system occurred (see Figure 68). The corresponding stiffness values were obtained by modifying the stiffness properties of the nails, given as $k_{connection-strut}= AE/L$, where A is the area of the nails, E the elasticity modulus and L the minimum length of embedment into the facing. The values for each of the connection struts stiffness required to correlate to the data are shown in Table 8.

Table 8: Stiffness Values Used for Connection Struts in Model

Drift (%)	$K_{connection-strut}$, AE/L (kN/m x 10^3)
0.05	19.51

0.1	13.15
0.3	9.76
0.5	7.21
0.75	5.94
1.0	5.51
1.5	4.67
2.0	3.82

The frame, both modeled and tested with pin connections, is represented by the dashed black element. The vertical elements were given properties corresponding to a 4 x 8 rough sawn dimension lumber section and the base and roof beams have section properties corresponding to a 4.5 x 5.5 southern pine glulam sections. Each section has respective material properties representative of those used in the test units. The contribution of the frame to the stiffness of the system was found to be significant due to the uplift and obtained during the test. E was given as 8275MPa (1.2ksi) by the program.

The spring element A modeled the uplift observed in the test units. The properties of the spring element consisted of a low moment of inertia ($I \cong 1 \times 10^{-25} \text{m}^4$) and AE/L, equal to 1523kN/m, was adjusted to match the uplift level at all drift levels. The spring assumes rotation of the model about the bottom-left corner, while the uplift of the test units was due to the base beam deforming by flexure due to the moment induced by the slab connection not being at the center of the frame connections. Therefore, the modeling of this element is also approximate. These behaviors are illustrated in Figure 81

.

a) Linear Analysis Model   b) Test Unit Behavior
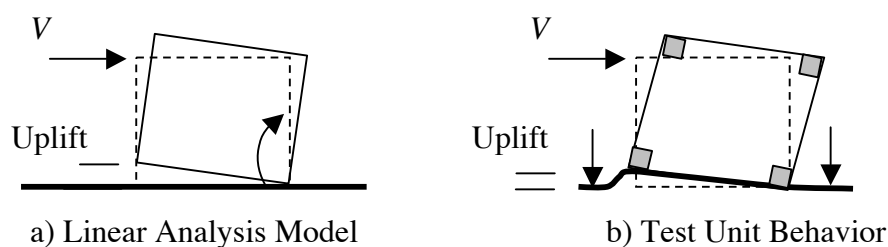
Figure 81: Comparison of Model Behavior vs. Observed Test Unit Behavior

Spring element *B* modeled the slip of the test units. Since very little slip with respect to the slab was observed, the spring was modeled as very stiff and was given a moment of inertia value $I = 500 \text{m}^4$. The *AE/L* value used for this element was $215 \text{x} 10^9 \text{kN/m}$.

8.3 ENERGY DISSIPATION

The hysteretic energy dissipation capacity of each test unit was calculated as described in Section 7.3.1 and presented in Section 6.2.2, Table 6 and Section 6.3.2, Table 7.

The ratio, *R*, for each of the test units was determined at 2% drift. Force-displacement values were not representative at subsequent loadings due to unit failure. The ratios obtained are conservative since the equivalent rectangular areas were based on the first absolute maximums of the hysteretic loops, and not reduced as the maxima of subsequent loops' degraded with each cycle. Therefore, the ratio, *R*, at 2% drift was approximately 13.5% and 11.7% respectively for unit 1 and 2. These ratios were converted to equivalent damping ratios, ζ, based on Equation 7.5, $\zeta = R \times 2/\pi$. The damping ratios were 8.6% and 7.4% respectively for unit 1 and 2.

Assuming an initial viscous damping of $\zeta_0 = 2\%$, then the total damping, ζ_{tot}, is given as follows:

$$\zeta_{tot} = \zeta + \zeta_0 \quad \dots\dots\dots\dots\dots\dots\dots\dots\dots\dots\dots\dots\dots.(8.6)$$

Hence, $\zeta_{tot\#1} = 10.6\%$, and $\zeta_{tot\#2} = 9.4\%$ respectively for unit 1 and 2. For design purposes, a damping ratio of $\zeta_{tot} = 10\%$ should be used.

The yield displacement, d_y, 19mm ($^3/_4$in) of the wall units is assumed to have occurred at approximately 0.75% drift.. The limit drift capacity of the wall units, γ_u, occurred at

approximately 3%. The maximum structural ductility, μ_{wall}, of the wall units is calculated from the following formula:

$$\mu_{wall} = \frac{\gamma_u}{\gamma_y} \dots\dots\dots\dots\dots\dots\dots\dots\dots\dots\dots\dots\dots\dots\dots\dots\dots\dots(8.7)$$

The ductility found experimentally is defined as $\mu_{wall} = \dfrac{3.0}{0.75} = 4$.

Figure 82 plots the equivalent damping ratios found experimentally as a function of the ductility of the test units.
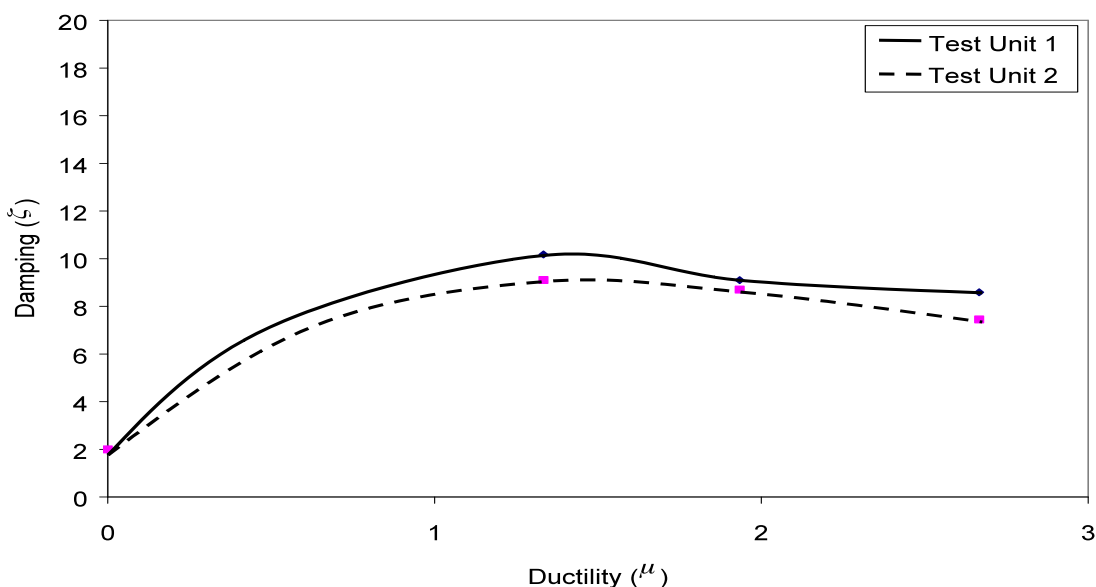
Figure 82: Equivalent Test Unit Damping Ratios, ζ, and Ductility, μ

8.4 SYSTEM DUCTILITY, OVERSTRENGTH AND RESPONSE MODIFICATION FACTORS

The ductility of the units was found to equal μ. If the equal displacement principle holds, then the ductility factor, μ, equal to 4, is equal to the response modification factor, R,

described in the UBC (1997) or FEMA 302 (1998). The system ductility reduction factor, R_d, the ratio of the elastic seismic force demand to the fully yielded structural strength (Newmark and Hall, 1982), must also equal 4.

A value equal to 1.0 is assigned to the overstrength factor, Ω_0, since the calculated base shear exceeds the capacity of the bilinear approximation. Also, the test units have limited lateral strength redundancy.

Therefore, the response modification factor is calculated by relationship C5.2.1-3 presented in the FEMA 302 provisions and determined by Uang (1991) shown below:

$$R = R_d \cdot \Omega_0 \ldots\ldots\ldots\ldots\ldots\ldots\ldots\ldots\ldots\ldots\ldots\ldots\ldots\ldots\ldots..(8.8)$$

The response modification factor is equal to $R = 4 \cdot 1.0$, or 4, as shown in Figure 83. Based on the elastic response, the elastic seismic force demand, V_E, and elastic seismic displacement demand, D_E, are respectively interpolated as 144kN (32.4kips) and 57mm (2.2in). These values are based on the design strength, V_y.
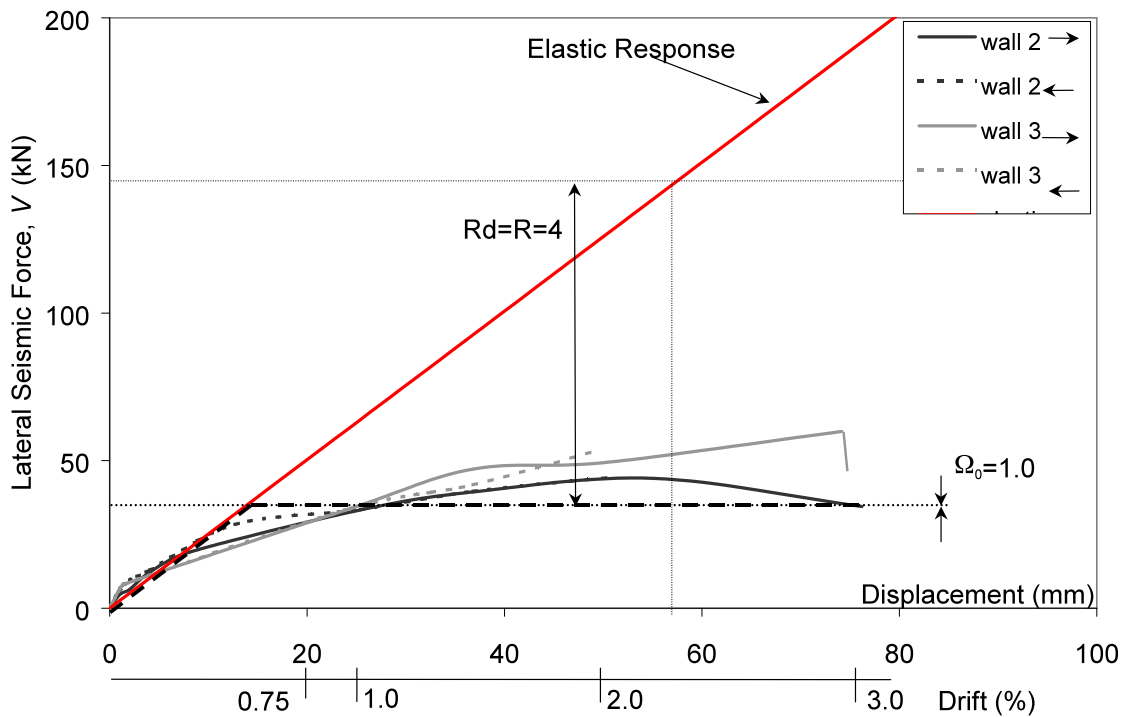
Figure 83: Elastic Response and Envelope Curves for Units 1 and 2 versus Drift

Designers using the1994 UBC requirements, have suggested the use of a reduction factor, R_w, equal to 6, by comparing the lateral resistance of straw-bale/facing wall system to that of a rigid concrete shear wall and counting on the allowable shear stress for cement stucco, as outlined in Chapter 25 (UBC, 1994). The author believes an R_w factor not higher than 4 should be used, based on the experimental findings that suggest the full shear stress capacity of the facings cannot be developed. The author's opinion is that the lateral resistance capacity of a rigid concrete shear member is superior to a straw-bale/facing wall.

8.5 DISTRIBUTED MASS SDOF OSCILLATOR MODEL OF UNITS AND EQUIVALENT IDEALIZED SDOF MODEL

It was intended to obtain a SDOF model to represent the behavior of the whole system. The wall system was first simplified as a distributed mass SDOF inverted pendulum structure with properties of the test units. This simplification is represented by Figure 84a, while 84b shows an idealized equivalent single mass SDOF oscillator.

a)Distributed Mass SDOF Model   b)Single Mass SDOF Model
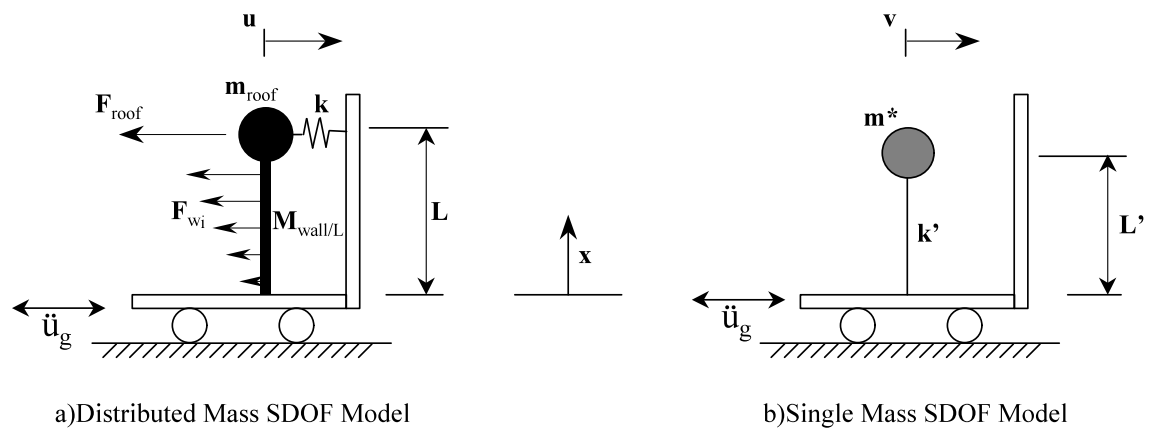
Figure 84: Inverted Pendulum Oscillator Models

In order to make the response of a distributed mass SDOF oscillator equal to that of the single mass SDOF simplified model of the wall, the following three requirements need to be satisfied:

i)   The center of the inertial forces of both models must be at the same height.

ii)   The same base shear, V_x, is applied to both models, hence the dynamic force applied to both models must be equal.

iii)   Both models needed to oscillate at the same period (T).

The mass of the pendulum, labeled m_{roof}, is representative of the dead and live loads specified in the UBC provisions for roof dead loads of 957Pa (20lbs/ft^2) and live loads

(which depend on geographic location and roof geometry) and associated by tributary area to the longest permitted unsupported roof dimension, 3048mm (10ft), under the construction codes that consider straw-bale construction (CTPCAZBC, NMBC). Influence of possible roof flexibility on the behavior was ignored. The mass distributed along the rod of the pendulum, $m_{wall/L}$, corresponds to the mass of the wall unit. It was assumed that the straw-bales and facings always acted compositely and gapping was ignored

The spring stiffness in Figure 84a was based on Equation 8.3, where κ was determined as 0.038 from test results. Figure 85 presents the inertial forces on the idealized structures.

a)Inertial Forces--
   Distributed Mass SDOF Model

b) Inertial Forces--
   Single Mass SDOF Model
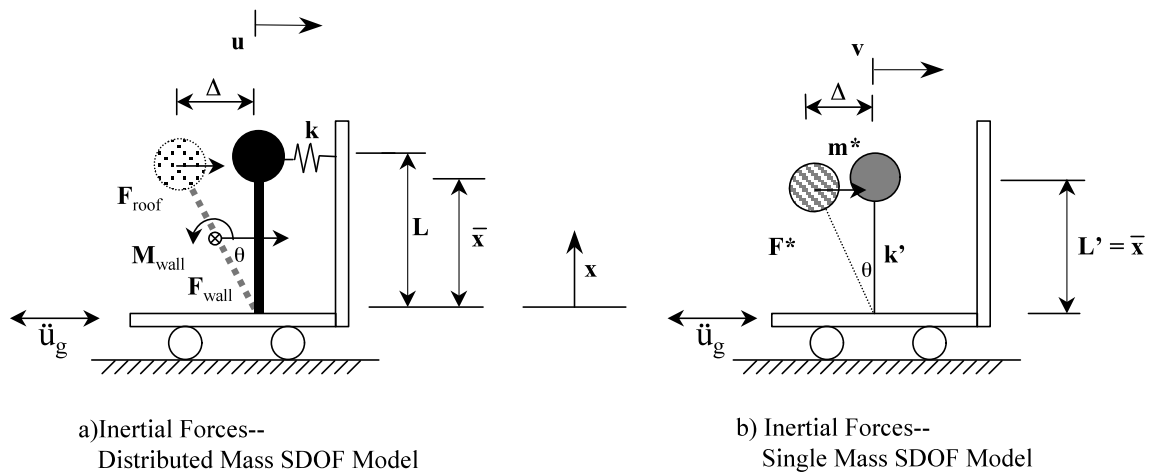
Figure 85: Inertial Forces Acting on Oscillators

The centroid of inertial forces, $\bar{x}$, for the distributed mass model is found from the first moment of forces, as shown in Figure 85a, in Equation 8.9.

$$\bar{x} \cdot \Sigma F = F_{roof} \cdot L + \int dF_{wall} \cdot x \dots\dots\dots\dots\dots\dots(8.9)$$

but since $dF_{wall} = dm_{wall} \cdot \ddot{u}$, where $dm_{wall} = \mu \cdot dx$, and μ is the mass per length of the rod used to simplify the wall unit. Since, $\ddot{u} = \ddot{\theta} \cdot x$, $dF_{wall} = \mu \cdot dx \cdot \ddot{u} = \mu \cdot dx \cdot \ddot{\theta} \cdot x$.

Similarly, $F_{roof} = m_{roof} \cdot \ddot{u}_{roof} = m_{roof} \cdot \ddot{\theta} \cdot L$. The moment in the rod due to the distributed mass is accounted for in this substitution. This can now be incorporated into Equation 8.10 to obtain the force centroid as:

$$\bar{x} = \frac{F_{roof} \cdot L + \mu \cdot \ddot{\theta} \int x^2 \cdot dx}{\Sigma F_{Distributed masses}} \quad \dots\dots\dots\dots\dots\dots\dots\dots\dots\dots (8.10)$$

Integrating the second part of this equation, and equating $\mu = m_{wall} / L$ and $F_{roof} = m_{roof} \cdot \ddot{u}_{roof}$, the center of the inertial forces is obtained as follows:

$$\bar{x} = \frac{m_{roof} \cdot L^2 \cdot \ddot{\theta} + m_{wall} \cdot \dfrac{L^2}{3} \cdot \ddot{\theta}}{F_{roof} + F_{wall}} \quad \dots\dots\dots\dots\dots\dots (8.11a)$$

$$\bar{x} = \frac{\left[m_{roof} + \dfrac{m_{wall}}{3} \right] \ddot{\theta} \cdot L^2}{m_{roof} \cdot \ddot{\theta} \cdot L + \mu \cdot \ddot{\theta} \int x \cdot dx} \quad \dots\dots\dots\dots\dots\dots\dots (8.11b)$$

$$\bar{x} = \frac{\left[m_{roof} + \dfrac{m_{wall}}{3} \right] \ddot{\theta} \cdot L^2}{m_{roof} \cdot \ddot{\theta} \cdot L + \dfrac{\mu \cdot \ddot{\theta} \cdot L^2}{2}} \quad \dots\dots\dots\dots\dots\dots\dots (8.11c)$$

$$\bar{x} = \frac{\left[m_{roof} + \dfrac{m_{wall}}{3} \right] \ddot{\theta} \cdot L^2}{m_{roof} \cdot \ddot{\theta} \cdot L + \dfrac{m_{wall} \cdot L}{2}} \quad \dots\dots\dots\dots\dots\dots\dots (8.11d)$$

$$\bar{x} = \frac{\left[m_{roof} + \dfrac{m_{wall}}{3} \right] \cdot L}{\left[m_{roof} + \dfrac{m_{wall}}{2} \right]} \quad \dots\dots\dots\dots\dots\dots\dots\dots (8.11e)$$

Equation 8.11e gives the centroid of inertial forces, equivalent for both the distributed and single mass models. Therefore, $L' = \bar{x}$ as shown in Figure 85b.

In order to satisfy the second requirement for equality of these models, the base shear, V_x, applied on both models must be equivalent. Both models must therefore resist the same dynamic forces. Hence, $\Sigma F_{Distributedmasses} = F^*$, where $F^* = m^* \cdot \ddot{\theta} \cdot L'$ and is the dynamic force on the effective mass, m^*, of the single mass SDOF model. The following substitution procedure may be done:

$$\Sigma F_{Distributedmasses} = F^* \ldots\ldots\ldots\ldots\ldots\ldots\ldots\ldots\ldots\ldots\ldots\ldots(8.12a)$$

$$m_{roof} \cdot L \cdot \ddot{\theta} + \int_0^L \mu \cdot dx \cdot \ddot{\theta} \cdot x = m^* \cdot L' \ddot{\theta} \quad \ldots\ldots\ldots\ldots\ldots\ldots\ldots....(8.12b)$$

$$m_{roof} \cdot L \cdot \ddot{\theta} + \mu \cdot \frac{L^2}{3} \cdot \ddot{\theta} = m^* \cdot L' \ddot{\theta} \ldots\ldots\ldots\ldots\ldots\ldots\ldots\ldots(8.12c)$$

$$m_{roof} \cdot L \cdot \ddot{\theta} + m_{wall} \cdot \frac{L}{2} = m^* \cdot L' \ldots\ldots\ldots\ldots\ldots\ldots\ldots\ldots\ldots\ldots(8.12d)$$

$$m^* = \left(\frac{m_{wall}}{2} + m_{roof} \right) \cdot \frac{L}{L'} \ldots\ldots\ldots\ldots\ldots\ldots\ldots\ldots..(8.12e)$$

The last requirement needed to satisfy the equality of the single mass model to that of the distributed mass model is the same period (T). The following EOM may be written for the distributed mass model, Figure 85a:

$$\left[m_{roof} + \frac{m_{wall}}{3} \right] \cdot \ddot{u} + k \cdot u = 0 \quad \ldots\ldots\ldots\ldots\ldots\ldots\ldots\ldots\ldots\ldots.(8.13)$$

where $u = \bar{x} \cdot \theta$ and $\ddot{u} = \bar{x} \cdot \ddot{\theta}$. From Figure 85b, the EOM for the undamped single mass model written in terms of v is:

$$m^* \cdot \ddot{v} + k' \cdot v = 0 \quad \ldots\ldots\ldots\ldots\ldots\ldots\ldots\ldots\ldots\ldots\ldots.(8.14)$$

Based on the equality relationships established for m^* and L', the two oscillators will have the same response to a ground motion, $\ddot{u}_g$, and Equations 8.13 and 8.14 will be equal. Therefore, $u = v$ (and hence $\ddot{u} = \ddot{v}$). The only unknown value in these equations is k', and can be solved for as shown:

$$k' = k \cdot \frac{\left(m_{roof} + \dfrac{m_{wall}}{3} \right)}{m^*} = k \cdot \frac{\left(m_{roof} + \dfrac{m_{wall}}{3} \right)}{\left(\dfrac{m_{wall}}{2} + m_{roof} \right)} \cdot \frac{L}{L'} = k \cdot \frac{\left(m_{roof} + \dfrac{m_{wall}}{3} \right)}{\left(\dfrac{m_{wall}}{2} + m_{roof} \right)} \cdot \frac{L}{\left(\dfrac{m_{roof} + \dfrac{m_{wall}}{3}}{\dfrac{m_{wall}}{2} + m_{roof}} \right) \cdot L} \quad \ldots..(8.15)$$

or more simply,

$$k' \equiv k \quad \ldots\ldots\ldots\ldots\ldots\ldots\ldots\ldots\ldots\ldots\ldots\ldots\ldots.(8.16)$$

A direct correlation to the requirement for equal dynamic forces can be made to verify this expression for the equivalent stiffness k': The stiffness of two systems must be identical if displacements at equivalent centers of inertial forces are equal.

The period of the SDOF oscillators shown in Figure 81 can be calculated from the relationship:

$$T = 2 \cdot \pi \sqrt{\frac{m}{k}} \quad \ldots\ldots\ldots\ldots\ldots\ldots\ldots\ldots\ldots\ldots\ldots.(8.17)$$

Concluding, these values are shown in Figure 86 for the SDOF idealized model.
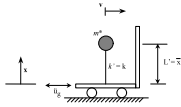
$$m^* = \left(\frac{m_{wall}}{2} + m_{roof} \right) \cdot \frac{L}{L'}$$

$$\bar{x} = \frac{\left[m_{roof} + \dfrac{m_{wall}}{3} \right] \cdot L}{\left[m_{roof} + \dfrac{m_{wall}}{2} \right]}$$

Figure 86: Resultant SDOF Idealized Model

The roof displacement, v, of the model shown will be less than the actual roof displacement of a structure, since it is being taken at the centroid of mass.

8.6 STRUCTURAL ROLE OF DIFFERENT ELEMENTS OF THE SYSTEM

Straw- It provided a surface where the facings were applied. The bond with the facings may prevent buckling effects from affecting the facing upon loading.

In-fill wall reinforcing bars- The #4 reinforcing bars helped the placement of the straw-bales during construction, increased the stability of the wall and provided limited in-plane and transverse lateral resistance.

Precompression- The precompression ties used made the in-fill wall denser, and prevented possible instability effects inherent of the soft, elastic properties of the straw-bales. Adequate precompression also eliminates the effects of creep in the in-fill wall and permit leveling of the roof beam before a roof is placed.

Frame- The frame connections were pinned, and provided no lateral resistance by itself. The frame in this type of structures provides support to the vertical loads. If larger drift levels were obtained, the frame may start providing lateral support as the frame elements begin crushing due to the rotations.

Facings- The facings provided the majority of the lateral resistance in the system.

Facing reinforcement- The 17-gauge stucco mesh increased the shear strength of the facings and provided the interface, together with the nails, for the connection between the facing and the frame.

Connection of frame and facing- The connection between the facing and the frame is the most crucial element in the resistance of lateral forces. It consists of nails attaching the facing to the frame by holding the 17-gauge stucco mesh close to the frame before application of the facings. If the connection is too strong, a brittle shear failure in the facings will occur at low displacement and high force levels. If it is too weak, a ductile failure will occur in the nails at large displacement and low force levels.

Connection of base beam to floor- The connection between the base beam and the slab was not rigid and allowed for vertical displacement (uplift) and horizontal displacement (slip). These displacements were sources of additional energy dissipation and contributed to the lateral load resistance of the system.

Connection of wall to roof- The connection should be adequate to keep the roof attached even at high drifts.

CHAPTER 9: DESIGN OF TYPICAL STRAW-BALE STRUCTURE AND ANALYSIS BY VARIOUS CODES

9.1 GENERAL DESCRIPTION OF THE STRUCTURE

The building that has been modeled is a post and beam type structure, with wheat straw-bales used as the in-fill material. It is based on a structure designed by Paul Weiner (Steen et al. 1994) but has been significantly modified. It is a one story residential building, chosen for a site just north of San Francisco, California, with proximity (≤ 2km (1.24mi)) to a seismically active fault. The detailed location is at 38° north latitude, and 122° longitude. Figure 87 shows a plan schematic of the structure, while Figure 88 shows elevation view of the structure.
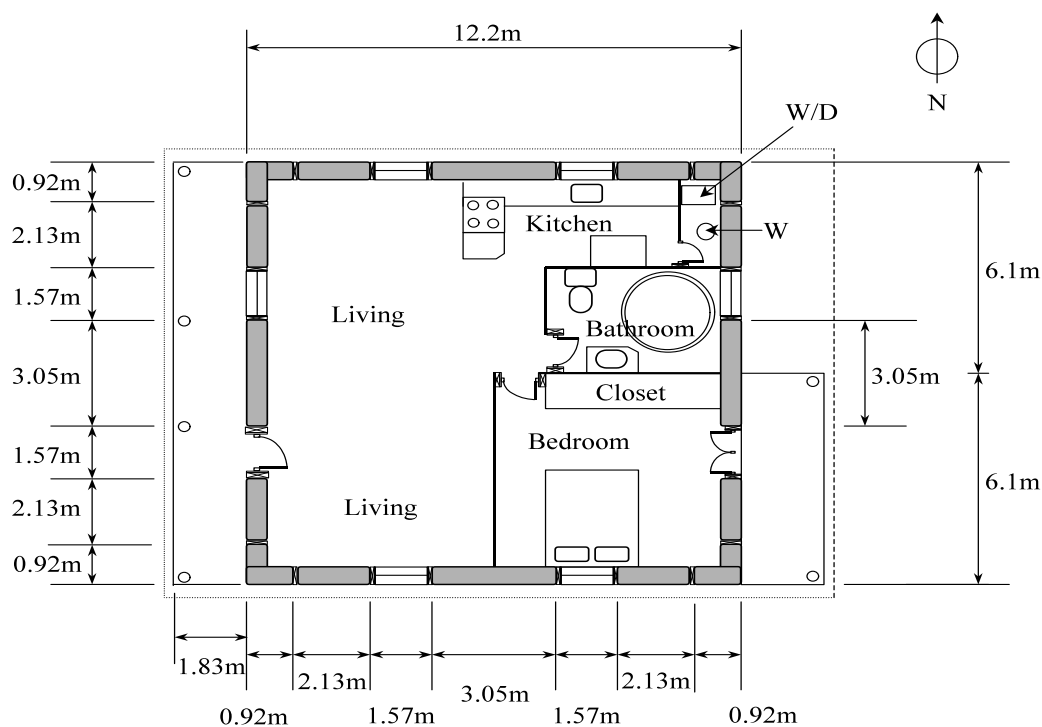
Figure 87: Plan Drawing of Model Structure
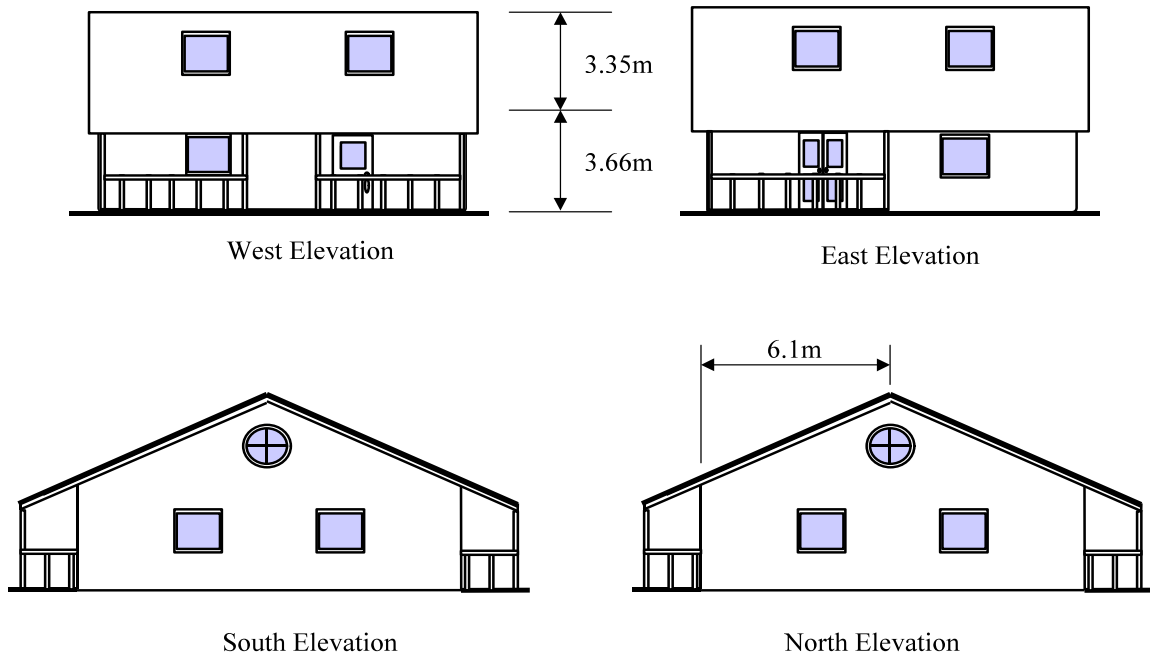
Figure 88: Elevation Drawings of Model Structure

The plan and elevation dimensions of the structure are as shown. The dead load of the straw-bale/facing walls, DL_{wall}, is assumed to be 346kN (77.7kips), or 28.3kN per horizontal meter (1943lbs per horizontal foot). The roof system has an area of 225m² (2420ft²) and is assumed to have a dead load, DL_{roof}, equal to 358.5kN (80.6kips). The total dead weight of the structure, W, is 704kN (158.3kips)

9.2 DETAILS

Straw-Bales-

The bales used were assumed to be made of wheat straw, bound by three polypropylene strings, with a moisture content ≤15%, and a density of 128.1kg/m³ (8.5pcf). They are assumed to have the following dimensions: Length 1219mm (48in), height 406mm (16in) and width 584mm (23in). They should be laid flat and in a running bond. The bales are assumed to be properly cut and re-tied as needed. #4 A615 steel reinforcing bars are

assumed to be used as vertical pinning reinforcement for each course of bales, starting on the second course of bales, 2 per bale and extending at least 305mm (1ft) into the bale directly below it. At the corners of the structure, a #4 A615 steel reinforcing bar should be bent into the staple shape shown in Figure 89, "stapling" each course corner, extending 305mm (1ft) into the bales.

#4 A615 Reinforcing bar

305mm
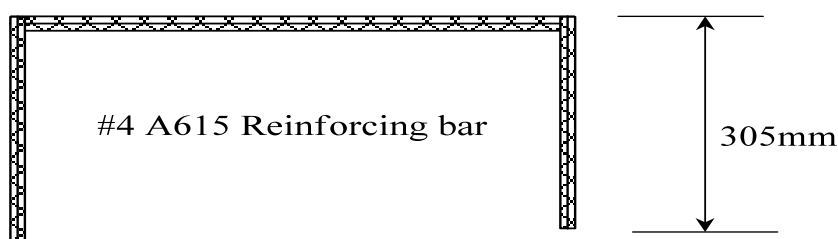
Figure 89: Staple for Corners in Straw-Bale Construction

Post and Beam Frame Elements-

The posts are assumed to be made of Douglas fir lumber and OSB sections. The post sections for window/door openings are assumed to be made from sections as shown in Figure 84, and according to the description of the built-up columns in Section 4.1.1. A total of 24 posts (built-up columns) are required for the structure, 6 per side. The posts are assumed to be connected to the floor by means of A36 steel plates, comparable in dimensions to those used for the units used in this study. These steel plates should be properly set into the perimeter grade beam as pouring occurs.

The beams should be 4.57m (15ft) long, 79.4mm by 190.5mm ($3^1/_8$in by 7½in) Douglas Fir glue laminated beams (AITC 117-88, 1988). A total of 12 beams with the above dimensions are necessary for the structure, 3 per side. A total of 24 grade A steel, 12-gauge (ASTM A446) splicing plates are to be used for splicing beams as needed on the perimeter. A total of 8 corner grade A steel, 12-gauge (ASTM A446) connector angles are assumed to be used to connect the corners of the perimeter beams. Connection to the

posts is assumed to be by means of steel A36 plates, comparable to those used in this study, as shown in Figure 90. 2 plates should be used per each connection, ensuring the out-of-plane shear capacity of the posts is not exceeded.
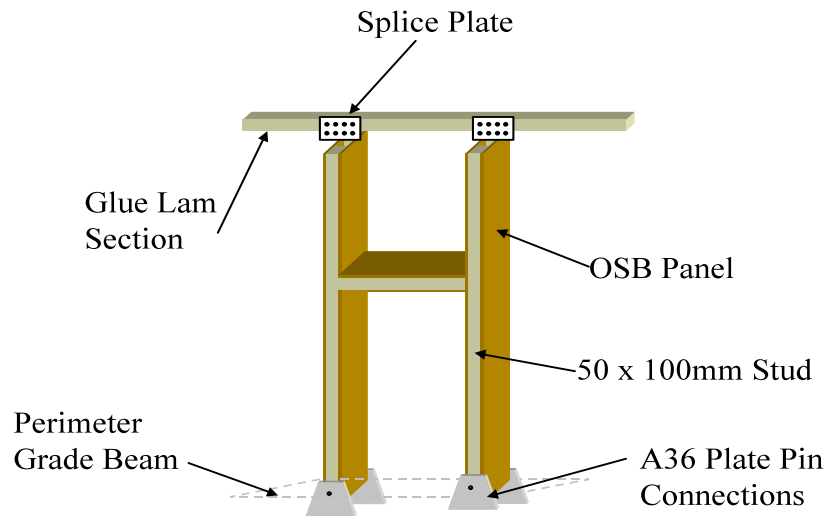
Figure 90: Post Framing Sections

Roof System-

The roof system is assumed to rely on 20 pre-fabricated 50 x 100m (2 x 4in) parallel chord scissors Douglas fir lumber trusses with mild steel connector plates at each joint. The slope of these trusses should be 28.8° with respect to the horizontal, which would make the height to mid-span length ratio of 3.4:6.1m (11:20ft). Pre-fabrication of these trusses assumes the manufacturer will have done an appropriate design to support all applicable loads. They are assumed to be attached firmly at a 610mm (2ft) off centers distance on the Glue laminated beams on the West and East walls. The attachment of these trusses to the perimeter beam needs to be done with mild steel plates. OSB panels with thickness 12.7mm (½in) are assumed for placing on top of the scissors trusses, with typical roof shingles attached on top for appropriate weather protection.

The roof system is assumed to remain rigid and firmly connected to the framing elements under lateral loading conditions.

Foundation/Floor System-

The floor of the structure is assumed to be a properly designed poured reinforced concrete slab. A reinforced concrete 610mm (2ft) thick perimeter grade beam is assumed to have been designed for support of all vertical loads. The grade beam is assumed to be 152mm (6in) above grade. The compressive strength of the concrete is assumed to be *f'c*= 31Mpa (4500psi). Sheet metal flashing, sealed at joints with caulking, is assumed to be placed on the perimeter as a moisture barrier.

Imbedded plastic hoses are assumed to have been placed prior to pouring for the precompression strapping to be run through. A total of 116 #4 A615 steel reinforcing bars, 457.2mm (1½ft) long, are assumed to be placed as to protrude 305mm (1ft) from the grade beam. The distance between each bar should be 406mm (16in), and set in the middle of the width dimension of the grade beam. Caulking is assumed to be used at the bar to sheet metal flashing connections. The 17-gauge stucco wire is assumed to be set into the slab, as shown in Figure 91.
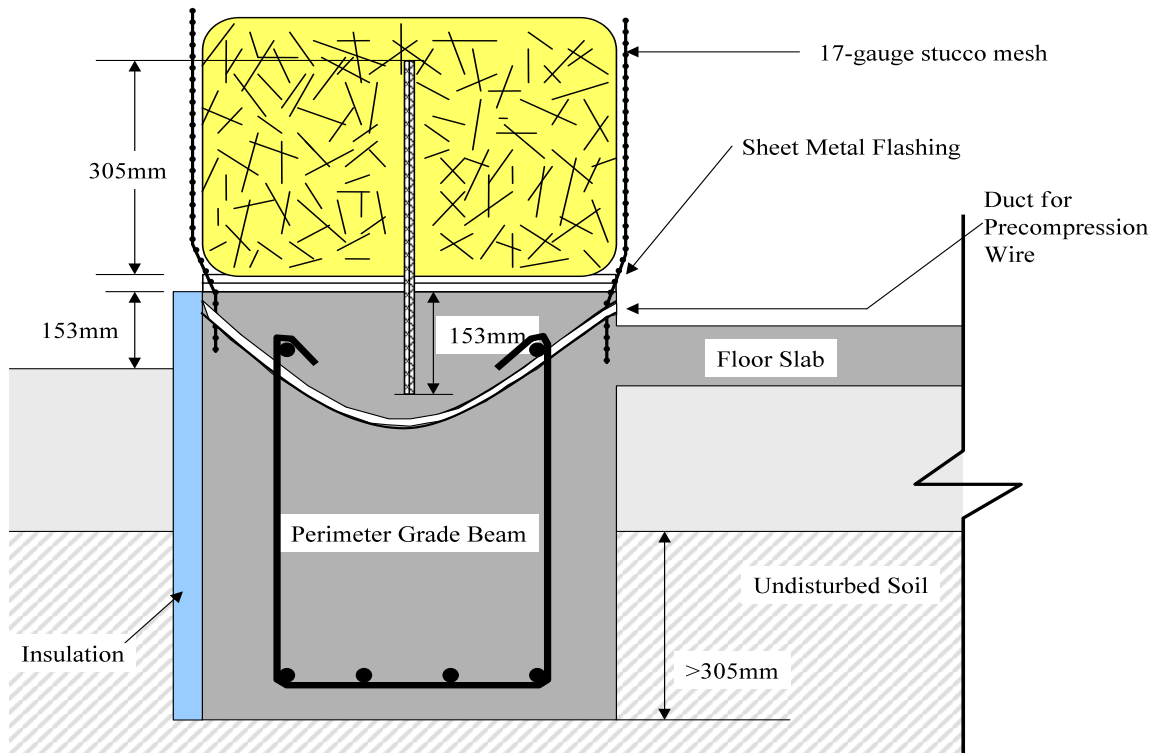
Figure 91: Foundation/Flooring System Cross-Section

It is assumed 305mm (12in) of the grade beam extends into undisturbed soil, as to not require any further foundation depth.

Precompression-

Precompression of the roof beams is assumed to be done with heavy fencing wire, similar to the one used in this study (12 gauge or higher). A total compression level of at least 0.6kN/m (71.9lbs/ft) should be applied to the walls prior to the installation of the roof.

Facings-

The reinforcement for the cover facings is assumed to be 17-gauge woven wire stucco mesh and expanded metal lath, attached to the in-fill wall and post and beam frame as described in Section 4.1.6. It is assumed to be set into the slab. The facing material is

assumed to be stucco, with a density, ρ, of 1600kg/m^3 (100pcf) and a compressive strength, $f'c$, of 17Mpa (2500psi), applied according to Section 4.1.7. The average thickness is assumed to be 38mm (1.5in) for the first two coats. The third coat does not contribute to the resistance capacity of the straw-bale/facing wall. The facing coats are to be applied by hand, with a curing time of at least 10 days for each coat.

9.3 DESIGN PROCEDURES

9.3.1 LOCAL BUILDING CODES

The CAPGSBC and NMBC guidelines were verified as the local building "code" for the proposed post and beam structure. The proposed straw-bales exceed the minimum dimensions and material properties requirements of both the CAPGSBC (Section 18944.35) and NMBC (Section 2.B) guidelines. The proposed orientation of the straw-bales and arrangement guidelines are met as described in the assumptions. The foundation/floor design meets the criteria of Section 2.D, E, F and H of the NMBC and Section 18944.40 of the CAPGSBC, which covers the floor/foundation, moisture barrier, reinforcements, and cover facings requirements. The maximum unsupported wall length (6.1m (20ft)) and height (3.7m (12ft)) restrictions in the NMBC are not exceeded by the proposed design. Both guidelines refer to the provisions for lateral and vertical loads as specified in the latest edition of the UBC.

9.3.2 UBC 1997 SEISMIC DESIGN PROVISIONS

The proposed site on which the structure is to be assumed to be erected is classified by the UBC provisions as Seismic Zone 4 and the type of Seismic Source is identified as A. This type of sources is defined as "Faults that are capable of producing large magnitude events (Moment Magnitude, $M_w \geq$ 7.0) and that have a high rate of seismic activity (Slip rate, $SR \geq$ 5mm/year)". The soil at the site is assumed to be "stiff", with a shear wave velocity, 183m/s (600ft/s) $\leq \overline{\upsilon}_S \leq$ 366m/s (1200ft/s). This type of soil characteristics leads the site to be classified as a Class D site. Based on these site characteristics and

seismicity maps accompanying the provisions, the following factors were obtained for calculations. The Seismic Zone Factor, Z, equal to 0.4, the Near Source Factor, N_v, equal to 2.0, the Seismic Coefficient, C_a, equal to $0.44 \cdot N_v$ or 0.88, and the Seismic Importance Factor, I, equal to 1.0. The Seismic Reduction Factor, R, will be taken as 4, according to Section 8.3 of this thesis. This evaluation of R is very approximate.

The period of the structure is calculated from Equation 30-8 of the UBC as shown below.

$$T = C_t \cdot (h_n)^{3/4} \dots \dots \dots \dots \dots \dots \dots \dots \dots \dots \dots \dots \dots .(9.1)$$

where the numerical coefficient, C_t, is given as 0.0488. The period of the proposed structure is calculated as $T = C_t \cdot (h_n)^{3/4} = 0.0488 \cdot (3.66)^{3/4} = 0.13s.$.

Based on the plan and vertical structural regularities of the proposed structure, the Static Force Procedure may be used for design. The design base shear, V, is calculated from Equation 30-6 of the UBC as:

$$V = \frac{2.5 \cdot C_a \cdot I}{R} \cdot W \dots \dots \dots \dots \dots \dots \dots \dots \dots \dots \dots \dots .(9.2)$$

The design base shear is:

$$V = \frac{2.5 \cdot C_a \cdot I}{R} \cdot W = \frac{2.5 \cdot 0.882 \cdot 1.0}{4} \cdot 704kN = 388kN$$

A 5% increase for possible torsional eccentricities makes the base shear equal to 407kN.

The structure as designed does not have adequate lateral resistance capacity to meet the design criteria for the proposed site, as the capacity is 83% of the design base shear. Additional elements providing lateral resistance equal to at least 17% of the design base shear are required for this design.

The vertical force distribution is calculated from Equation 30-15 of the UBC, shown below.

$$F_x = \frac{(V - F_t) \cdot w_x \cdot h_x}{\sum_{i=1}^{n} w_i \cdot h_i} \quad \ldots\ldots\ldots\ldots\ldots\ldots\ldots\ldots\ldots\ldots\ldots\ldots\ldots.(9.3)$$

Since the proposed structure is one-story, both i, x and n are equal to 1, and the vertical force distribution, F_x, is equal to V.

The story drift limitation, Δ_M, is calculated based on Section 1630.10.2 of the UBC as $\Delta_M = 0.025 \cdot h_t = 0.025 \cdot 3.66m = 91.5mm$.

9.3.3 FEMA 302 1998 (NEHRP 1997 SEISMIC DESIGN PROVISIONS)

The Occupancy Importance Factor, I, is 1.0, and the Seismic Use Group I for the proposed structure. The site on which the structure is assumed to be erected is classified by FEMA 302 provisions as Seismic Zone 4 and the type of Seismic Source is identified as A.

The soil at the site is assumed to be stiff clay, classified as Type D with a shear wave velocity, 183m/s (600ft/s) $\leq \overline{v}_S \leq$ 366m/s (1200ft/s). Based on these site characteristics, and referencing seismicity maps 3 and 4, the following coefficients were obtained for calculations. The Site Coefficient, F_v, equal to 1.5 for a 1-period MCE Spectral Acceleration, $S_i=0.5$, the MCE Spectral Response Accelerations for a 1-second Period, S_{M1}, equal to $F_v \cdot S_1$ or 0.75, and the DE Spectral Response Acceleration at 1-second Period, S_{D1}, equal to $\frac{2}{3} S_{M1}$ or 0.5. The Response Modification Factor, R, will be taken as 4, according to Section 8.3 of this thesis. This evaluation of R is very approximate.

The approximate fundamental period of the structure is calculated from Equation 5.3.3.1-1 of FEMA 302 as shown below.

$$T_a = C_t \cdot (h_n)^{3/4} \ldots\ldots\ldots\ldots\ldots\ldots\ldots\ldots\ldots\ldots\ldots\ldots (9.4)$$

where the numerical coefficient, C_t, is given as 0.0488. The period of the proposed structure is calculated as $T_a = C_t \cdot (h_n)^{3/4} = 0.0488 \cdot (3.66)^{3/4} = 0.13s$.

Based on the plan and vertical structural regularities of the proposed structure, the Equivalent Lateral Force Procedure may be used for design. The seismic base shear, V, is calculated from Equation 5.3.2 of NEHRP, shown below:

$$V = C_s \cdot W \ldots\ldots\ldots\ldots\ldots\ldots\ldots\ldots\ldots\ldots\ldots\ldots\ldots (9.5)$$

The Seismic Response Coefficient, C_s, is calculated based on Equation 5.3.2.1-2 of NEHRP as:

$$C_s \leq \frac{S_{D1}}{T_a \cdot (R/I)} \ldots\ldots\ldots\ldots\ldots\ldots\ldots\ldots\ldots\ldots\ldots\ldots (9.6)$$

The Seismic Response Coefficient is therefore equal to $C_s \leq \dfrac{0.5}{0.13 \cdot (4/1.0)} \leq 0.96$.

The seismic base shear is:

$$V = C_s \cdot W = 0.96 \cdot 704kN = 676kN$$

A 5% increase for possible torsional eccentricities makes the base shear equal to 710kN.

Under the FEMA 302 provisions, this structure, as designed, does not have adequate lateral resistance capacity to meet the design criteria for the proposed site, as the capacity is 48% of the design base shear. Additional elements providing lateral resistance equal to at least 52% of the design base shear are required for this design.

For seismic zones with the same soil classification but with a 1-period MCE Spectral Acceleration, S_1, less than or equal to 0.3, the proposed structure has adequate structural capacity under the FEMA 302 provisions.

The vertical force distribution of seismic force is calculated from Equation 5.3.4-1 of the provisions, shown below:

$$F_x = C_{vx} \cdot V \quad\ldots\ldots\ldots\ldots\ldots\ldots\ldots\ldots\ldots\ldots\ldots\ldots\ldots\ldots\ldots(9.7)$$

The Vertical Distribution Factor, C_{vx}, is determined from Equation 5.3.4-2:

$$C_{vx} = \frac{w_x \cdot h_x^k}{\sum_{i=1}^{n} w_i \cdot h_i^k} \quad\ldots\ldots\ldots\ldots\ldots\ldots\ldots\ldots\ldots\ldots\ldots\ldots\ldots\ldots(9.8)$$

Since the proposed structure is one-story, both i, x and n are equal to 1, and the vertical force distribution, F_x, is equal to V.

The story drift limitation, Δ_M, is calculated based on Table 5.2.8 of the NEHRP provisions as $\Delta_M = 0.025 \cdot h_{sx} = 0.025 \cdot 3.66m = 91.5mm$.

The Design Response Spectrum for the structure is presented in Figure 92. The Design Spectral Response Acceleration, S_a, is calculated from Equation 4.1.2.6-1 shown below:

$$S_a = 0.6 \frac{S_{DS}}{T_0} \cdot T + 0.4 \cdot S_{DS} \quad\ldots\ldots\ldots\ldots\ldots\ldots\ldots\ldots\ldots\ldots\ldots(9.9)$$

The period T_0 is calculated as $0.2 \cdot S_{D1}/S_{DS}$ or 0.33s. The Spectral Acceleration is then equal to: $S_a = 0.6 \frac{0.5}{0.33s} \cdot 0.13s + 0.4 \cdot 0.83 = 0.449\,s$.
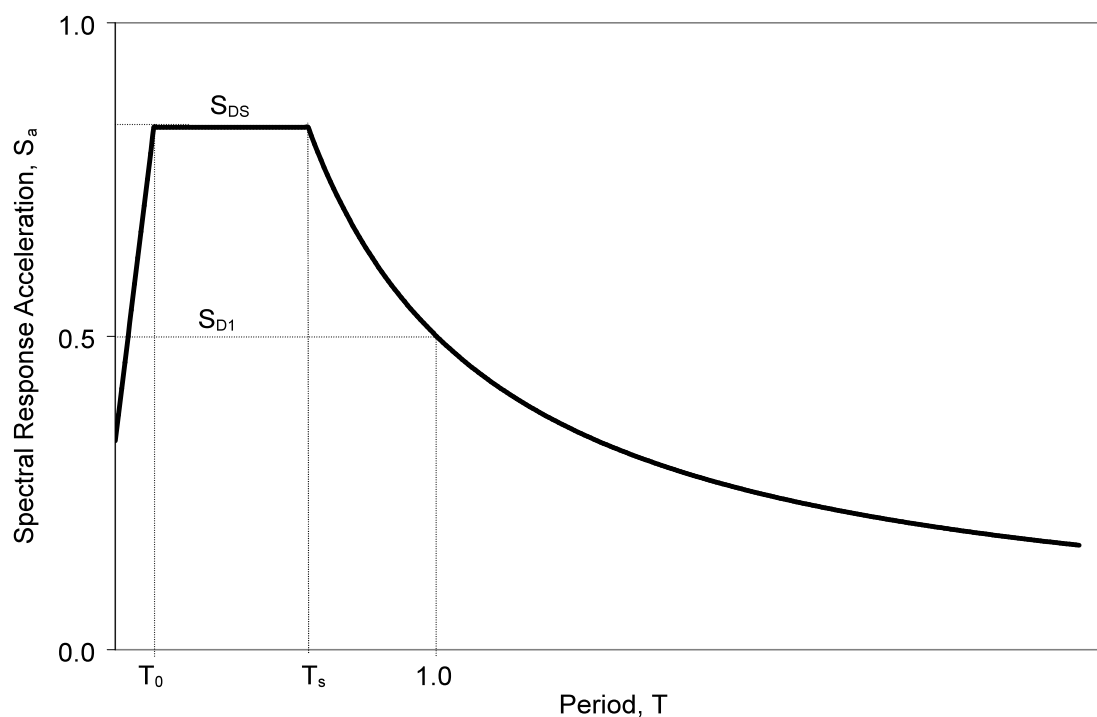
Figure 92: Design Response Spectrum

9.3.4 EXPECTED ENVELOPE CURVES

Considering degradation of the shear modulus, G, occurring at the same rate as observed in the wall models used for this study, expected structural envelope curves for the model structure, can be plotted as shown in Figure 93. The idealized response of an elastic structure with an initial shear modulus, G_i, representative of the elastic capacity of the wall models studied, is plotted too. The base shear values calculated by the UBC and NEHRP provisions are also plotted in Figure 93.

The base shear calculated by UBC and NEHRP exceed the capacity of the proposed structure by 13% and 50% respectively, as seen graphically.
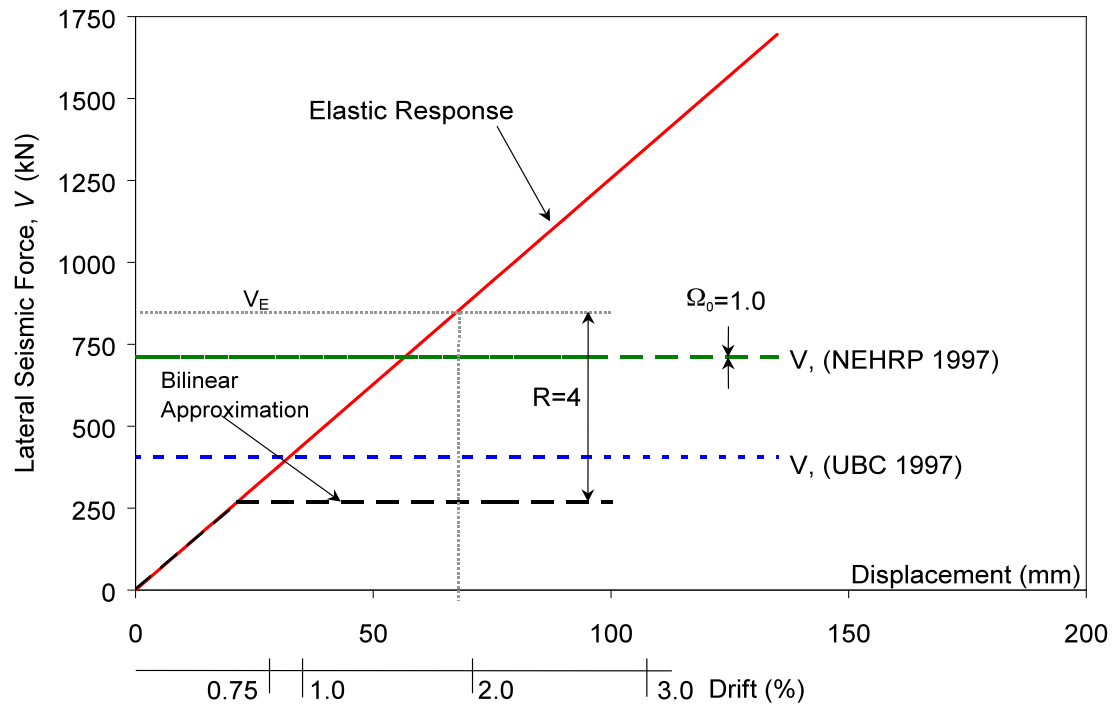
Figure 93: Expected Structural Envelope Curves and Calculated Base Shear Demand for Proposed Structure

9.3.5 ATC 40 PROVISIONS

In order to use the Capacity Spectrum Technique for assessing the performance of the proposed structure at the determined seismic demand displacements, the envelope and demand curves should be compared on a Acceleration-Displacement, S_a- S_d, plot. The design response spectrum shown in Figure 92 obtained by the FEMA 302 provisions was selected. Figure 94 shows the corresponding elastic response (5% damped) and reduced response spectra for a Type C structure, characteristic of pinched hysteretic loops, in the ADRS format. A performance point could not be established, since the equivalent bilinear representation of the capacity spectrum did not cross the reduced response spectrum for 10% damping. This equivalent viscous damping, ζ_{Tot}, was defined in Section 8.3. The displacement at top of structure will be larger than at centroid of mass.
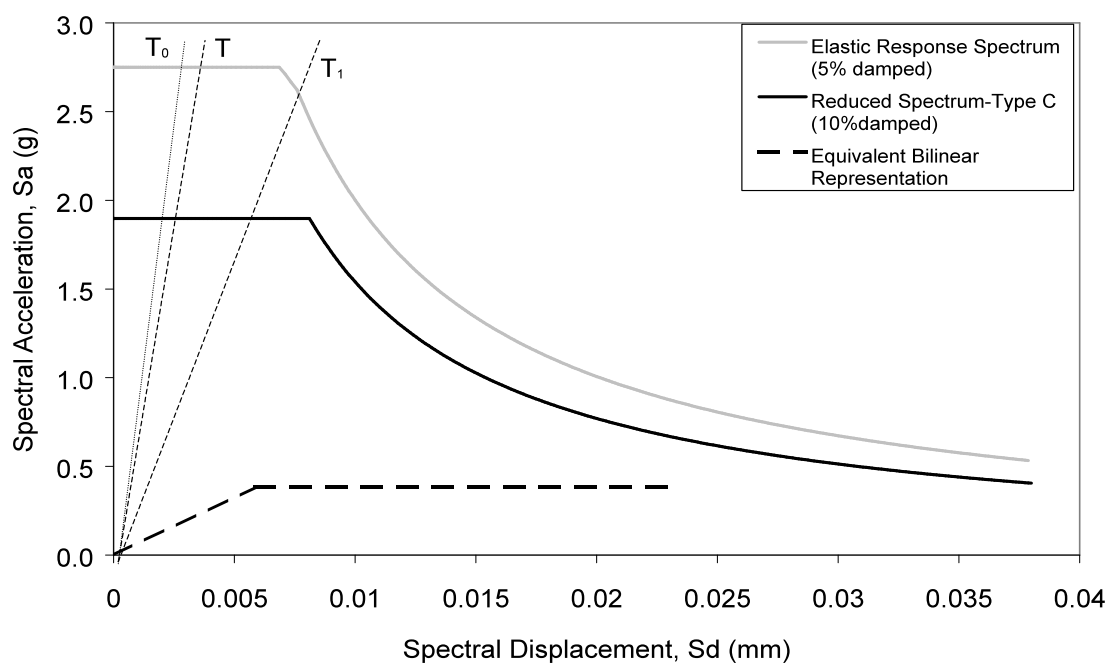
Figure 94: Acceleration-Displacement Response Spectrum (ADRS) for Model Structure

9.4 EXPECTED SEISMIC PERFORMANCE OF STRUCTURE MODELED

The structure suggested has no plan or vertical structural irregularities. The center of mass and torsional rigidity are located in the center of the structure. However a, 5% increase to the calculation of the base shear has been included as a factor of safety against possible eccentricities.

Based on the design strength determined in Section 8.1, 36kN or 14.8kN/m (8.1kips or 1.0kips/ft), the lateral resistance capacity, V_y, of the proposed structure in any direction is equal to 270kN (61kips), as seen in Figure 89.

The structure has a lateral resistance capacity 13% lower than the seismic base shear demand calculated by the UBC provisions (1997). Under these provisions, the structure has inadequate capacity and requires additional lateral resisting elements.

The structure has a lateral resistance capacity 50% lower than the seismic base shear demand calculated by the FEMA 302 provisions (1998). Under these provisions, the structure has inadequate capacity and requires additional lateral resisting elements.

Under the ATC-40 guidelines, the structure represented as a bilinear oscillator does not have adequate capacity and a performance point based on the reduced response spectrum for 10% damping could not be established to enable a displacement-based design.

9.5 DESIGN RECCOMENDATIONS BASED ON SEISMICITY

The base shear demand is a function of the seismicity and the structural mass. While the structure described above was not able to meet the FEMA 302 (1998) requirements for the san Francisco seismicity and the structural mass. For different masses, demand spectra may be plotted for a particular seismic zone, as shown in Figure 95. Demand curve 1 corresponds to the demand of the mass of the proposed structure as designed with 100% of the design mass. Demand curve 2, where the bilinear representation meets the demand, represents 58% of the mass of demand curve 1. Since the walls are a significant portion of the total mass, the roof mass must be reduced by 85% to get a total net mass for the structure of 58% of the original mass. If the characteristics of the wall elements are kept constant, (3.66m high and 9.1m long each), the maximum roof load that may be applied is 15% of the roof load used for the analyzed design.
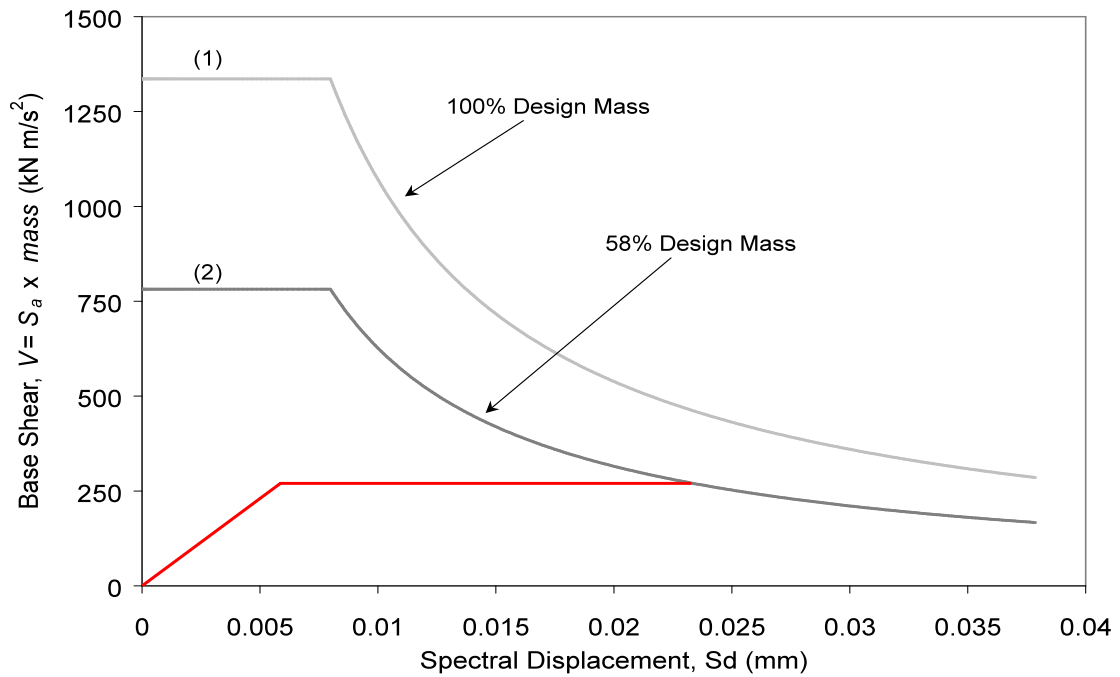
Figure 95: 10% Damped Base Shear Demand versus Spectral Displacement

The lateral force capacity required for design is a function of the roof area for the specific seismic zone for which the proposed structure was intended. The maximum tributary area of roof, A_{roof}, for a wall element may be calculated per horizontal unit of wall, L_{wall}, as shown in Figure 96. For demand curve 2, the maximum tributary area of roof, $A_{SF\text{-}roof}$, per horizontal meter of wall, $L_{SF\text{-}wall}$, is equal to 1.9m^2/m for this seismic zone. This wall system is therefore not appropriate for use in a zone of high seismicity. In another seismic zone, the maximum roof tributary area per horizontal meter will be different.
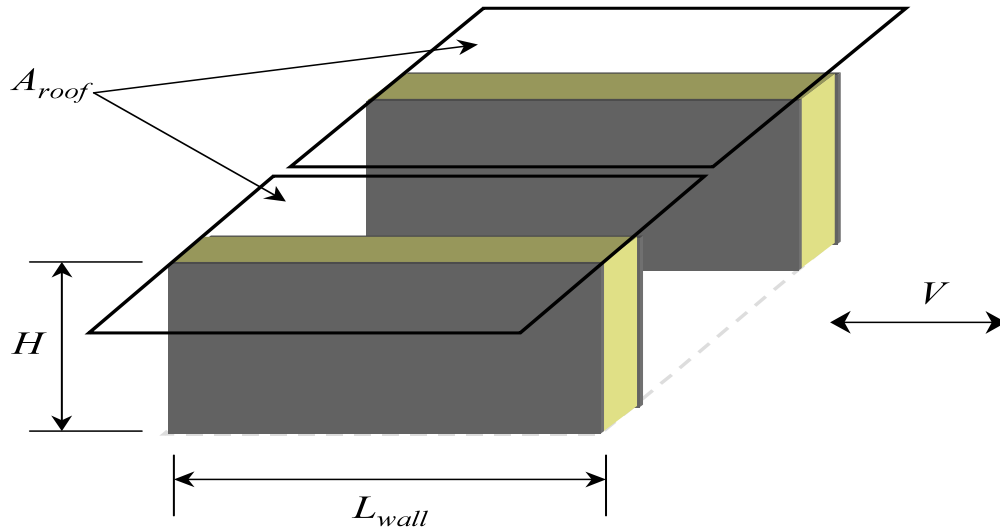
Figure 96: Schematic of Maximum Tributary Area per Horizontal Unit of Wall

Equation 9.5 calculates the base shear based on a Seismic Response Coefficient, C_s, which which is dependent of the seismic zone. An equation to determine the maximum tributary area of roof, A_{roof}, for 1 horizontal meter of wall, associating the coefficient corresponding to the proposed site, C_{SF}, equal to 0.96, and those of other zones, C_s^*, may be developed as:

$$A_{roof} / L_{wall} = 1.9(m^2/m) \cdot \frac{C_{SF}}{C_s \,^*} \ldots\ldots\ldots\ldots\ldots\ldots\ldots..(9.10)$$

The centroid of mass, determined from Equation 8.12e, can be related the length of wall and roof area as:

$$m^* = \left(\frac{m_{wall}}{2} + m_{roof} \right) \cdot \frac{x}{\overline{x}} = \left(\left(\frac{L_{wall} \cdot (H_{wall} \cdot \rho_{wall})}{2} \right) + A_{roof} \cdot DL_{roof} \right) \ldots\ldots.(9.11)$$

where the density and the height of the wall, H_{wall}, ρ_{wall}, may be expressed as a constant, k_{wall}. The design dead load, DL_{roof}, may vary for each design. The height of the centroid of

mass, $\bar{x}$, may be found by Equation 8.11e. Furthermore, the centroid of mass, m^*, and length of wall, L_{wall}^* required for adequate lateral resistance can be associated with the total mass, m, and required length of wall, L_{wall}, may be related as:

$$\frac{m^*}{L_{wall}^*} \geq \frac{m}{L_{wall}} \ldots\ldots\ldots\ldots\ldots\ldots\ldots\ldots\ldots\ldots\ldots\ldots\text{(9.12)}$$

This equation may be expressed as a constant, k_{ml}. For the structure as described above for the San Francisco site, k_{ml} is found to equal:

$$k_{ml} = \frac{m}{L_{wall}} = \frac{58\% \cdot W}{L_{wall}} = \frac{58\% \cdot 704kN}{9.1m \times 2walls} = 22.44\frac{kN}{m}$$

For different seismicity, constant k_{ml} may be modified as:

$$k^* = k_{ml} \cdot \frac{C_s^*}{C_{SF}} \ldots\ldots\ldots\ldots\ldots\ldots\ldots\ldots\ldots\ldots\ldots\ldots\text{(9.13)}$$

This equation is related to the Equation 9.13 in terms of length of wall, 3.66m (12ft) high required for a roof area as:

$$L_{wall} \geq m^* \cdot k^* \ldots\ldots\ldots\ldots\ldots\ldots\ldots\ldots\ldots\ldots\ldots\text{(9.14)}$$

The length of wall required to support a certain roof area with a particular design dead load is found by incorporating Equation 8.11e into Equation 9.12, and including constant k^*, as follows:

$$L_{wall} \geq \frac{k^* \cdot \left(\dfrac{L_{wall} \cdot k_{wall}}{2} + A_{roof} \cdot DL_{roof}\right)^2}{\dfrac{L_{wall} \cdot k_{wall}}{3} + A_{roof} \cdot DL_{roof}} \ldots\ldots\ldots\ldots\text{(9.15)}$$

This quadratic equation is based on the assumption that the shape of the demand spectrum does not change much between seismic zones. The equation obtained is approximate, since the period of the structure is not corrected for the effect of mass or seismic force reduction and is not applied to the scaling down method used to generate the demand spectrum in Figure 96. The approximation cannot be scaled down linearly because the period lines radiate from the bottom left corner of the graph.

For a response spectrum based on the FEMA 302 provisions, this approximation is applicable, as the peak spectral acceleration response for short periods may be scaled down linearly by the seismic response coefficient, R, equal to 4 (Section 8.3), as shown in Figure 97. The difference between the design level spectra and the resistance level of the structure may be calculated and factored into Equation 9.15 and from the spectral acceleration of the structure by including a further reduction factor to k^{**}. This additional coefficient is a ratio of the shear resistance of the design strength of the structure and the calculated base as:

$$k** = k* \cdot \frac{0.0735d(b_p\sqrt{f'_{cp}} + b_s\sqrt{f'_{cs}}}{V_{NEHRP97}} \quad \ldots\ldots\ldots\ldots\ldots.(9.16)$$

This coefficient is equal to $k** = \dfrac{270kN}{704kN} \cdot k* = \dfrac{1}{2.63} \cdot k*$ for the analyzed structure.
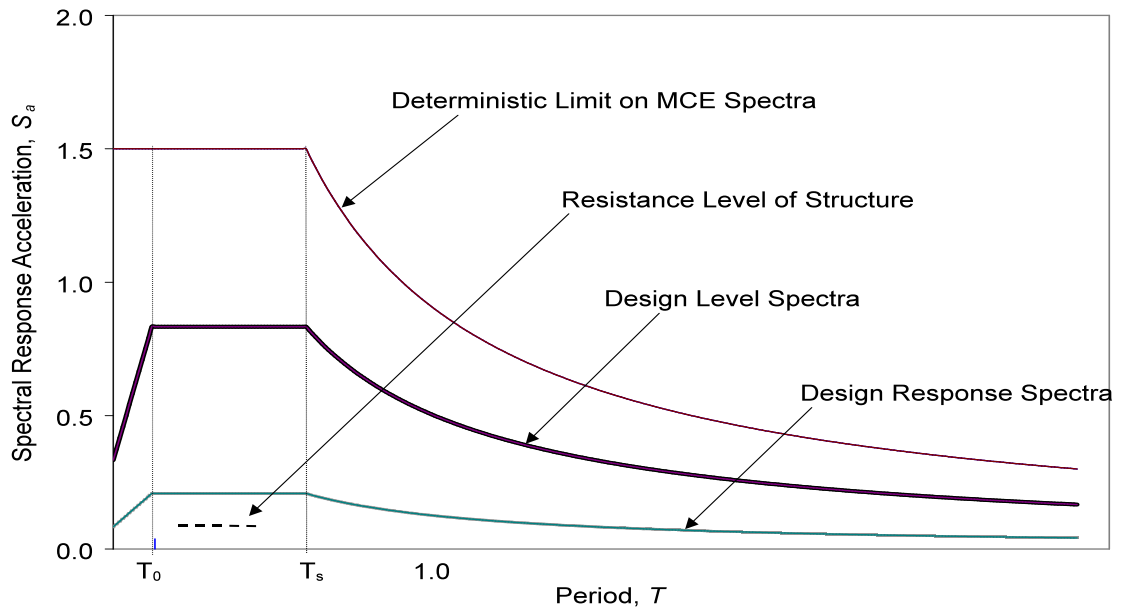
Figure 97: Reduction of Response Spectrum Calculated by NEHRP (1998)

For example, in Pullman, WA, the Seismic Response Coefficient, C_s, is lower. Assuming the site soil is Type D, the following coefficients are determined from seismicity maps: A Site Coefficient, F_v, equal to 2.4 for a 1-period MCE Spectral Acceleration, S_1, equal to 0.1, the MCE Spectral Response Accelerations for a 1-second Period, S_{M1}, equal to $F_v \cdot S_1$ or 0.45, and the DE Spectral Response Acceleration at 1-second Period, S_{D1}, equal to $\frac{2}{3} S_{M1}$ or 0.16.

The Occupancy Importance Factor, I, is 1.0, and the Seismic Use Group I for the proposed structure. The Response Modification Factor, R, will be taken as 4, according to Section 8.3 of this thesis.

The approximate fundamental period of the structure was calculated from Equation 9.4 as

$$T_a = C_t \cdot (h_n)^{3/4} = 0.0488 \cdot (3.66)^{3/4} = 0.13s.$$

The Seismic Response Coefficient, C_s, is calculated based on Equation 5.3.2.1-2 of FEMA 302 as:

$$C_s \leq \frac{S_{D1}}{T_a \cdot (R/I)} \quad \text{..(9.17)}$$

The Seismic Response Coefficient is therefore equal to $C_s \leq \dfrac{0.16}{0.13 \cdot (4/1.0)} \leq 0.31$.

The base shear is equal to:

$$V = C_s \cdot W = 0.31 \cdot 704 kN = 218 kN$$

A 5% increase for possible torsional eccentricities makes the base shear equal to 230kN.

The structure for a lower seismicity site, such as Pullman, has adequate lateral resistance as designed, with a factor of safety over 1.17. If the equation to determine the length of wall required, L_{wall}, was solved for the calculated area of roof, A_{roof}, it wold be found that less length of wall is necessary than the one suggested in the model structure.

CHAPTER 10: CONCLUSIONS

10.1 CONCLUSIONS

Two single story wall units with straw-bale in-fill and cement-stucco facing on one side and gypsum-based plaster facing on the other side in a wooden post and beam frame were subjected to repeated in-plane cyclic lateral loads at the roof level. Tests to determine the material properties were also carried out to enable an understanding of how lateral load is resisted. It was found that:

1. The facings were the stiffest parts of the system and carried the majority of the lateral load. The straw-bale in-fill was relatively flexible with very limited lateral force resistance. It serves as a surface for application of the facings and limits buckling and possible collapse of the facing. The post and beam frame was pinned and carried very little lateral force. As cycles were applied the facings tended to move away from the straw.

2. The facings were observed to crack and spal at the corners of the units. No damage was observed at the middle of the facings. Significant uplift occurred.

3. It was found that both test units reached peak strengths of greater than $V = 0.0735d(b_p\sqrt{f'_{cp}} + b_s\sqrt{f'_{cs}})$. Here f'_{cp} is the compressive strength of the plaster, f'_{cp} is the compressive strength of the stucco, b_p is the average thickness of plaster facing, b_s is the average thickness of stucco facing and d is the wall length. The second test had a strength of 27% larger than the first test due to confinement of the facings within the frame. The peak strengths were 44% of that estimated strength capacity for shear failure of reinforced concrete members by ACI-318 (1995), $V = 0.1667\sqrt{f'_{cp}}b_w d$.

4. The equivalent lateral stiffness of the facings was found to be 0.038GA/L where G is the shear modulus of the material based on a Poisson's ratio of 0.15, and the elastic modulus, E, is based on the material strengths, f'_c, and density w. A is the plan area of the facings and L is the wall height. The coefficient of 0.038 is significantly less than unity as a result of uplift, slip and cracking of the facings beside the nails.

5. Drifts of greater than 3% were reached for each frame before the strength dropped to less than 80% of the peak strength. This related to a displacement ductility of 4%.

6. The seismic performance of a straw-bale structure meeting the geometric requirements specified in the California Proposed Guidelines for Straw Bale Construction and City of Tucson and Pima County Arizona Building Code and New Mexico Building Codes, and assuming hysteretic characteristics similar to those in the tests was investigated using the UBC (1997), FEMA 302 (1998) and ATC-40 (1996) codes. It was found that while the structure did not meet the seismic criteria for these codes in zones of near fault high seismicity, it was satisfactory for zones of lower seismicity.

7. A simple model was developed using a linear analysis program to describe the relative component of panel deformation, frame/facing connection and uplift drifts to the total drift and to allow strengths in each component to be obtained.

8. The required length of wall per unit of roof area may be calculated for a structure with similar hysteresis characteristics to those of the test units is given in the form of:

$$L_{wall} \geq \frac{k * \cdot \left(\dfrac{L_{wall} \cdot k_{wall}}{2} + A_{roof} \cdot DL_{roof} \right)^2}{\dfrac{L_{wall} \cdot k_{wall}}{3} + A_{roof} \cdot DL_{roof}} \quad \ldots\ldots\ldots\ldots(9.15)$$

where $k*$ is the mass of a structure, subjected to lateral forces and supported by a length of wall. It is modified by a ratio of the seismic Response Coefficient, C_s, of any site, to that of the analyzed site.

This quadratic equation may be modified by a ratio of the base shear design of any site to that of the analyzed one and used conservatively with the FEMA 302 spectra.

10.2 RECOMMENDATIONS FOR FURTHER RESEARCH

Only two walls were tested. This number was not sufficient to give the required confidence for design of general straw-bale-stucco-facing walls for residences in regions of moderate or high seismicity. The sensitivity to and the desirability of slip and uplift of the frame on the overall performance should be understood.

Information on the connection between frame and facings is desirable to model the behavior of a post and beam straw-bale in-fill wall more accurately. A more precise testing of the effect of the connection interface can allow a non-linear behavior analysis. Tests are required to also understand the behavior of frames with different details, such as the thickness of facings, precompression of bales, and connections between the frame and the roof, as well as to the foundation.

BIBLIOGRAPHY

ACI-318 Building Code and Commentary, American Concrete Institute. Detroit, 1995

ATC-40 *Seismic Evaluation and Retrofit of Concrete Buildings Report No. SSC 966-01 and -02*. Applied Technology Council, November 1996.

Bainbridge, David. "An Introduction to Straw-Bale Building." Laguna Beach, CA: Earthword, EOS Institute, 1993.

Bou-Ali, Ghailene. "Straw-Bales and Straw-Bale Wall Systems." Master's Thesis: Civil Engineering Department, University of Arizona, 1992.

Burkhardt, Ross. "Straw Bale Construction." from The Real Goods Solar Living Sourcebook, 9th ed. White River Jct., VT: Real Goods Trading Corp., 1996. pp. 43-46.

Canada Mortgage and Housing Corporation, Housing Technology Incentives Program. "An Innovative Straw/Bale Mortar Wall System." NHA 5799 84/08. Ontario, Canada.

Chapman, Linda and Platts, Bob. *Prestressed Nebraska System Testing Summary*. The Last Straw No. 14, Spring 1996. Tucson, AZ.

Code for Design of Concrete Structures for Buildings CSA A23.3-1978, Canada Standards Agency, 1978, Ontario.

"Developing and Proof-Testing the 'Prestressed Nebraska' Method for Improved Production of Bale Fibre Housing" Report by Firehouse Ltd. with Scanda Consultants Ltd. Ottawa, 29 February 1996.

Eisenberg, David. *Straw Bale Construction and the Building Codes-A Working Paper, v. 1.5, February 1996*. Development Center for Appropriate Technology, Arizona.

FEMA-302 <u>NEHRP Recommended Provisions for Seismic Regulations for New Buildings and other Structures 1997 Ed</u>.: Building Seismic Council. Washington DC, 1998.

Hames, Shannon. "Shannon's Page on Straw-Bale Construction." Internet Site: www.geocities.com/athens/acropolis/8308.

King, Bruce. <u>Buildings of Earth and Straw.</u> Sausalito, CA: Ecological Design Press, 1996.

<u>LRFD Manual of Steel Construction</u> 2nd Ed.:AISC. Chicago, 1994.

MacGregor, James. Reinforced Concrete-Mechanics and Design, 3rd Ed.: Prentice-Hall. Upper Saddle River, 1997.

Nelson, Jared. "Effects of Long-Duration, Long-Period Ground Motion on Bridge Performance," *PEER A2 Project*: Civil and Environmental Engineering Department, Universtiy of Washington, 1998.

Newmark N. M., and J. W. Hall, 1982, *Earthquake Spectra and Design*, EERI Monograph Series, Earthquake Engineering Research Institute, Oakland, CA.

Park, R. and Paulay, T. <u>Reinforced Concrete Structures</u>: John Wiley and Sons. New York, 1974

Simmons, Bryce. *Straw Bale Test Report, SHB Job No. C93-9914*: November 17, 1993. SHB AGRA Inc., Albuquerque.

Stafford, Chris and Tichy, Robert. "Compression and Lateral Load Tests of Two-String Straw Bale Walls." Test Report: Wood Materials and Engineering Laboratory, Washington State University, 1995.

Steen et al. <u>The Straw Bale House.</u> White River Jct., VT: Chelsea Green Publishing Co. 1994.

Thompson et al. Straw Bale Construction-A Manual for Maritime Regions. Nova Scotia, Canada: Straw House Herbals-Solterre Design, 1993. 18pp.

Welsch, R.L. "Sandhill Baled-hay Construction." *Keystone Folklore Quarterly*. Spring 1970. pp.16-34.

APPENDIX A